Fluorogenic Derivatization of Pro-Quinoidal Species:
From Biogenic Amines to Protein Bound 3-Nitrotyrosine

By

Joshua M. Woods

Submitted to the graduate degree program in Pharmaceutical Chemistry and the Graduate Faculty of the University of Kansas in partial fulfillment of the requirements for the degree of Doctor of Philosophy.

_____

Chairperson John F. Stobaugh

_____

Christian Schöneich

_____

Susan M. Lunte

_____

Michael Wang

_____

Robert C. Dunn

Date Defended: August 21, 2014

The Thesis Committee for Joshua Woods

certifies that this is the approved version of the following thesis:

Fluorogenic Derivatization of Pro-Quinoidal Species:

From Biogenic Amines to Protein Bound 3-Nitrotyrosine

_____

Chairperson John F. Stobaugh

Date approved: August 21, 2014

Table of Contents

Fluorogenic Derivatization of Pro-Quinoidal Species:

From Biogenic Amines to Protein Bound 3-Nitrotyrosine

The focuses of this dissertation are an examination and advancement of chemistries for the fluorogenic derivatization of the analysis of proquiniodal species. The term proquinoidal species specifically refers to a group of biologically active compounds that easily may be oxidized to the corresponding quinones or imino-quinones. Catechols (Cs), catecholamines (CAs), and 5-hydroxyindoles (5-HIs) are classes of biogenic amines that affect neuroregulatory functions such as mood and appetite. While the determination of these classes of substances has been the accomplished by a variety of techniques over the past several decades, a recent approach has been their conversation to a fluorescent product by use of the fluorogenic reagents benzylamime (BA) or diphenylethylenediamine (DPE).

In the first section of this work, a critical examination of these derivatization chemistries is undertaken through product isolation, derivatization kinetics investigations, and yield determination for three substances that represent each analyte class. While not investigated in detail, it is recognized that 3-nitrotyrosine residues in peptides and proteins (a post-translational modification that has been associated with various age related pathologies such as atherosclerosis, neuropathies and others conditions), when reduced to the corresponding 3-aminotyrosine residues, undergo an analogous derivatization reaction to the catechol class. Application of the described derivatization reaction to such substances is an obvious and valuable extension of the present findings. Results obtained from the initial finding indicated that improvements regarding the physical-chemical properties of the DPE and/or BA regents would be highly useful in future applications directed toward the analysis of 3-nitrotyrosine residues, particularly as regards solubility and selective isolation of the formed product.

The approach described herein relies on the reduction of the 3-NY residue to the corresponding 3-aminotyrosine (3-AY), with subsequent derivatization by either BA or DPE. Enhancement of the existing derivatization reagents is explored through chemical modification of the reagents through the attachment of various substituents for the purpose of enhanced isolation and/or detection, increasing reagent aqueous solubility, maximization of single production formation, and allowing for the incorporation of stable isotopes. Recognizing that samples of biological origin are present as a complex mixture, further to the alluded to selectivity achieved via reagent design, significant improvements of chromatographic peak capacity were additionally sought. Efforts toward this goal included the fabrication of an Extreme Ultra-Pressure Liquid Chromatography (XUPLC) system, which utilized long columns packed with sub-2µm particles (75 µm id x 0.5-2.0 m L; packed with 1.9 µm BEH C18 particles) necessitating operation at 30,000 psi.

An overall goal was the integration of the results obtained from these two differing but complimentary research areas. The derivatization investigations revealed the derivatization reactions to be complete with 2 hours, with yields for Cs of no less than 70% when either reagent, BA or DPE, was utilized. Further reagent design and evaluation efforts were directed toward the characterization of BA and DPE that was elaborated to possess a sulfonic acid moiety, which provided for enhanced aqueous solubility and a selective sample preparation handle via strong anion exchange solid phase extraction. An alternate approach was the elaboration of each base regent to the dimethylamino-analog, again with the motivation being enhanced aqueous solubility but now potentially better electrospray ionization properties for mass spectrometry. Efforts in the XUPLC area revealed the expected gain in resolution and concurrent increased peak capacity. In summary, this dissertation describes advances in the utilization of existing reagents, the preparation and characterization of new reagent analogs and describes an advanced chromatographic system. All of these aspects are expected to be of high valuable

in the analytical chemistry of catechol determinations and the related area of 3-nitrotyrosine residues present in peptides and proteins.

Acknowledgements

The work contained within this thesis would not be possible without the support of several different people, all who have helped me grow as a person and a scientist. Thank you, John Stobaugh, for giving me a chance to prove myself within the graduate program. I certainly was not qualified to enter the program due to the troubled time I had during my undergraduate career. However, you helped me to secure a spot in the graduate program that has allowed me to prove I am capable of more than my undergraduate transcripts would show. Additionally, you took the time to teach me to focus on the details required to be a successful chemist, and for that I will be forever grateful. Thank you to my dissertation committee: Christian Schöneich, Sue Lunte, and Michael Wang. I appreciate the support and guidance you all have provided through the many challenges I encountered throughout working on my research project. Thank you, Bob Dunn, for both serving on my dissertation committee and for fueling my excitement over chemistry during undergrad.

I was fortunate enough to make several close friends during my time in graduate school. If I had not entered the pharm chem program at the same time as Justin Thomas, Randy Logan, and Jessica Creamer, it would not have been such a rewarding experience. We were able to help each other pass through demanding coursework and struggle through challenging examinations at a time when the program was undergoing restructuring. I look forward to our lasting friendships and will never forget the several great times we had as we enjoyed the city of Lawrence together. A special thanks to Jordan Stobaugh. I was fortunate enough to meet you in undergrad in the dreaded physical chemistry classes. You have continuously pushed me towards achievements I would not otherwise dream of.

My family has provided unending support through all of my education. Thank you to my parents who are always there to encourage me through difficult times and remind me the hard parts of life are usually temporary. I certainly would not have survived grad school without the help of my grandma, and my Aunt Julie and Uncle Scott. My wife and I were fortunate enough to be able to live near family who

were eager to help us raise our children. I can't thank you all enough for helping my wife and I raise Jaina and Juliet during such a challenging time of life.

Finally, thank you Rachel. Your support throughout the last six years made this thesis possible.

Chapter 1

Introduction

1.3 Introduction

The following body of work describes the development of methodologies, which aim at enhancing the analysis of proquinoidal compounds. Proquinoidal compounds, which are elaborated in greater detail in the following sections and in chapter 2, refer to any compound which can be oxidized to a corresponding quinoid or iminoquinoid. The oxidized form represents a highly reactive electrophilic species that is amenable to further reactions that eventually result in a product of enhanced analytical detectability. This introduction provides an overview and brief highlights of the rational for which analytes are examined in subsequent chapters along with the biological importance of those analytes. While numerous detection methods have been used for the detection of proquinoidal substances, the following body of work details current efforts in the refinement of usage of current reagents and the development of newer reagents for the derivatization of these substances, with fluorescence and mass spectrometry being targeted as the primary means of detection.

Analytes of Interest

Catechols, Catecholamines, and 5-Hydroxindoles

Catechols, catecholamines, and 5-hydroxyindoles are an important series of biological compounds which are related in both the way they are endogenously synthesized and in the bioregulatory roles they perform[1]. Perhaps the most extensively studied within these classes of compounds is dopamine[2], a catecholamine which affects the mood and appetite[3]. Regulation of dopamine levels within the brain also has implications for disease states such as schizophrenia and Parkinson's disease [4]. The well-established route for endogenously synthesized DA begins with tyrosine,

which is hydroxylated at the 3 position by tyrosine hydroxylase to form l-3,4-dihydroxyphenylalanine (L-DOPA)[5]. L-DOPA, itself a catecholamine, can then be decarboxylated by DOPA decarboxylase to dopamine[6]. Oxidation of dopamine by dopamine β-hydroxylase creates norepinephrine, a potent catecholamine which acts as a hormone for stress and memory[7]. NE can be further modified by phenylethanolamine metyltransferase to epinephrine, a similar hormone responsible for regulating heart rate and the fight-or-flight response[8].

Serotonin (5-HT) is another biogenic amine responsible for behavior and sleep[9]. Similar to how catecholamine synthesis begins with an amino acid, the series of biologically relevant 5-hydroxyindoles begins with tryptophan. Although most 5-HT synthesis occurs within the gut, synthesis in the brain begins within serotonergic neurons via hydroxylation of tryptophan at the 5 position by tryptophan hydroxylase creating 5-hydroxytryptophan (5-HTP) [10]. 5-HTP is subsequently acted upon by 5-HTP decarboxylase, producing 5-HT[11]. 5-HT can be metabolized through two distinct pathways. Arylalkylamine N-acetyltransferase can acetylate the primary amine on serotonin, producing N-acetyl-serotonin[12]. Monoamine oxidases are also capable of degrading 5-HT by oxidation of the primary amine to create 5-hydroxyindoleacetic acid (5-HIAA)[13].

Not only are these catechols, catecholamines, and 5-hydroxyindoles all biologically significant, they also share a high degree of structural similarity and fall into the description of proquinoidal substances. As these compounds share similar roles in bioregulation, they can all be found within a commonly analyzed compartment for neuroregulation, the cerebrospinal fluid [14]. Although this is not a comprehensive list of mood altering endogenous small molecules found within the brain, it should serve to highlight the degree of complexity one may encounter during analysis of relevant matrices. As such, comprehensive separation, proper identification, and accurate quantitative measurements are crucial for clinical evaluation of relevant disease states. These classes of proquinoidal compounds will be further elaborated upon along with their analysis in Chapter 2.

Protein Bound 3-Nitrotyrosine

Protein bound 3-nitrotyrosine (P3NY) is a post-translation modification (PTM) found to accumulate in several age related diseases. It is a highly studied modification due to its relative stability when compared to other oxidative modifications. Because of its relation to the aging process, there is a high degree of interest in the role it plays in several disease states from cancer to Alzheimer's[15].

Early investigations into formation of P3NY focused upon peroxynitrite as a source for protein oxidation. Extensive work has shown that inflammation of tissue corresponds to an increase in nitric oxide release which can react with superoxide to form peroxynitrite. Peroxynitrite itself can degrade to form a hydroxyl radical, a potent oxidant, and nitrogen dioxide. These two degradation products support the chemical rational for the oxidation of tyrosine to P3NY[16]. Peroxynitrite has been shown to readily oxidize tyrosine to P3NY *in vitro* and is used as a way to easily produce nitrated protein samples needed in the development of analytical methods[15]. Continued investigations have shown that there are multiple paths for the formation of P3NY, but peroxynitrite and its degradation products are thought to remain a prominent source for protein oxidation.

There is much debate regarding whether or not P3NY is a PTM of relevance or if it is just a consequence of other oxidative mechanisms within disease states[16]. Work done by MacMillan-Crow et. al. showed peroxynitrite exposure can result in nitration of Tyr34 in manganese superoxide dismutase (MnSOD)[17]. Tyr34 resides in the active site of MnSOD and nitration at this site results in complete inactivation of MnSOD. This loss of function shows a primary way in which P3NY can responsible for cellular damage and play a role in formation of disease states and has been heavily implicated as a cause for ALS. An additional PTM of interest is the nitration of Tyr74 in cytochrome c. Exposure to nitrating conditions has been shown to produce site directed nitration of cytochrome c[18]. Although cytochrome c

has been shown to exhibit weak activity as a peroxidase, after nitration of Tyr74, peroxidatic activity is shown to increase [19]. The consequence of this gain of function is still under investigation.

Historically, P3NY has been detected through western blot analysis by use of antibodies against P3NY. Such approaches suffer from lack of specificity of the antibodies which lead to lack of reproducibility. Additionally, cleanup prior to western blots are laborious and time intensive. Within the past decade, approaches for P3NY analysis have focused on reduction of P3NY to protein 3-aminotyrosine and subsequent derivatization. Initial approaches focused in the development of new derivatization reagents are described in Chapter 3. Continued elaboration of these approaches and utilization of newly developed derivatization reagents is described in Chapter 4.

1.3 Preferred Methods Analysis

High performance liquid chromatography (HPLC) is the preferred method of separation found within this body of work. A typical conventional HPLC is composed of a liquid pump, an autoinjector, a packed chromatography column, and can be connected to a wide range of detectors. Reverse phase chromatography is the most common separation format utilized in the following work. A conventional reverse phase column is typically a metal tube from five to 25 cm in length with a 4.6 mm inner diameter. The column is packed with a stationary solid-phase material composed of 2-10 µm particles whose chemical composition is commonly C18 chains bonded to a silica backbone. The analytical sample is introduced to the head of the column by the auto-injector, which transfers the sample of interest from a vial onto the column. Mobile phase is then pumped through the column. As analytes partition from the solid phase to the mobile phase, they move along the length of the column (when in the mobile phase) and begin to separate. This separation phenomenon is based on differences in the rate of partitioning which is governed by the analytes affinity, or selectivity, towards both the solid phase and

the mobile phase. After an analyte has eluted from the column, it can be detected by a variety of methods mentioned in subsequent paragraphs.

The historical precedence for HPLC has shown while it may never be the best method of separation for a single set of analytes, being typically inferior in plate counts to gas chromatography and capillary electrophoresis, it is a robust mode of separation for small molecules, peptides, and even proteins. The robustness of HPLC, along with its compatibility with most forms of detection, has made it a favored means of separation. The theoretical background of HPLC and advancement of the technology is explored further in the appendix chapter to this thesis.

HPLC coupled with electrochemical detection (ECD) has been widely used for detection of catechols. ECD works with HPLC by placing a pair of electrodes post column in the effluent and applying a potential across the electrodes. As molecules pass the electrodes they can be reduced at the cathode or oxidized at the anode, which makes this form of detection ideal for proquinoidal compounds. However, ECD can exhibit issues with selectivity, require long acquisition times, and require pmols of material due to poor sensitivity[20].

Recently, mass spectrometry has been utilized in the detection of proquinoidal compounds due to its high specificity and ever increasing sensitivity[21]. Mass spectrometers typically consist of an ionization source followed by a detector capable of separating gas phase ions. There are several different sources for both ionization and detectors for separation. The mass spectrometer utilized within this work was a quadrupole time of flight (QToF) hybrid mass spectrometer with an electrospray ionization (ESI) source.

Electrospray ionization is a soft ionization technique where the liquid flow from an HPLC is aerosolized by a non-reactive nebulizing carrier gas (typically nitrogen). This aerosol spray enters an electric field where the droplets deform until reaching its Raleigh limit. At this limit they explode producing subsequently smaller droplets[22]. Heat can be applied to assist in the evaporation of solvent

from the smaller droplets which results in the analyte taking on charge from the mobile phase forming a gas phase ion that is directed via electric fields towards the mass analyzer.

Quadrupole mass analyzers are composed of four cylindrical metal rods of equal dimensions arrayed parallel to each other. The rods act in two sets with a radio frequency voltage being applied to each set with a DC voltage applied over the RF voltage. These voltages direct gas phase ions down the center of the quadrupole and act as a mass filter.

A ToF mass analyzer is composed of two regions. In the first region, ions are allowed to collect on a microsecond time scale and then an electric potential is applied. The gas phase ions absorb kinetic energy which accelerates them into the field free region. The time required for analytes to reach the detector plate is determined by their mass as $E = mv^2$ where E is energy, m is mass, and v is velocity. As the ions are given the same energy, their mass determines the velocity with which they move through the field free region resulting in separation of different masses.

As access to highly sensitive mass spectrometers is not always guaranteed, a different means of detection of proquinoidal compounds is through derivatization to produce a fluorescent reporter molecule. This has been classically accomplished through use of ethylenediamine as a derivatization reagent[23]. This approach at detection later expanded to utilize diarylethylenediamines[24]. Such derivatizations were expanded as it was realized benzylamine can also produce a fluorescent product under oxidative conditions[25]. This derivatization scheme is favored for a variety of reasons. First, the necessary reagents are widely available at low cost when compared to other reagents used for fluorescence measurements. The derivatization only produces a fluorescent product when a catechol or 5-hydroxyindole is present, making for a highly selective reaction. Finally, the fluorescence profile exhibits excitation/emission spectra of 360/460 nm, which is outside a large portion of auto-fluorescence that occurs with relevant biological samples [26]. In addition to the highly sensitive and

selective nature of these favored fluorescent derivatization reactions, the products allow detection of femtomole (fmol) amounts of analyte or less [27].

1.4 Summary and Specific Aims

The goal of the present work was to enhance the analysis of biologically relevant proquinoidal compounds. The first series of these compounds found in Chapter 2 are catechols, catecholamines, and 5-hydroxyindoles. Work on those compounds aims to further elaborate upon previously established derivatization protocols using benzylamine (BA) and 1,2-dihydroxyphenylethylenediame (DPE) as derivatization reagents. This is accomplished through derivative product isolation, establishing reaction rate profiles, and comparing relative yields for both classes of reagents. With derivatization work from Chapter 2 as a foundation, Chapter 3 explores synthetic routes towards modification of BA and DPE. The goal of that work is to provide added functionality to aid in analysis of the other proquinoidal target: protein 3-nitrotyrosine. Finally, Chapter 4 utilizes the newly synthesized reagents and shows initial work featuring comparisons of those reagents.

[1] Y.-B. Wu, J.-H. Wu, Z.-G. Shi and Y.-Q. Feng, *Journal of Chromatography B* **2009**, *877*, 1847-1855.
[2] D. E. Vaillancourt, D. Schonfeld, Y. Kwak, N. I. Bohnen and R. Seidler, *Mov Disord* **2013**.
[3] E. Stice, S. Yokum, D. Zald and A. Dagher, *Curr Top Behav Neurosci* **2011**, *6*, 81-93.
[4] a) A. A. Macdonald, K. N. Seergobin, A. M. Owen, R. Tamjeedi, O. Monchi, H. Ganjavi and P. A. Macdonald, *PLoS One* **2013**, *8*, e74044; b) K. E. Furth, S. Mastwal, K. H. Wang, A. Buonanno and D. Vullhorst, *Front Cell Neurosci* **2013**, *7*, 102.
[5] J. D. Elsworth and R. H. Roth, *Experimental Neurology* **1997**, *144*, 4-9.
[6] H. Ueno, T. Iwata, N. Koshiba, D. Takahashi and K. Toshima, *Chem Commun (Camb)* **2013**, *49*, 10403-10405.
[7] D. F. Manvich, L. Depoy and D. Weinshenker, *J Pharmacol Exp Ther* **2013**.
[8] Q. Wu and M. J. McLeish, *Arch Biochem Biophys* **2013**, *539*, 1-8.
[9] M. Some and A. Helander, *Life Sciences* **2002**, *71*, 2341-2349.
[10] J. D. Fernstrom and R. J. Wurtman, *Science* **1971**, *173*, 149-152.
[11] K. Ponicke, U. Gergs, I. B. Buchwalow, S. Hauptmann and J. Neumann, *Mol Cell Biochem* **2012**, *365*, 301-312.
[12] M. Barbera, B. Mengual, J. M. Collantes-Alegre, T. Cortes, A. Gonzalez and D. Martinez-Torres, *Insect Mol Biol* **2013**.
[13] a) A. M. Cesura and A. Pletscher, *Prog Drug Res* **1992**, *38*, 171-297; b) M. B. Youdim, D. Edmondson and K. F. Tipton, *Nat Rev Neurosci* **2006**, *7*, 295-309; c) R. B. Silverman, X. Lu, G. D. Blomquist, C. Z. Ding and S. Yang, *Bioorg Med Chem* **1997**, *5*, 297-304.
[14] a) T. Suominen, P. Uutela, R. A. Ketola, J. Bergquist, L. Hillered, M. Finel, H. Zhang, A. Laakso and R. Kostiainen, *PLoS One* **2013**, *8*, e68007; b) E. Legangneux, J. J. Mora, O. Spreux-Varoquaux, I. Thorin, M. Herrou, G. Alvado and C. Gomeni, *Rheumatology (Oxford)* **2001**, *40*, 290-296.
[15] P. Pacher, J. S. Beckman and L. Liaudet, *Physiol Rev* **2007**, *87*, 315-424.
[16] J. M. Souza, G. Peluffo and R. Radi, *Free Radic Biol Med* **2008**, *45*, 357-366.
[17] L. A. MacMillan-Crow, J. P. Crow and J. A. Thompson, *Biochemistry* **1998**, *37*, 1613-1622.
[18] J. M. Souza, L. Castro, A. M. Cassina, C. Batthyany and R. Radi, *Methods Enzymol* **2008**, *441*, 197-215.
[19] L. C. Godoy, C. Munoz-Pinedo, L. Castro, S. Cardaci, C. M. Schonhoff, M. King, V. Tortora, M. Marin, Q. Miao, J. F. Jiang, A. Kapralov, R. Jemmerson, G. G. Silkstone, J. N. Patel, J. E. Evans, M. T. Wilson, D. R. Green, V. E. Kagan, R. Radi and J. B. Mannick, *Proc Natl Acad Sci U S A* **2009**, *106*, 2653-2658.
[20] a) G. M. Cao and T. Hoshino, *Chromatographia* **1998**, *47*, 396-400; b) J. Cummings, L. M. Matheson and J. F. Smyth, *J Chromatogr* **1990**, *528*, 43-53.
[21] Z. D. Peterson, D. C. Collins, C. R. Bowerbank, M. L. Lee and S. W. Graves, *Journal of Chromatography B* **2002**, *776*, 221-229.
[22] D. C. Taflin, T. L. Ward and E. J. Davis, *Langmuir* **1989**, *5*, 376-384.
[23] a) H. Weil-Malherbe and A. D. Bone, *Biochem J* **1952**, *51*, 311-318; b) J. Harley-Mason and A. H. Laird, *Tetrahedron* **1959**, *7*, 70-76.
[24] Y. Umegae, H. Nohta, M. Lee and Y. Ohkura, *Chem Pharm Bull (Tokyo)* **1990**, *38*, 2293-2295.
[25] H. Nohta, M.-K. Lee and Y. Ohkura, *Analytica Chimica Acta* **1992**, *267*, 137-139.

[26] a) M. Fritzsche and C. F. Mandenius, *Anal Bioanal Chem* **2010**, *398*, 181-191; b) M. Monici in *Cell and tissue autofluorescence research and diagnostic applications*, *Vol. Volume 11* (Ed. M. R. El-Gewely), Elsevier, **2005**, pp. 227-256.
[27] T. Yoshitake, J. Kehr, K. Todoroki, H. Nohta and M. Yamaguchi, *Biomed Chromatogr* **2006**, *20*, 267-281.

Chapter 2

The Derivatization of Proquinoidal Analytes with 1,2-Diphenylethane-1,2-Diamine (DPE) and Benzylamine (BA): An Investigation of Products, Yields, Kinetics and Reagent Selectivity

The Following work has been submitted for publication to Chromatographia

2.1 Introduction

In the present investigation, the term proquinoidal analytes refers any of a group of substances that possess structural moieties allowing for their facile conversion to reactive quinoidal or iminoquinoidal products in the presence of mild oxidizing agents. Substances such as 2-hydroxyphenols [1], 2-aminophenols [2-4] and 5-hydroxyindoles [1] that may possess a variety of substituents (e.g., alkyl, amino-alkyl, carboxy-alkyl) at different positions fulfill these requirements. **Figure 2-1** illustrates structures and initial oxidation products for model analytes (**1a, 1b, 5**) and the biologically relevant substance, epinephrine (**3**), which exhibit this property.

From a broader perspective, substances of biological interest with this feature include the catecholamines (CAs), catechols (Cs), 5-hydroxyindoleamines (5-HIs) [1], and post-translational modifications (PTMs) of protein tyrosine residues, such as protein-DOPA (P-DOPA) [5] and protein 3-nitrotyrosine (P-3NY) [6], which becomes proquinoidal upon reduction to the protein-3-aminotyrosine (P-3AY) [2]. A non-exhaustive list of examples for the first three groups include; the CAs epinephrine (E), norepinephrine (NE) and dopamine (DA); the Cs, 3,4-dihydroxyphenylacetic acid (DOPAC), 3,4-dihydroxymandelic acid (DOMA) and 3,4-dihydroxyphenylethyleneglycol (DOPEG); and the 5-HIs, serotonin (5-hydroxytryptamine, 5-HT), 5-hydroxytryptophan (5-HTP) and 5-hydroxyindoleacetic acid (5-HIAA), with P-DOPA and reduced P-3NY (P-3AY) representing the last category. Each of the substances arises from biosynthetic modification of the two amino acids, tyrosine [7] and tryptophan [8]. CAs and 5-HIs represent substances serving as neurotransmitters that are important in various CNS functions [7-10], while in contrast the Cs arise from deamination of CAs, and are of interest in various disease states [11-13]. P-3NY is a stable post-translational modification (PTM) of protein tyrosine residues, which is

formed as a result of exposure to reactive nitrogen species (RNS) and thus serves as a biomarker of oxidative stress [6].

Due to the involvement of CAs, Cs and 5HIs in a myriad of biologically important activities, there has been a long-standing and continuing interest in the development of methodologies for their sensitive and selective determination in biological tissues and fluids. Because of their inherent ease of oxidation (pro-quinoidal nature), liquid chromatography with electrochemical detection (LCEC) has been established for the determination of these analyte classes since the 1980s. In a recent publication, Yamaguchi provides an overview that summarizes attributes and limitations of the emergence and continued advances in LCEC for their determination [1]. Over the same timeframe, and continuing for the next two-decades, the Ohkura and Yamaguchi groups, described the fluorogenic derivatization of various CAs and Cs with diphenylethylenediamine (DPE) [1,14] and 5-HIs [1,15], with benzylamine, respectively (BA). Each derivatization reaction is initiated by an oxidation step to form a reactive quinoidal intermediate (**Figure 2-1: 2,4,6**) followed by reaction with the fluorogenic reagents in a series of steps, in each case culminating in the formation of a fluorescent 2-phenylbenzoxazole (PBO) moiety within the overall product structure (**Figure 2-2: 7a,7b,8,9**) [15,16].

During the development of these derivatization reactions, the researchers reported structures of the fluorescent products, initially for 5-HIs with BA [15] (**Figure 2-2: 9**) and subsequently for CAs with DPE [16] (**Figure 2-2: 8**). With respect to 5-HIs derivatized with BA, the product structure was based on prior reports of substances possessing analogous structural features [17,18], while the structure of product (**8**), resulting from derivatization of the epinephrine (**3**) with DPE, was elucidated via isolation and characterization by MS and NMR techniques [16]. Similar products would be expected from the derivatization of all 3,4-dihydroxyphenylethylamines (**Figure 2-2: 8**). In a prior publication it was noted that when various CAs and Cs were derivatized with DPE, the fluorescent products all exhibited similar excitation (~350 nm) and emission (~480 nm) spectra [14]. However, the specific structure of products

resulting from DPE or BA derivatization of Cs was not reported. Due to our interest in developing methodology for the aforementioned PTMs of protein tyrosine, there was a need to elucidate the product resulting from derivatization of Cs with BA and/or DPE. Using 4-methylcatechol (4MC; **1a**) as a model of P-DOPA and 2-aminocresol (2AC; **1b**) as a model for reduced P-3NY (P-3AY), previously we have reported that derivatization of 4MC (**1a**) or 2AC (**1b**) with BA leads to the formation of the 6-benzylamino-2-phenylbenzoxazole (BAPBO) [2] (**Figure 2-2: 7a**). Subsequently, in unpublished research we found that derivatization of 4MC (**1a**) with DPE resulted in the 6-amino-2-phenylbenzoxazole (APBA) (**Figure 2-2: 7b)**. The details of this reaction will be reported herein.

The determination of these analyte classes with these regents has been a continually evolving process. As previously noted BA was initially used for the derivatization of 5-HIs, but in a following publication Yamaguchi et al. report the simultaneous determination of serotonin and norepinephrine via pre-column derivatization with BA [19]. This approach follows a previous report where it was established that BA (and various substituted analogs) undergoes reaction with CAs to apparently form the same products as those obtained from DPE [20]. More recently Yamaguchi and co-workers have developed a two-step reagent addition sequence for derivatization of samples containing each analyte class [21]. The methodology was based on an initial rapid derivatization of 5-HIs with BA (2 minutes at room temperature), followed by derivatization of the CAs and Cs by addition of DPE and the "accelerator" glycine (gly) [14] using a higher reaction temperature (20 minutes at 50 °C). Interestingly, it was asserted that 5-HIs have low or no reactivity towards DPE and that CAs and Cs have low or no reactivity towards BA, thus enabling the described selective derivatization of these analytes with different reagents; however, the selective reactivity claims seem to be in contrast to the BA based method previously noted. Upon close scrutiny, the claims of reagent-analyte reactivity selectivity would appear to be questionable. For example, in the first step the transformation of 5HIs by BA is clearly rapid; however, it is not obvious that DPE is unreactive with the quinoid intermediate formed from 5-

HIs. Further, upon execution, of the second step by the addition of DPE/gly there will be substantial quantities of BA remaining to react with the CAs and Cs. In the case of CAs, whether DPE or BA mediates the formation of the fluorescent benzoxazole is irrelevant, with the same product being formed in either case. With regard to Cs, previously we have observed that reaction with BA leads to formation of BAPBO (**Figure 2-2: 7a**) derivatives [2] and, with data to be presented herein, that APBA (**Figure 2-2: 7b**) products are formed from reaction with DPE. Thus in the two-step protocol the potential arises for the formation of two products from Cs when both BA and DPE are present as reagents. From a chemical standpoint one may question the claim that 5-HIs exhibit low or no reactivity towards DPE. Since reaction of DPE with quinoidal intermediates arising from CAs (**Figure 2-1: 4**) and Cs (**Figure 2-1: 2**) leads to the formation of substituted PBO derivatives (**Figure 2-2: 8** and **7b**), it would seem plausible that as BA reacts with 5-HI derived quinoid substances (**Figure 2-1: 6**) to form PBO derivatives (**Figure 2-2: 9)**, a similar result would be obtained from reaction of the quinoid with DPE (**Figure 2-1: 6**). In this regard, we have observed that reaction of BA or DPE with 5-HIs and certain other ortho-quinones results in the formation products analogous to **9 (Figure 2-2)**.

One additional aspect of basic chemical interest is the use of gly as an "accelerator" in the DPE derivatization of CAs and Cs. Past publications describe the preparation of the DPE reagent as a solution being composed of gly and DPE, the gly component being present at equivalent or higher concentrations with respect to the DPE. Typical derivatization protocols result in DPE (and gly) being present in molar excess of 10^5-10^6 as compared to the analytes. With the reaction being conducted at high pH values, typically pH 10, a large fraction of the gly will be present as the nucleophilic species (free amine), and with respect to the quinoidal species arising from Cs or 5-HIs (**Figure 2-1: 2** and **6**) there is the potential for the interception of such intermediates by nucleophilic gly, thus creating an alternate non-productive reaction pathway leading to an overall diminished yield of the desired fluorescent product.

In the preceding paragraphs, many aspects of DPE and BA mediated fluorogenic derivatization of proquinoidal analytes of biological interest (5-HIs, CAs, Cs) were presented. Further it was pointed out that reduced P-3NY (P-3AY) substances, due to their proquinoidal nature would exhibit much of the same chemistry, thus the model substances 4MC (**Figure 2-1: 1a**) and 2AC (**Figure 2-1: 1b**) would be expected to possess similar chemical reactivity and undergo similar reaction pathways with either of the noted reagents. However, there are details of these reactions that have not been explored in the past or perhaps could be further clarified. Many of these aspects will be addressed presently using several substances where the products of the reactions are probed by mass spectrometry, and in other cases using various substances as models (**Figure 2-1: 1a, 3,5**) for 5-HIs, CAs and Cs. As noted previously, presently we will report the product of DPE with the model 5-HI **5 (Figure 2-1)** and the model catechol **1a (Figure 2-1)** and we have prepared the products **7a**, **7b**, **8** and **9 (Figure 2-2)** thus enabling derivatization reaction yield determinations. In the present investigation, the derivatization kinetics of these reactions are explored, including the role played by the "accelerator" gly in DPE derivatizations, which we expect to be of particular interest in the derivatization of Cs where the internal nucleophile (β-amino-alkyl substituent of the CAs) is absent in the Cs family of analytes. Finally, we will report results obtained from the derivatization of 4MC conducted with BA, DPE and gly, present in various combinations.

2.2 Experimental

2.2.1 Reagents and Solvents

Benzylamine (BA), meso-1,2-diphenylethylenediamine (DPE), 4-methylcatechol (4MC), 5-benzyloxyindole-2-carboxylic acid ethyl ester, palladium on carbon (Pd/C), N-cyclohexyl-3-

aminopropanesulfonic acid (CAPS), formic acid (FA), 2-amino-p-cresol (2AC), ammonium bicarbonate, and potassium hexacyanoferrate ($K_3Fe(CN)_6$) were obtained from Sigma-Aldrich (St. Louis, MO, USA) and were used as received. Methanol (MeOH), hexanes (Hx), methylene chloride (CH_2Cl_2), acetone ($(CH_3)_2CO$), tetrahydrofuran (THF), and ethyl acetate (EtOAc) were all HPLC grade and purchased from Fisher Scientific (Pittsburgh, PA, USA). Purified water was obtained from a Labconco Water ProPS Filtration Apparatus (Labconco Corporation, Kansas City, MO, USA).

2.2.2 Mass Spectrometry and NMR

The University of Kansas Mass Spectrometry & Analytical Proteomics Laboratory preformed high-resolution molecular mass determinations using a Q-Tof-2™ mass spectrometer (MicroMass Ltd., Manchester UK) equipped with an electrospray ion source. HPLC-F-MS determinations utilized for product screening were conducted with the following system: a Waters Associates Alliance 2690 chromatograph, Shimadzu RF-535 fluorescence detector and a MicroMass QuattroMirco™ mass spectrometer. NMR spectra were acquired used a Bruker Avance DPX 400 instrument and Bruker 500 MHz instrument equipped with a dual carbon/proton cryoprobe.

2.2.3 HPLC-Fluorescence Detection (HPLC-F)

General Aspects. All kinetic and yield data was collected on a Shimadzu LC-10 series HPLC consisting of an SLC-10A vp system controller, two LC-10AD vp pumps, and SIL-10AD vp auto-injector and a RXL-10A xl fluorescence detector set at 360 nm excitation and 460 nm emission. Separations were performed with a Phenomenex® HPLC column (4.6 mm x 150 mm; ODS-3 particles, dp 5µm, pore 100 Å). Mobile phase A (MP-A) (consisted of 0.1% FA in 90:10 H_2O:MeOH and mobile phase B (MP-B)

consisted of 0.1% FA in 10:90 H_2O:MeOH. Unless otherwise noted, 20 µL injection volumes were throughout with a 1.0 mL/min flow rate.

Chromatographic Details. Protocol 1: For the 4MC/DPE(**1a→7b**) derivatization, isocratic chromatography was conducted using 30:70 MP-A:MP-B. *Protocol 2:* All other kinetic and yield investigations (**1a→7a; 3→8**; **5b→9b**) used an isocratic separation with 100% mobile phase B. *Protocol 3*: For the investigation of reactions containing a mixture of products, starting conditions used 30:70 MP-A:MP-B, followed by a linear gradient to 100% MP-B over 5 minutes, a 5 minute hold, then a return to the initial conditions with a 5 minute re-equilibration time prior to the next injection. *Yield Determinations*. For yield investigations, peak areas of the peaks of interest resulting were compared against single point calibrations of the previously synthesized reference substances for determination of required reaction times and resulting yields.

2.2.4 Synthesis of Derivatization Products - General Aspects

The derivatization products (**7a**, **7b**, **8**, and **9**) that were used in the yield investigations were prepared according to the procedures described in the following paragraphs. In each case the products were purified by preparative chromatography, and provided the expected results for ^{1}H NMR and high resolution mass spectrometry (HRMS). Only the E (**8**) reference substance was not subjected to HRMS as it was similar in all respects a previously reported preparation [16]. Each preparation provided a single peak, which co-eluted with the *in situ* generated derivatization product, when examined by HPLC with fluorescence detection.

*Synthesis of the 4MC/BA Reaction Product (**7a**).* The 4MC/BA reaction product was synthesized according to a previously published procedure [2]. To a 500 mL RBF, a solution of 2.0 g of 4-MC dissolved in 125 mL of MeOH was added to 125 mL of purified H_2O. Solid $K_3Fe(CN)_6$ (5.0 g) was slowly added to the

solution, following by addition of BA (25 mL) over 1 hr. After stirring for 3 hrs, MC (200 mL) was added to the dark brown reaction mixture and stirring continued an additional 0.5 hr. Subsequently, the reaction was filtered, the organic phase recovered and washed 5x with equal volumes of H_2O, recovered and dried with $Mg(SO_4)_2$, and concentrated *in vacuo* (~10 mL). Product isolation was accomplished by low-pressure preparative chromatography (25mm x 200 mm glass column) on silica gel (200-440 mesh, 60 Å), utilizing a mobile phase composed of EtOAc:Hx (2:8). The desired fraction, visualized on-column by exposure to the long wavelength of a hand-held UV lamp (Model UVGL-25; UVP, Upland, CA), was collected, and the solvent evaporated under reduced pressure to provide a solid, which after recrystallization from $CH_3)_2CO/H_2O$ and drying (80 °C for 4 hrs in vacuo) resulted in yellow crystals, m.p. 143 °C (uncorrected). ^{1}H NMR ($(CD_3)_2CO$)) δ 7.1 (2H, m), 7.5(3H, m), 7.4 (5H, m), 7.25 (1H, t, J = 7.3), 6.65 (1H, s), 4.5 (2H, s), 2.35 (3H, s) (spectra available in supplementary information); MS (ESI) m/z calc. for $C_{21}H_{19}N_2O$ $[M+H]^+$: 315.1497, found: 315.1501.

*Synthesis of the 4MC/DPE Reaction Product **(7b**.* To a solution of **7a** (0.5 g) in THF (20 mL) contained in a 100 mL RBF was added Pd/C (50 mg), the headspace purged with hydrogen, and the flask fitted with hydrogen filled balloon. The resulting suspension was magnetically stirred for 24 hours, followed by filtration through a Celite pad, the solvent removed *in vacuo* to provide a solid, which was taken up in EtOAc and purified by low-pressure preparative chromatography (25mm x 200 mm glass column) on silica gel (200-440 mesh, 60 Å), utilizing a mobile phase composed of EtOAc:Hx (25:75). The product containing fraction was isolated and the solvent removed in vacuo to provide solid 7b, 218 °C (uncorrected). ^{1}H NMR (DMSO) δ 8.1 (2H, m), 7.55 (3H, tdd), 7.35 (1H, s), 6.9 (1H, s), 5.1 (2H, s), 2.2 (3H, s) (spectra available in supplementary information); MS (ESI) m/z calc. for $C_{14}H_{13}N_2O$ $[M+H]^+$ 225.1028, found: 225.1008.

*Synthesis of E/BA Product (**8**).* To a stirred solution of epinephrine (1.65 g), prepared by dissolution in equal parts of MeOH:H_2O (650 mL), was added BA (10 mL) and solid $K_3Fe(CN)_6$ (5.92 g),

followed by additional BA (10 mL). The reaction was continued for 4 hrs, after which time the MeOH was removed *in vacuo* and the remaining aqueous reaction mixture extracted 3x with 100 mL aliquots of CH_2Cl_2. The combined extracts were dried with anhydrous $Mg(SO_4)_2$, the filtered to provide a dark solution, which was initially fractionated by low-pressure preparative chromatography (25mm x 600 mm glass column) on silica gel (200-440 mesh, 60 Å), utilizing a mobile phase composed of ACN. The long wavelength fluorescent band, visualized on-column by exposure to the long wavelength of a hand-held UV lamp (Model UVGL-25; UVP, Upland, CA), was collected, and the solvent evaporated to yield a dark liquid, which was re-fractionated using a mobile phase of CH_2Cl_2:ACN (3:1). The fluorescent band was collected and the solvent evaporated *in vacuo* to provide a brownish solid product **8** that requiring further purification by preparative HPLC. Preparative HPLC was conducted using a Phenomenex™ Luna 10µ-PREP C18(2) column (250 x 21.2 mm) using the following chromatographic conditions and parameters: MP-A 0.1% FA in H_2O, MP-B 0.1% FA in MeOH; flow rate 4.0 mL/min. Approximately 20 mg of solid was dissolved in 5 mL of MeOH and 50 µL injected per chromatographic run with was conducted according to the following program: time zero, 100% MP-A followed by a linear ramp to 100% MP-B over 10 min and hold for 4 min, then return to the 100% MP-A and hold for 5 min. The desired peak was collected form each run (30 total), combined, the solvent evaporated to leave **8.** ^{1}H NMR ($CDCl_3$) δ 8.2 (2H, m), 7.6 (1H, s), 7.5 (3H, m), 6.6 (1H, s), 5.3 (1H, dd), 4.5 (1H, dd,), 3.5 (2H, m), 2.8 (3H, s), which is in agreement with the previously reported spectra [16].

*Synthesis of 5-hydroxyindole-2-carboxylic acid ethyl ester (5HI-2-CAE) (**9b**).* To a THF solution (50 mL) of 5-benzyloxyindole-2-carboxylic acid ethyl ester (5.0 g) contained in a 250 mL RBF was added Pd/C (0.5 g). The flask was purged with hydrogen and fitted with hydrogen filled balloon. The suspension was magnetically stirred for 24 hrs, filtered through a thin pad of Celite. Addition of H_2O (200 mL) resulted in formation tan colored needles, which were dried *in vacuo* at 80 °C to provide the intermediate 5-hydroxyindole-2-carboxylic acid ethyl ester, which was used without further purification. [Analytical

data: ^{1}H NMR δ 11.6 (1H, s), 9.05 (1H, s), 7.25 (1H, d, 8.8 Hz), 6.95 (2H, m), 6.8 (1H, dd, J = 8.5 Hz, J = 2.35 Hz), 4.1 (2H, q, J = 7.15 Hz), 1.35 (3H, t, J = 7.1 Hz); MS (ESI) m/z calc. for $C_{11}H_{10}NO_3$ $[M+H]^+$: 204.0661, found: 204.0645]. To a solution of this intermediate (0.75 g), prepared in THF (75 mL) and MeOH (50 mL), contained in a 500 mL RBF, was added an aqueous solution (150 mL) of $K_3Fe(CN)_6$ (8.0 g), followed by addition of a BA solution (5 mL dissolved in 75 mL of THF) over 1.5 hrs, with stirring continuing for 1 hr. Subsequently the reaction solution was extracted with EtOAc (200 mL), the organic layer recovered and washed an additional 2x with an equal volume of H_2O, followed by *in vacuo* concentration to approximately 10 mL, which was subjected to low-pressure preparative chromatography (30 mm x 600 mm glass column) on silica gel (200-440 mesh, 60 Å), utilizing a mobile phase composed of EtOAc:Hx (10:90). The desired fraction was collected and evaporated to provide **9b** as a solid product. ^{1}H NMR (DMSO) δ 9.2 (1H, s), 8.35 (2H, m), 7.75 (1H, dd, J = 2.15 Hz, J = 0.95 Hz), 7.65 (1H, d, J = 8.85 Hz), 7.55 (3H, m), 7.45 (1H, dd, J = 9.0 Hz, J = 1.0 Hz), 4.45 (2H, q, J = 4.60 Hz), 1.5 (3H, t, 7.15 Hz) (spectra available in supplementary information; MS (ESI) m/z calc. for $C_{18}H_{15}N_2O_3$ $[M+H]^+$: 307.1083, found: 307.1072.

2.2.5 Derivatization for Kinetic and Yield Determinations

A diluent buffer solution consisting of 50% CAPS (0.3 M, pH 10.0) and 50% MeOH, was used for all dilutions, being discarded after one week. For ammonia incubation studies, a NH_4HCO_3 (0.1 M, pH 8.1) buffer was substituted for the CAPS buffer in the diluent solution. Stock solutions (1.0 mM) of the synthesized products (**7a**, **7b**, **8** and **9b**) were prepared in MeOH and stored at 4 °C, then diluted 100 nM with MeOH immediately prior to injection. Analyte stock solutions (1.0 mM) of **1a**, **3** and **5b** were prepared in methanol, stored at 4 °C, and diluted to 1 µM with MeOH:H_2O (1:1) to prior to derivatization. Stock solutions of the derivatization reagents BA (0.3M) and DPE (0.3M) were prepared

daily in the diluent buffer solution. Stock solutions of $K_3Fe(CN)_6$ (10 mM) and gly (0.3M) were prepared in the diluent buffer solution and used within 24 hours. Derivatizations were conducted by adding the following solutions to a 1.7 mL auto-sampler vial in the following order: 700 µL diluent buffer; 100 µL analyte; 100 µL $K_3Fe(CN)_6$, and 100 µL of derivatization reagent. This resulted in reaction concentrations of 100 nM analyte, 1mM $K_3Fe(CN)_6$, and 30 mM derivatization reagent. For derivatizations containing glycine, the following solutions were added to a 1.7 mL auto-sampler vial in the following order: 600 µL of diluent buffer, 100 µL of analyte, 100 µL of $K_3Fe(CN)_6$, and 200 µL of gly:DPE (1:1). This provided for reaction concentrations of 100 nM analyte, 1 mM $K_3Fe(CN)_6$, 30 mM glycine and 30 mM DPE. The same procedure was used for investigation of the ammonia loading experiments with the exception being that NH_4HCO_3 buffer was substituted for the CAPS buffer and the analyte solution containing $K_3Fe(CN)_6$ was incubated at room temperature for 0, 1, 2, and 4 hours prior to addition of BA. In all experiments, after the completion of all reaction components (and during incubation periods) the vials were sealed, vortex mixed for 5 seconds, and then loaded into the autosampler at room temperature. Injections (20 µL) were made every 10 minutes.

2.2.6 Derivatization of 4MC Exploring Reagent Selectivity and Gly Effect

The results of these experiments are shown in **Figure 2-16A-B**, with the details of each derivatization as follows. **Figure 2-16A**, the derivatization of 4MC (**1a**) with BA (~100-200 nM final concentration) was conducted as described in the previous section. **Figure 2-16B**, the derivatization of 4MC (**1a**) with DPE was conducted according to the standard protocol, except 100 µL of **7a**, (4MC-BA product), was substituted for 100 µL of the diluent buffer solution. **Figure 2-16C**, 4MC (**1a**) was derivatized with BA and DPE, with 100ul of the diluent buffer being substituted by 100 µL of the additional reagent solution. **Figure 2-16D**, 4MC (**1a**) was derivatized with BA per the standard protocol,

with the diluent buffer being 600 µL, and as described in the previous section 200 µL of gly:DPE solution utilized in order to examine the effect of each reagent in the presence of gly. In all cases the total reaction volume was 1.7 mL and the reaction conducted for 1.5 hours at ambient temperature prior to determination by HPLC-F *protocol 3* (described in a previous section) using 40 µL injections.

2.3 Results and Discussion

2.3.1 Products from Derivatization of 5-HIs with BA and DPE

BA has been reported as a fluorogenic reagent for 5-HIs in the early 1990s [15], with the structure of the product based on the previously known transformation (oxidative conditions followed by reaction with BA) of 1,4-dimethyl-6-hydroxycarbozole [17,18], a substance possessing the 5-hydroxyindole moiety within the overall structure. The reaction sequence is based on the transformation of analyte **5** (**Figure 2-1**) through the quinoid intermediate **6** (**Figure 2-3**) to the PBO **9** (**Figure 2-3)**. Presently, this reaction has been investigated using 5-hydroxyindole and 5-hydroxyindole-2-carboxlic ethyl ester (5-HI-2-CAE) as model analytes. For 5-hydroxyindole, the derivatization reaction was conducted using BA or DPE, with the products subjected to LC-FL-MS analysis. For each reagent, the fluorescent products (**Figure 2-2: 9a and 9b**) co-eluted chromatographically, exhibited the same fluorescence properties (excitation and emission maximum of 375 nm and 475 nm) and the same mass spectrum, $[M+H]^+$ m/z = 235 [22]. Product **9a** was found to be unstable when attempts to isolate preparative quantities were undertaken (likely due to oxidation with positions 2 and 3 being unsubstituted) [22]. To avoid this liability, the reference standard sought was prepared from reaction of 5-hydroxyindole-2-carboxylic acid ethyl ester (**Figure 2-1: 5b**) with BA resulting in product **9b** (**Figure 2-2**). LC-MS characterization of the **9b** provided the expected mass spectrum; $[M+H]^+$ m/z = 307 [22]. As

in the previous case, when analytical scale derivatizations of **5b** (**Figure 2-1**) were conducted with either BA or DPE identical products were produced. These overall chemical pathways are summarized in **Figure 2-2**, with the proposed detailed reaction pathway for PBO formation shown in **Figure 2-5**. Aspects regarding the mechanism, kinetics and yield of these reactions, for each reagent, will be presented in a following section.

2.3.2 Products from Derivatization of CAs with BA and DPE

The fluorescent product resulting from the derivatization of the catecholamine epinephrine (**Figure 2-2, 8**) was isolated and characterized by NMR and MS a number of years ago [16]. Prior publications have described the use of both reagents, DPE [23] and BA [19], for the derivatization of various catecholamines, with apparently the same fluorescent product being obtained from the use of either reagent and in all cases the fluorescent spectra and chromatographic properties support this conclusion. Presently the derivatization of **8** (**Figure 2-2**) was conducted on the analytical scale using BA and DPE, and product formed from each reagent co-eluted chromatographically, displayed identical fluorescence properties (excitation and emission maximum of 360 nm and 460 nm, respectively), and exhibited identical mass spectra, $[M+H]^+$ m/z = 267 (data not shown). In order to obtain a reference standard, the derivatization was conducted on the preparative scale using a slight modification of the previously published procedure (details are provided in the experimental section), with the major difference being the use of BA instead of DPE. The product (**Figure 2-2, 8**) was isolated, purified and found to exhibit identical chromatographic properties as the derivative formed from either reagent on the analytical scale. A proposed product formation mechanism is shown in **Figure 2-9**. Kinetic, yield and mechanistic aspects for this product and CAs in general will be discussed in a following section.

2.3.3 Products from Derivatization of Cs with BA and DPE

In a previous publication from these laboratories [2], the product arising from BA derivatization of Cs such as 4MC (**Figure 2-1: 1a**) and the o-aminophenol 2AC (**Figure 2-1: 1b**) was reported and is depicted by structure **7a** (**Figure 2-2**). At the onset of this prior research, it was not immediately obvious that this derivatization reaction would result a 6-amino substituted PBO (**Figure 2-2: 7a**); however, in prior reports [14] and confirmed in our past investigation, it was noted the product formed exhibited fluorescent characteristics similar to those observed with the CA derivatives. While similar fluorescent properties were noted for the derivatization of 4MC with DPE, a detailed examination of the product formed via use of DPE was not reported. In order to probe the structures of the products formed, 3,4-dihydroxycinnamic acid (DHCA) and 4MC were derivatized with BA and DPE and the reaction solutions examined by LCMS [22]. The product formed from BA derivatization of DHCA exhibited a mass spectrum of $[M+H]^+$ m/z = 371 and for 4MC derivatized with BA $[M+H]^+$ m/z = 315 (previously reported)[2], which is consistent with the **7a** type general structure presented in **Figure 2-2** with R_1: $CH=CHCO_2H$ and CH_3, respectively. In the case of DPE, DHCA exhibited a mass spectrum of $[M+H]^+$ m/z = 281 and for 4MC $[M+H]^+$ m/z = 225. In each case, the DPE derived product was found to have a -90 Da MW shift as compared to the BA product. As noted in our earlier investigation, the presence of a 6-amino substituent on the PBO structure is necessary to provide for the observed fluorescence characteristics, thus suggestive of a product bearing a 6-amino substituent for the DPE based products as compared to the 6-benzylamino substituent, which has been previously established for the BA based products, with this structural difference being illustrated by **7b** versus **7a** in **Figure 2-2**. While this conclusion is clearly supported by the fluorescence and MS data [22], further proof was sought by the independent synthesis of the **7b** type derivative for 4MC. In general, we have found that the preparative scale synthesis of various PBO derivatives from reaction of the requisite catechol with DPE prove problematic due the

formation of a multiple unknown substances along with the desired product. As a result **7b** was prepared from the known **7a** via catalytic reduction to remove the N-benzyl substituent (details for the preparation of each compound are described in the experimental section). This product was found to provide identical chromatographic, fluorescence and mass spectral properties to the analytical scale derivatization product previously noted and was used as a reference standard in the characterization of the yield and kinetic studies of this reaction. Clearly DPE is serving as an amine donating agent in the derivatization of Cs. The mechanistic aspects of this role will be discussed in a following section.

2.3.4 Rate, Yield, and Mechanism for 5-HICAE derivatization with BA and DPE

The next aspect of this investigation was the characterization of the derivatization kinetics and yield of the model 5-HICAE (**Figure 2-1: 5b**). The model selected was based on considerations of perceived product stability and accessibility of the synthetic route. As compared to serotonin and other 5-HIs, 5-HICAE possesses a 2-carboxyethyl substituent rather than a 3-alkyl substituent on the indole ring system, which was perceived to not substantially bias the derivatization kinetics as substances substituted in either position should readily undergo oxidation to the reactive quinoid intermediate. The reaction was conducted at ambient temperature in an autosampler vial and periodically analyzed by HPLC-F until completion of the reaction as evidenced by an unchanging maximal product peak area. The concentrations of reactants were as follows: 5-HICAE, 100 nM; $K_3Fe(CN)_6$, 0.1 µM; BA or DPE, 30 mM, which resulted in a relative ratio of 1:10:300,000 analyte to oxidant to reagent, respectively. Chromatograms illustrating the time course for derivatization of 5-HICAE with BA are shown in **Figure 2-3**. Time course plots of data obtained from 5-HICAE derivatization with three differing reagent systems (BA, DPE or DPE plus gly) are shown in **Figure 2-4,** with a summary of these data presented in **Table 1**. Interestingly, product yield was observed to be ~ 35% irrespective of which reagent was used or if gly

was present with DPE. However, the reaction was complete within 20 minutes with BA, as compared to 50 minutes with DPE. As noted earlier, DPE does form the same product as BA in the derivatization of 5-HIs and the present results contradict the earlier claim that DPE exhibits low or no reactivity towards this class of analytes, albeit a slower reaction was observed.

As regards the mechanism whereby the same product is formed from either reagent, a plausible reaction scheme is shown in **Figure 2-5**. As in all of the analyte classes investigated, the reagent undergoes a nucleophilic addition to the quinoidal intermediate, followed by tautomerization reforming the aromatic system, followed by oxidation to form the o-iminoquinone (**6→10→11→12**). Continuing towards PBO formation, the imine subsequently shifts to the Schiff base (**12→13**), which undergoes cyclization (**13→14**) and subsequent formation of the fluorescent product (**14→9b**), a step that is likely completed via a radical mediated process, where H_2 is eliminated when BA is used as the regent, or BA is eliminated (fission of the DPE molecule) in the case of DPE as reagent. The key sequence of reactions from **12→9b** previously has been reported for the elaboration of an o-quinone to the PBO with BA [24], thus leading strong credence to the presently proposed reaction sequence. With regard to DPE, the only difference would lie in the final step where the DPE molecule undergoes a symmetrical fission (**14→9b**); however, this would involve the generation of a benzyl radical, a highly plausible step.

2.3.5 Rate, Yield, and Mechanism for CA derivatization with BA and DPE

Continuing this line of investigation, similar experiments were performed for the derivatization of the CA epinephrine (E) (**Figure 2-1: 3**). The reaction conditions and relative concentrations of all reactants were as noted in the previous section. Chromatograms showing the progress of this reaction are shown in **Figure 2-6** and, as in the previous case time course plots of data obtained for E derivatization with the three different reagent solutions (BA, DPE or DPE plus gly) are presented in

Figure 2-7, with an overall summary of the time to completion and yield data summarized in **Table 1**. Examination of these data reveal that irrespective of the reagent system utilized, including the presence of gly that was previously claimed to function as an "accelerator", there was no substantial difference in time required to complete the derivatization nor difference in product yield.

A plausible reaction sequence for the various steps involved in the transformation of CAs to the PBO products of general structure **8** is presented in **Figure 2-8**. In this case the initially formed o-quinone undergoes an intramolecular Michael addition with subsequent tautomerization followed by a further oxidation to form adrenochrome, which then reacts with the reagent forming an o-iminoquinone (**4→15→16→17→18**). As in the case of the previously discussed 5-HIs, this type of intermediate (**18**) proceeds along the same reaction pathway to ultimately produce the observed fluorescent PBO product (**8**). In the present case, the time for completion of the derivatization reaction and yield was invariant with respect to the reagent system utilized, which is in contrast to the previous situation where derivatization with DPE required more than twice the reaction time as compared to BA. Apparently once the reaction sequence reaches intermediate **15** (**Figure 2-8**), despite significant differences in overall steric bulk, either reagent is equally facile in proceeding to formation of the PBO product (**Figure 2-8: 8**). Of note, the intramolecular Michael addition **(4→16**) serves as a product defining step in the overall sequence, as will be seen in the next section, this feature is also found in the derivatization of Cs with either reagent and once the sequence reaches intermediate **17**, either reagent serves to complete formation of the fluorescent PBO product via the illustrated steps (**17→18→19→20→8).** As noted above, the conversation of a p-amino-substituted o-quinone to a PBO derivative has been described via the proposed reaction sequence [24].

2.3.6 Rate, Yield, and Mechanism for Cs derivatization with BA and DPE

The Cs are the remaining class of targeted analytes to be invested, with 4-MC being selected as the model catechol. When 4MC was derivatized with BA or DPE as individual reactions PBO products were observed; however, the PBO formed from reaction of BA possesses a 6-(N-benzyl)-amino substituent (**Figure 2-12: 7a**), while derivatization with DPE results in a PBO bearing a 6-amino substituent (**Figure 2-12: 7b**). These experiments were conducted in the same manner as described earlier utilizing the three reagent systems (BA, DPE or DPE plus gly). Chromatograms presented in **Figure 2-9** and **Figure 2-10**, display the time course for the PBO product formed from derivatization with the BA regent and the DPE reagent (absent gly), respectively, with the data being summarized by the plots shown in **Figure 2-11**. An overall summary of the results is presented in **Table 1**, where unlike the CA case, the different reagent systems now result in significant differences in time to completion and yields of the PBO product. Derivatization of with BA resulted in completion of the reaction in ~30 minutes yielding ~ 88%, while in the case of DPE (gly absent) a longer reaction time was required, ~75 minutes and a slightly diminished yield of ~74% was observed. In the experiment where the "accelerator" gly was present with DPE, the reaction was indeed completed in a shorter time, 20 minutes in the presence of gly *versus* 75 minutes in the absence of gly, albeit with a substantially diminished yield, 74% in the absence of gly *versus* 38% in the presence of gly.

A plausible explanation of these results can be found in the reaction sequence shown in **Figure 2-12,** with the **26→27** transformation being elaborated in **Figure 2-13**. The catechol 4MC undergoes an initial reaction forming the electrophilic o-quinone **2a**. In contrast to CAs where a facile intramolecular reaction is operative (**Figure 2-8**), in the present case nucleophilic BA or DPE intercepts **2a**, forming the pathway directing intermediates **21** or **25,** for BA or DPE, respectively. For BA, the reaction sequence **21→22→23→24→7a** follows, which is similar to the pathway previously described for the catecholamines (**Figure 2-8**), ultimately resulting in the formation of the PBO product **7a**. However, in the case of DPE intermediate **25** apparently serves as the amine donor in a transamination reaction

resulting in formation of intermediate **27**, which then proceeds through the PBO forming reaction sequence resulting in **7b** formation. It appears that conversion of intermediate **26 to 27** requires multiple steps. A transamination involving BA undergoing reaction with an o-quinone substrate previously has been reported [24]. In the present case, DPE or DPE/gly exclusively resulted in the transamination reaction leading to 27 formation, which was not observed with the use of BA as illustrated in the reaction sequence **22 → 23→24→7a** (**Figure 2-12**). A possible explanation for the divergence the DPE and BA reaction pathways is shown in the scheme of **Figure 2-13** where oxidation results in the conversion **of 26→30**, followed by a tautomerization to form **31**, which can undergo further oxidation and tautomerization to result in the key species **32**. The transformation of **31→32** is of particular note when one considers BA versus DPE. For BA, to affect the observed transamination, the imine **31** would require nucleophilic attack (excess BA, $^{-}$OH or H_2O) to form a tetrahedral intermediate whose fragmentation completes the amine-transfer to the analyte. This is not observed. Alternatively for DPE, the transformation of **31→32** is highly plausible, being driven by the extended conjugation between the DPE phenyl-rings and continuing throughout the analyte skeleton. Once formed **32** is subject to nucleophile attach by any of the species previously noted as well as gly if included in the reagent solution. With **27** being a good leaving group, intermediate **33** undergoes a facile breakdown to effect transamination, a result that is exclusively observed.

As to the role of the "accelerator" gly, past derivatization protocols have frequently incorporated gly in a 1.5-fold molar excess as compared to DPE [14,21]. In basic media, the gly primary amine would be a competing nucleophile and undergo reaction with the o-quinone **2a→29**. If gly does serve in this role, this would result in an analyte consuming non-productive pathway (NPP) leading to a diminished yield, which is observed in the present experiments (**Table 1**). As to the acceleration of the reaction rate, any species capable of reacting with the analyte or intermediates along the product formation pathway in a non-productive fashion, would give the appearance of an enhanced product

formation rate, but would be expected to result in a diminished yield. Referring to the kinetic scheme of **Figure 2-14** and the associated kinetic equations (eq. 1 and eq. 2), one can readily see the result of such a competition, both from the perspective of rate and yield of the desired product. The rate of formation of **7b** is quantitatively described by **eq.1**, with the applicable rate constant k_{obs} being related to the sum of the path rate constants, thus giving the appearance of an "accelerator" effect when gly undergoes a non-productive competing reaction. Quantitatively the expected yield is shown by **eq. 2**, where it is seen that the productive pathway (k_1) is a fraction of all processes competing for the analyte, thus predicting a diminished yield when such a kinetic situation is operative, as appears to be true in the present case (**Table 1**). Based on this kinetic analysis and the present data, there would appear to be no basis for the long-standing use of gly as an accelerator in DPE derivatizations of Cs and in fact its inclusion in the reagent solution is detrimental with respect to product yield.

2.3.7 Formation of the DPE Product using BA via Ammonia Loading

As noted in the previous section, the derivatization of Cs with BA or DPE results in the formation of differing products, with the former reagent resulting in a substantially more hydrophobic product as compared to the latter, **7a** versus **7b** (**Figure 2-12**). From a chromatographic standpoint, the conversion of analytes to highly hydrophobic products can result in excessive elution times in an isocratic format and when utilizing reversed-phase gradient elution one may encounter numerous poorly resolved peaks late in the elution profile. With regard to the physical-chemical properties of the reagents, DPE possesses poor aqueous solubility as compared to BA, resulting in the need to conduct derivatization reactions in media containing a high percentage of a co-solvent such as methanol. While acceptable in many cases, the broader application to the P-3NY problem via derivatization of the 3AY-type products obtained by reduction [3,4] is problematic due to the poor solubility of peptides in such solvent systems.

This issue created an interest in exploring the feasibility of producing a DPE-type derivative (**Figure 2-12: 7b**) via the use of BA by using a modified reaction protocol. Recognizing the reactive nature of the intermediate o-quinone type substances (**2a**) and the present results with gly, which indicate that reactive amines can undergo Michael addition, a series of experiments were planned to evaluate the potential for the dynamic installation of an amino-group at what will become the 6-position. This was undertaken by exposing 4MC to a reaction solution containing $K_3Fe(CN)_6$ and an ammonia source (ammonium hydroxide or ammonium bicarbonate) for timed intervals prior to addition of BA. The initial feasibility was evaluated by LC-F-MS characterization of the reaction products formed and revealed two fluorescent products, with the early eluting peak exhibiting $[M+H]^+$ m/z = 225 and the latter eluting peak exhibiting $[M+H]^+$ m/z = 315, which corresponds to the DPE product (**7b**) and the BA product (**7a**), respectively [22]. Utilizing the **7a** and **7b** product standards additional experimentation was undertaken where pH 8.1 ammonium bicarbonate was incubated with 4MC for various times prior to the addition of BA. These data (**Figure 2-15)** reveal that simultaneous exposure to the ammonia source and BA result in the predominate formation of the BA product (66%) as compared to the DPE product (28%), while in contrast after one hour of exposure to the ammonia source prior to the addition of BA resulted in predominate formation of the DPE product (75%) and as compared to the BA product (3%). Continued exposure to ammonia prior to BA resulted in virtually no BA product being formed with the DPE product clearly dominating; however, the maximum yield of the DPE product occurred with the one hour pre-exposure, with increasing times providing a continuing decreasing yield trend, which is obviously due to the competition of unknown side-reactions in the formation of the ammonia addition product, 4-amino-5-methylcatechol, and its fate prior to formation of the comparatively stable PBO products, **7a** and **7b**. A further interest in the use of the ammonium-based buffer lies in its compatibility with LC-MS methods, which is of interest in our continuing investigations in the proteomics area; however, the present data

suggest that this problem may best be addressed via the synthesis of an appropriate water soluble DPE analog.

2.3.8 Reagent Selectivity and Further Aspects of the gly Effect

As described earlier, protocols for the derivatization of mixtures containing 5HIs, CAs and Cs, have advocated the use of a two-step procedure where the 5HIs were first derivatized with BA (ambient temperature, 2 min), and subsequently the remaining targets subjected to derivatization with DPE/gly (50 °C, 20 min) [21]. The basis of the approach was a claimed low or no reactivity of DPE towards 5HIs and vice versa for BA towards CAs and CS. Based on the present results summarized in **Table 1** this clearly is not the case as either reagent converts 5HI type analytes to the desired fluorescent product, albeit taking twice the reaction time for DPE, which indicates each reagent is participating in the observed conversion. With regard to CAs, the present data indicate that the desired transformation is effected by either reagent in equal times with similar yields. As regards Cs, derivatization with DPE/gly appears to be an inferior approach, as substantially decreased yields results (Table 1), while use of DPE alone results in a similar yield as that attained by BA, but at more than double the reaction time, which is the reverse of the previously claimed kinetic selectivity and in this case [21], two differing fluorescent products would be formed. To achieve similar kinetic selectivity one would simply conduct the reaction at an elevated temperature in the presence of BA and DPE, which would be expected to lessen the presently observed selectivity, thus moving towards equalization for the reaction of each reagent with the Cs type analyte.

To further confirm the above conclusions, a selective group of experiments was conducted for 4MC (**1a**) derivatization with each reagent separately (BA or DPE), combined (BA and DPE) and combined in the presence of gly (BA and DPE and gly), with the results being displayed in **Figures 2-16**

through 2-19. **Figure 2-16** illustrates the derivatization of 4MC (**1a**) with BA, to provide a single major peak eluting at 14.5 min and exhibits co-elution with the isolated standard (**7a**). In **Figure 2-17** illustrates the result obtained from derivatization of 4MC (**1a**) with DPE in a solution spiked with ~100 nM **7a**. The DPE product **7b** eluted at 5.7 min, standard 7b eluting as before being unaffected by the derivatization process. These two experiments clearly show that each reagent reacts with 4MC (**1a**) to form the expected differing products; however the next experiment was used to probe reagent selectivity as each reagent was initially present. Examination of **Figure 2-18** reveals that 4MC is exclusively transformed to the BA-type product (**7a**), a result that is not unexpected based on the prior results summarized in **Table 1**. In a last and perhaps most critical comparison, 4MC (**1a**) was derivatized with both reagents (BA and DPE) in the presence of gly, a situation that is widely used in past protocols [21,25] (**Figure 2-19**). The resulting chromatogram reveals, the transformation of 4MC (**1a**) to the expected BA (**7a**) and DPE (**7b**) products in approximately equivalent amounts and the appearance of multiple unknown fluorescent products, with the peak eluting at 8.8 min being formed in a significant amount. It is not clear why the DPE related product **7b** forms in the presence of gly, whereas it was not observed in the previous experiment (**Figure 2-18**); however, there is the possibility of conversion of the gly adduct **29** (**Figure 2-13**) to **7b** through a series of reactions (PBO formation and gly substituent decarboxylation and dealkylation) but further investigation is required to support such speculation and is beyond our present objectives. Careful scrutiny of early publications reveals the use of gly as an accelerator was advocated in the fluorometric derivatization of CAs [14]; however, a following publication noted use of the DPE/gly for dopamine derivatization resulted in two peaks when used in the pre-column format [26]. The present results together with the note prior results clearly indicate that gly serves no analytically useful purpose and in fact is a substantial detriment when used with these fluorogenic derivatization reagents.

2.4 Summary and Conclusions

In the present investigation we have confirmed the products formed from derivatization of 5HIs and CAs; however we have additionally shown that both DPE and BA undergo reaction with each analyte to form the same products in each case. Further we have presently shown that derivatization of Cs with BA and DPE lead to different fluorescent products exhibiting similar fluorescence characteristics and are of the same general class (PBO). The preparation of reference standards allowed the determination of product yields for these determinations, and significantly revealed that inclusion of gly in the reagent solution results in a substantially reduced yield for Cs derivatization. The kinetic data generated essentially dispel earlier claims regarding selectivity, such as the non-reactivity or low-reactivity of DPE with 5HIs and vice versa in the case of CAs and Cs where DPE was previously noted to be reactive and BA to be of low-reactivity or non-reactive. Based on an appreciation of the reaction mechanism for the derivatization of CS, in particular 4MC in this study, we explored the possibility of installing a less hydrophobic 6-amino group instead of a 6-benzyl group via pre-incubation prior the addition of BA to complete fluorescent product formation, and while successful, a diminished yield was observed thus damping enthusiasm for this approach to achieve formation of a less hydrophobic derivative. A series of comparative derivatizations were performed where it was shown that the expected products were attained through the use of BA or DPE alone, or the BA product obtained when used in the presence of DPE in the derivatization of 4MC, which meets expectations according to the kinetic results obtained. Finally the use of gly to serve as an accelerator or exhibit any role in achieving selectivity is clearly not viable and is in fact detrimental and is not recommended to be used in conjunction with these reagents. The results obtained from DPE derivatization of Cs suggest that it could be advantageous to prepare a DPE-type reagent that bears a hydrophilic substituent providing for greater aqueous solubility, thus the

use of this reaction in the determination of peptides bearing the 3-NY modification, the need for which we noted in the introduction.

2.5 Chapter 2 Figures

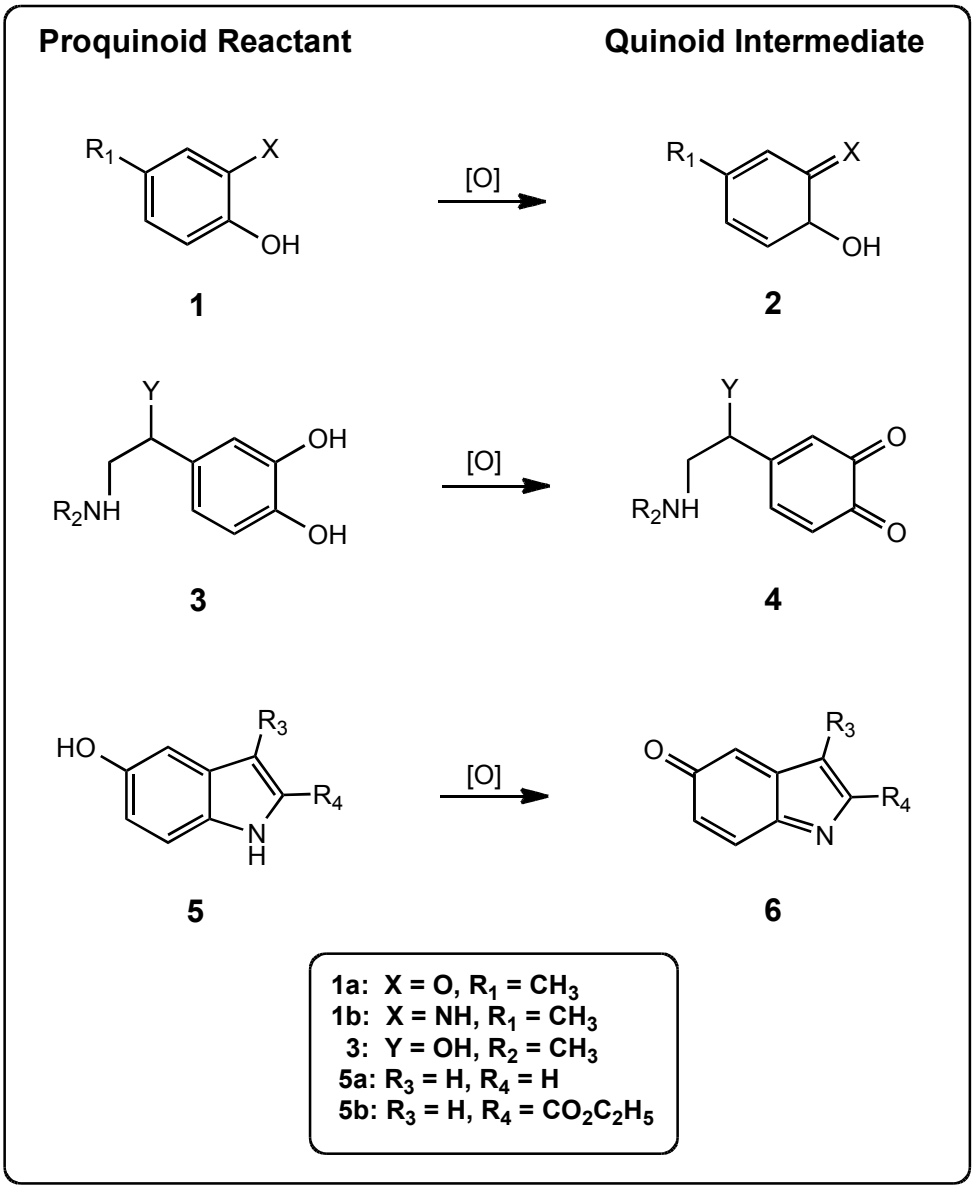

Figure 2-1. Structures of proquinoid substances of relevance to the present investigation

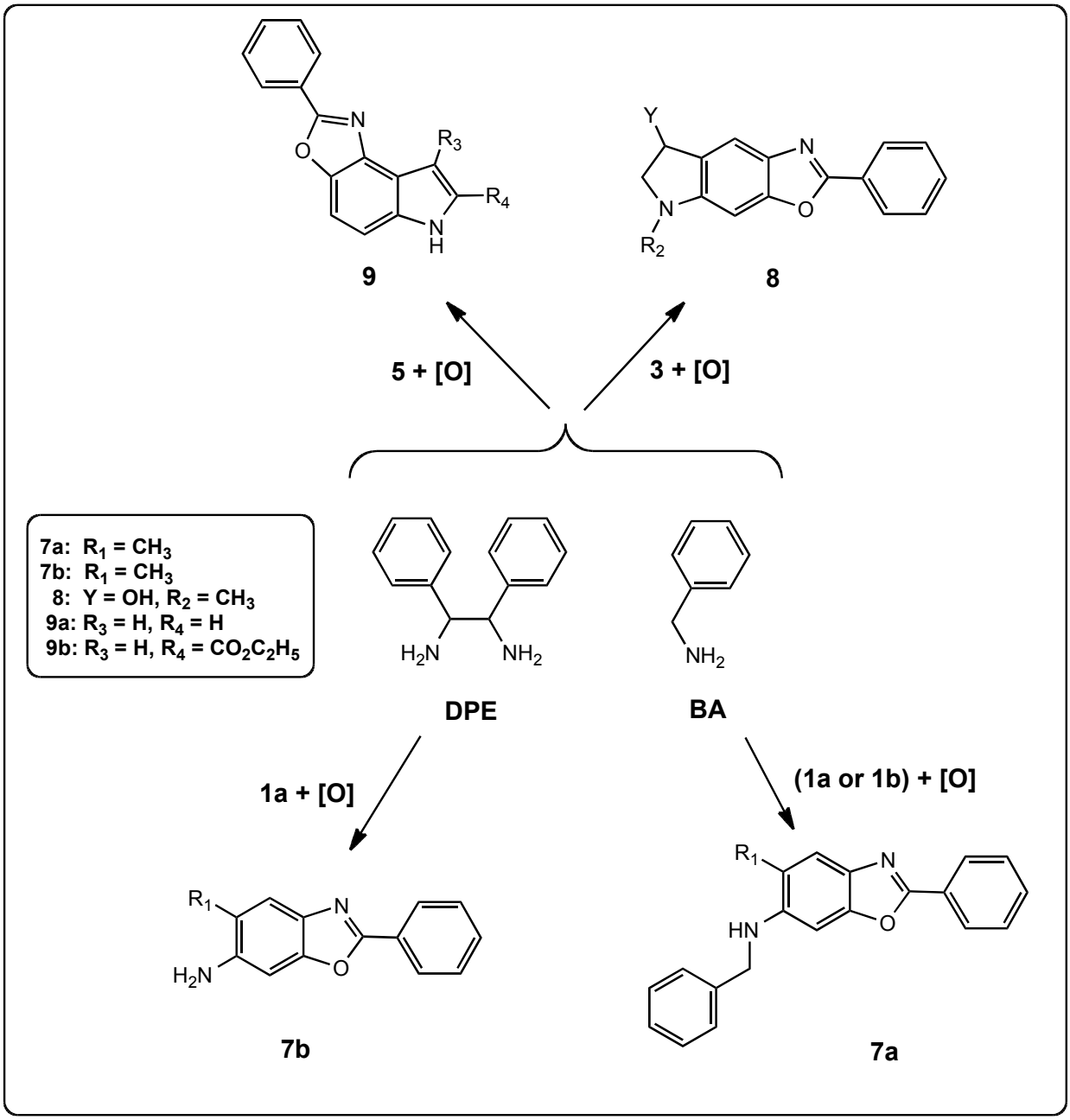

Figure 2-2. Products obtained from the reaction of DPE and BA with the proquinoid structures illustrated in Figure 2-1.

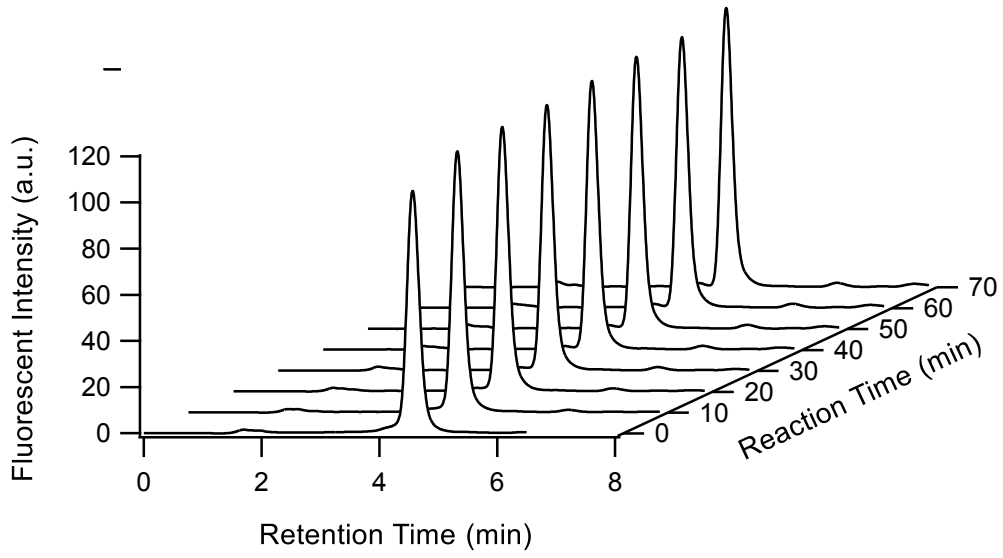

Figure 2-3. HPLC-F chromatograms illustrating the time course of product formation from derivatization of 5-HI-2-CAE (5b) with BA

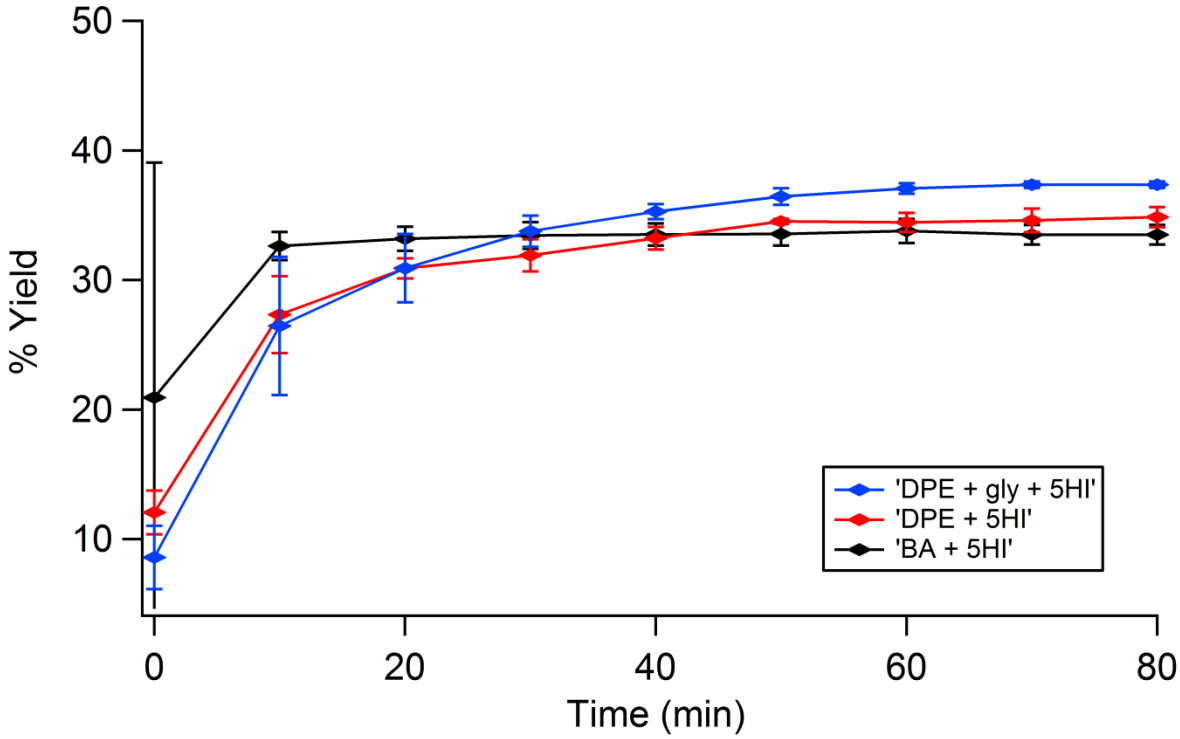

Figure 2-4. Time course of product formation from derivatization of 5-HICAE (5b) with BA, DPE and DPE in the presence of gly.

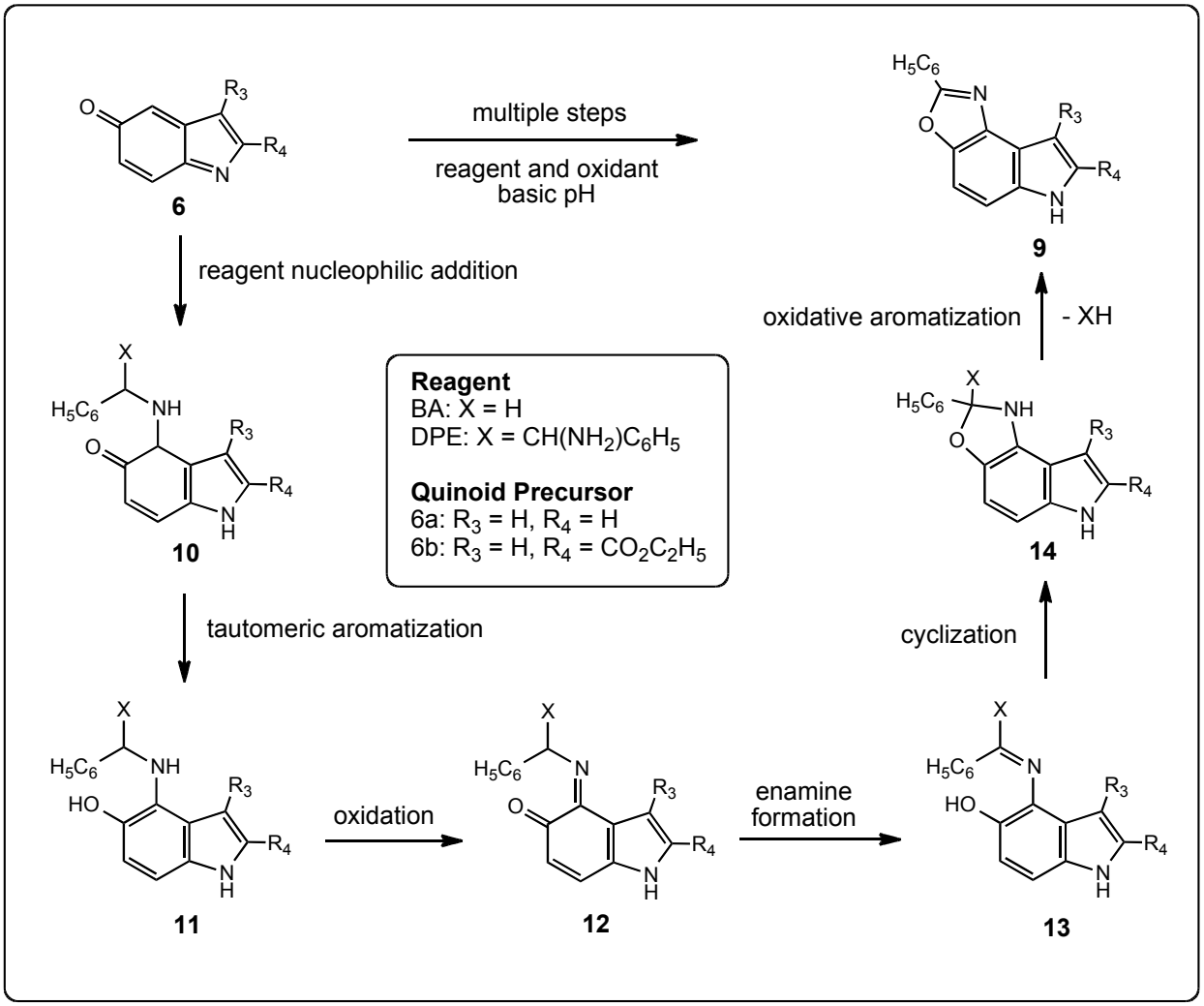

Figure 2-5. Proposed reaction sequence for product formation for derivatization of 5-HIs with BA or DPE

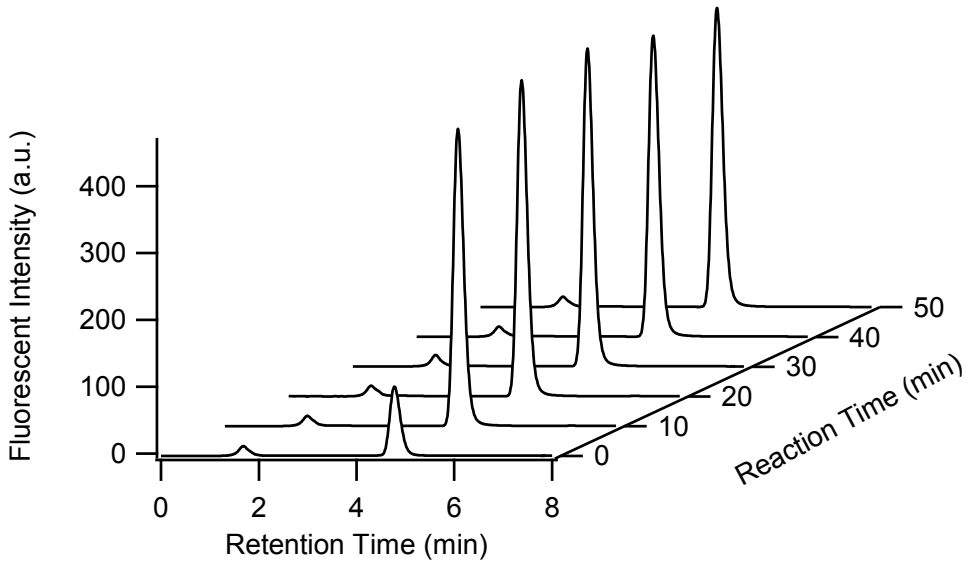

Figure 2-6. Cascade chromatograms showing product formation from the reaction between E (3) and BA.

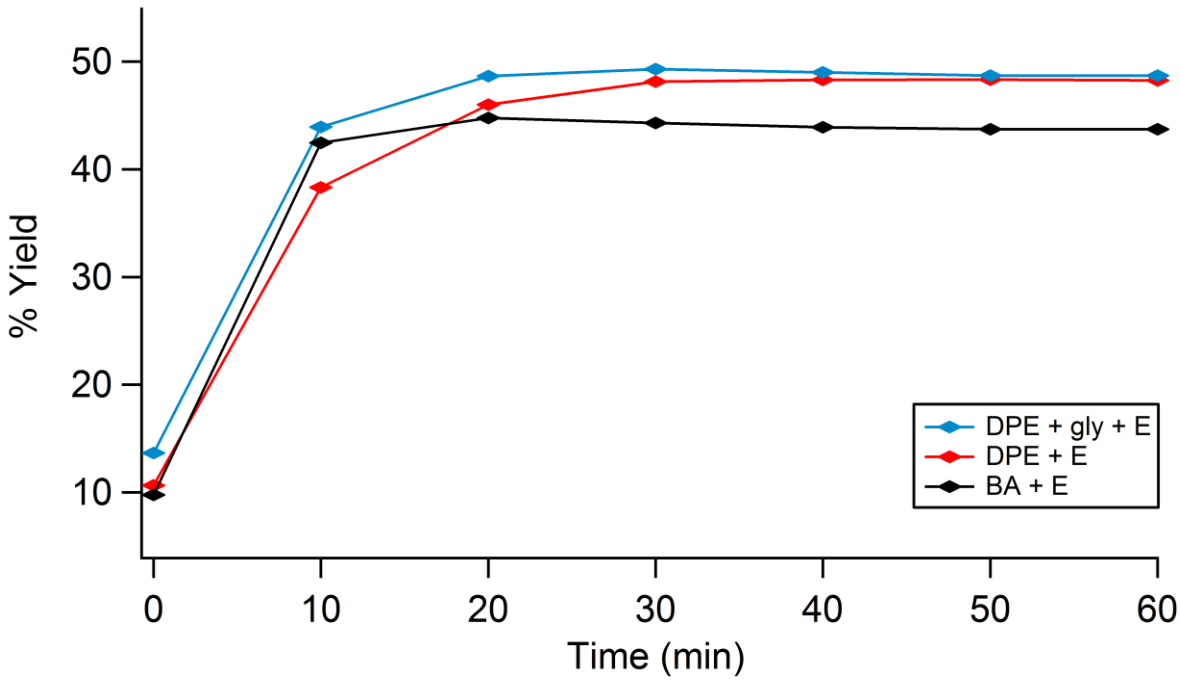

Figure 2-7. Reaction progress for the derivatization of E (3) with different reagents and combinations.

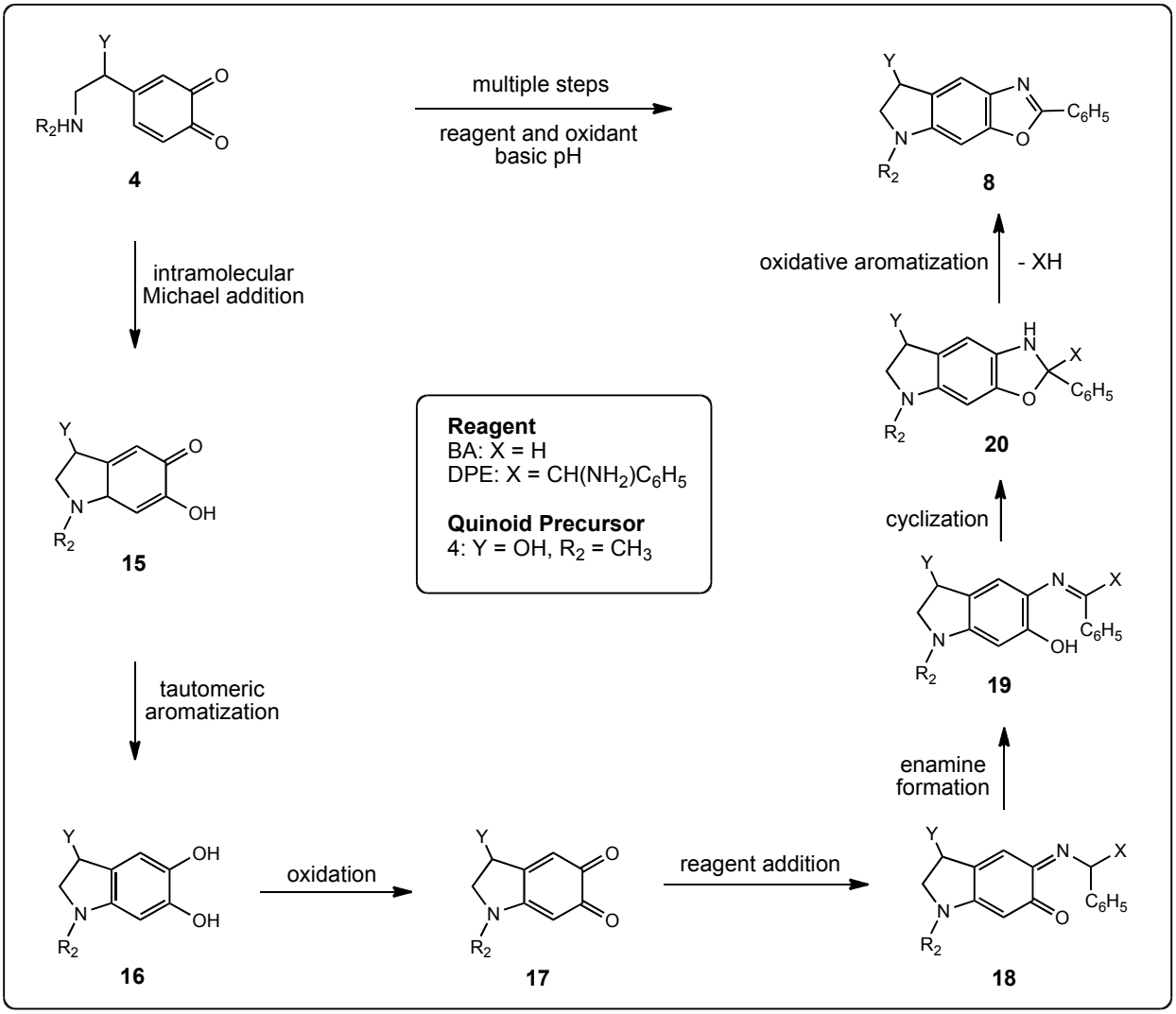

Figure 2-8. Proposed reaction sequence for product formation for derivatization of CAs with BA or DPE.

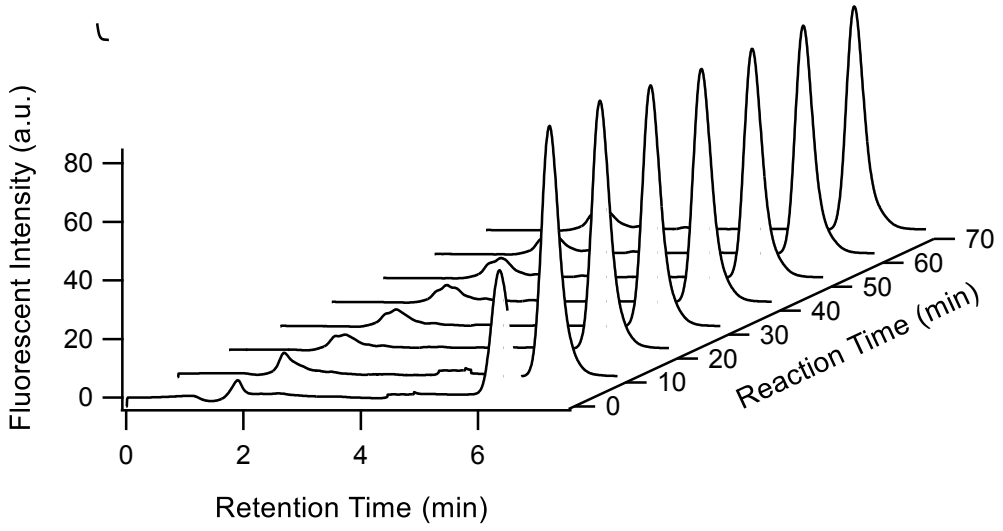

Figure 2-9. Cascade chromatograms showing product formation from the reaction between 4-MC and BA.

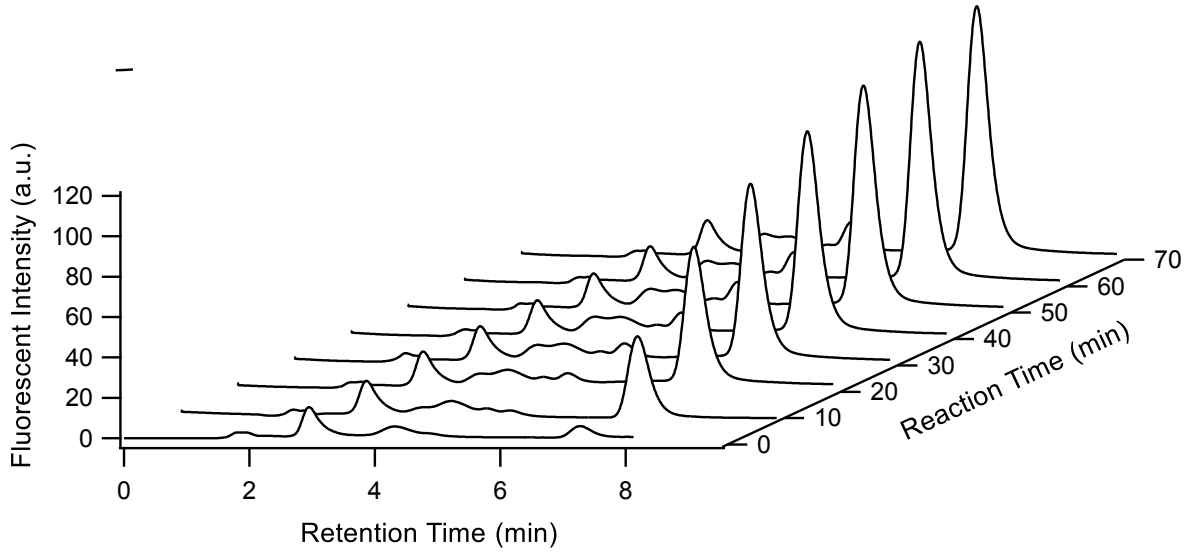

Figure 2-10. Cascade chromatograms showing product formation from the reaction between 4-MC and DPE.

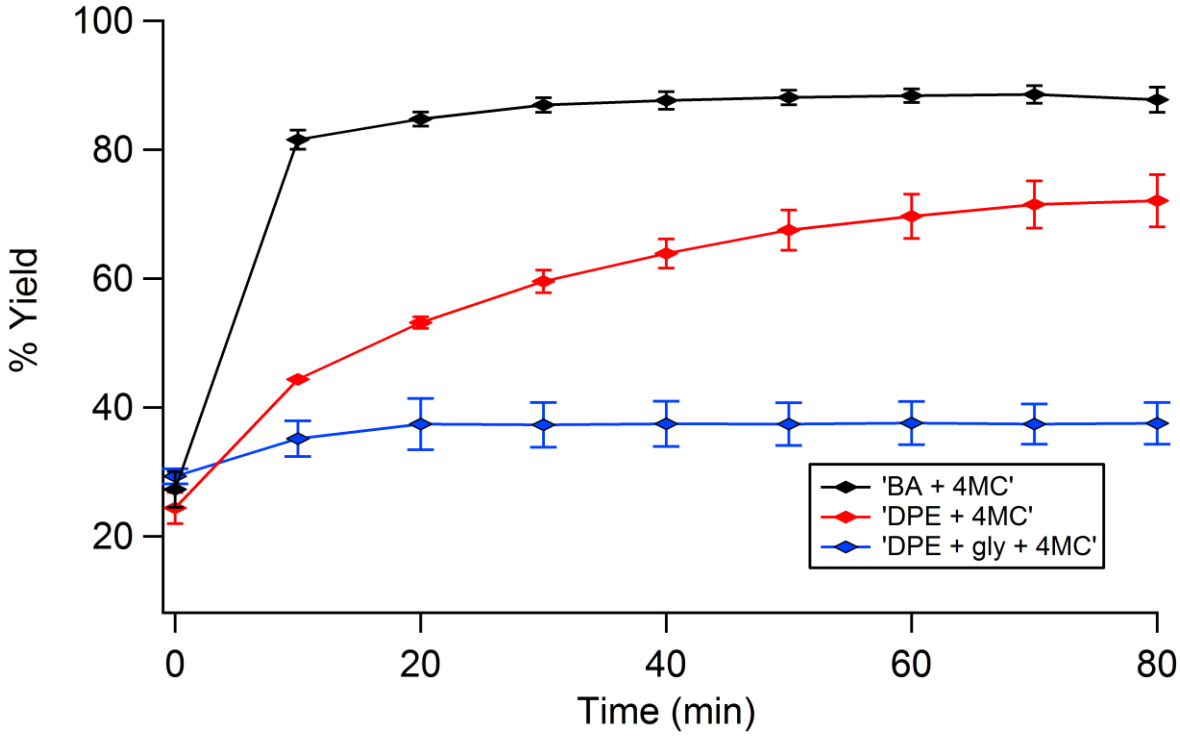

Figure 2-11. Reaction progress for the derivatization of 4MC (1a) with different reagents and combinations.

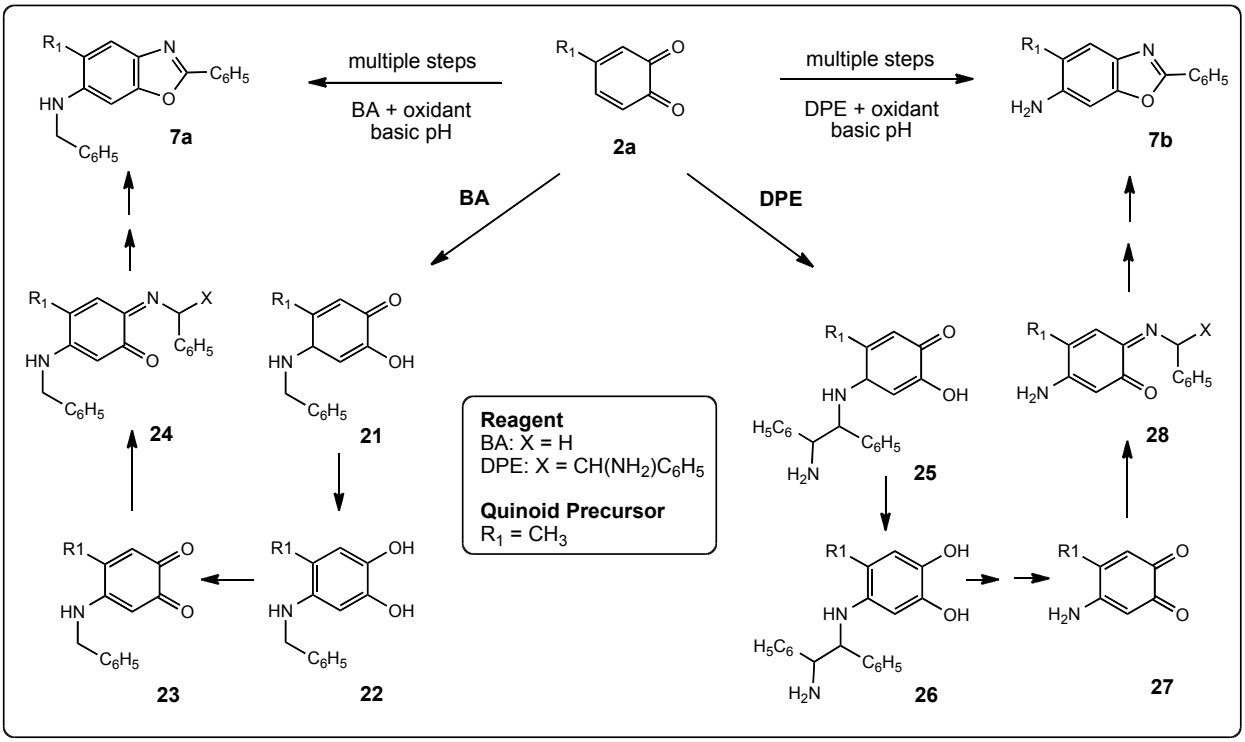

Figure 2-12. Proposed reaction sequence for product formation for derivatization of Cs with BA or DPE.

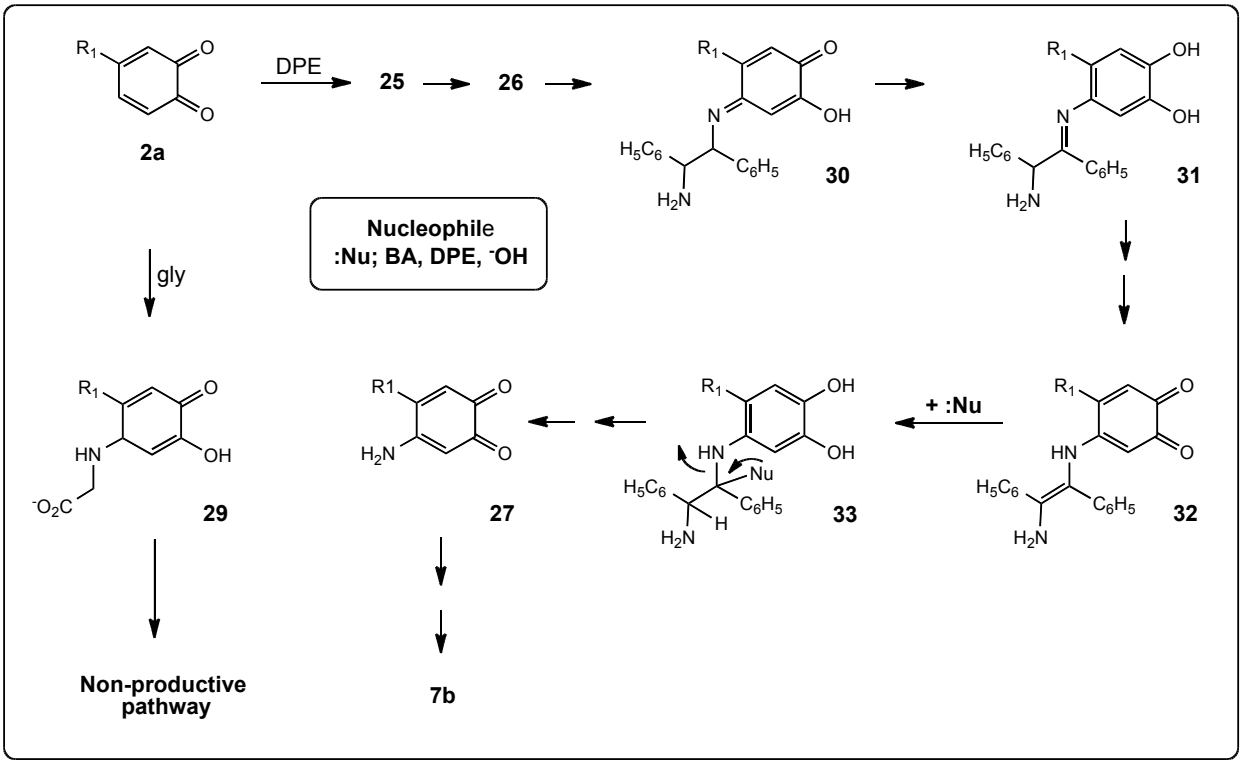

Figure 2-13. Proposed reaction sequence illustrating the non-productive role of gly and DPE transamination in the derivatization of Cs.

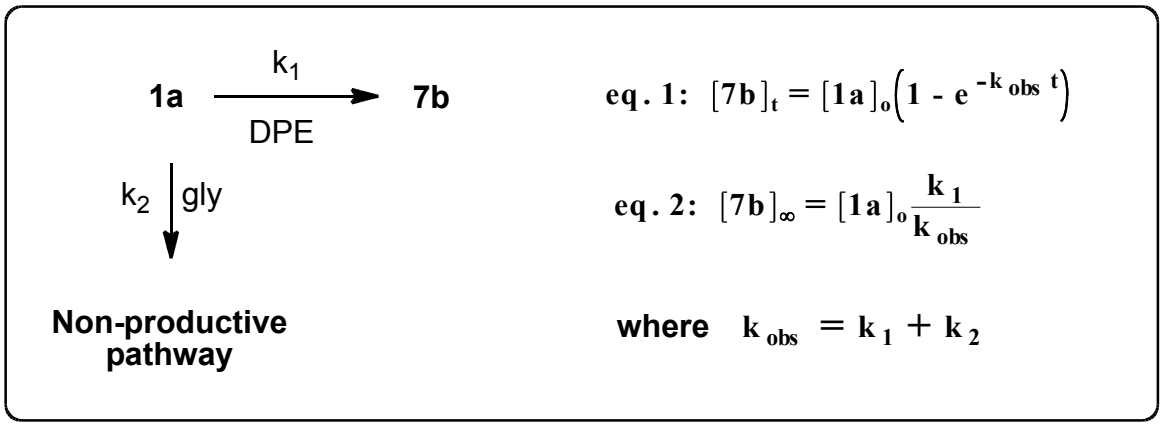

Figure 2-14. Kinetic scheme illustrating the apparent "accelerator" and non-productive role of gly in the derivatization of Cs with DPE.

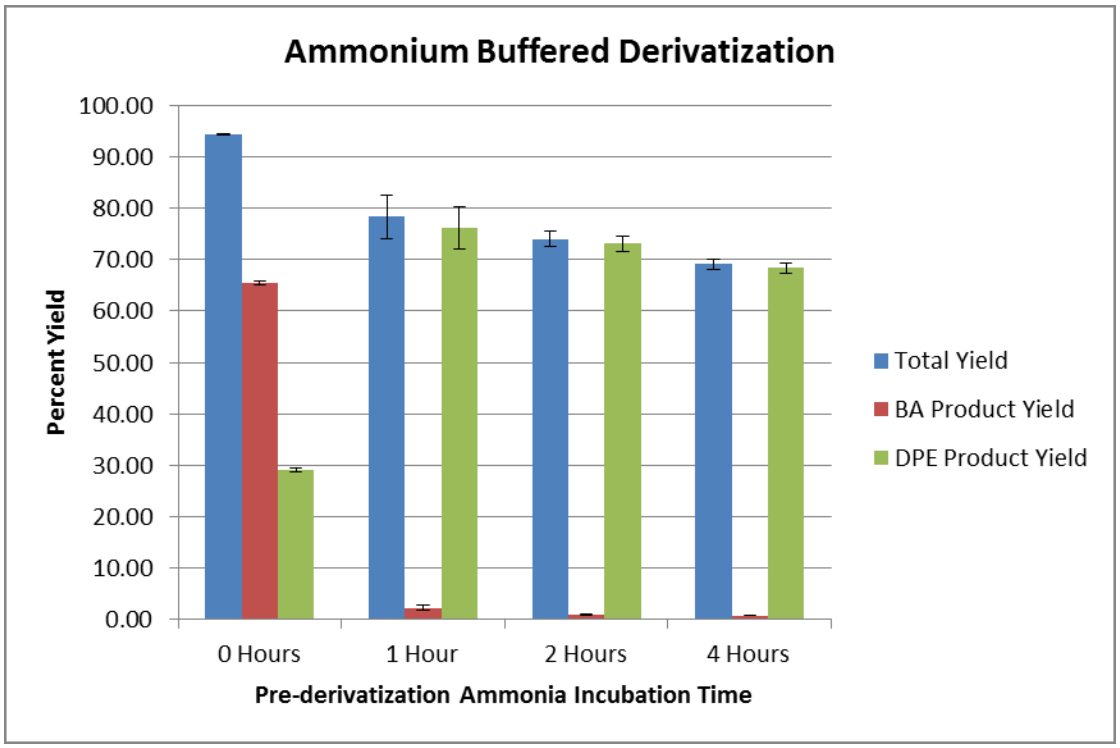

Figure 2-15. Derivatization yields of the reaction between 4MC and ammonium bicarbonate for various incubation times followed by addition of BA.

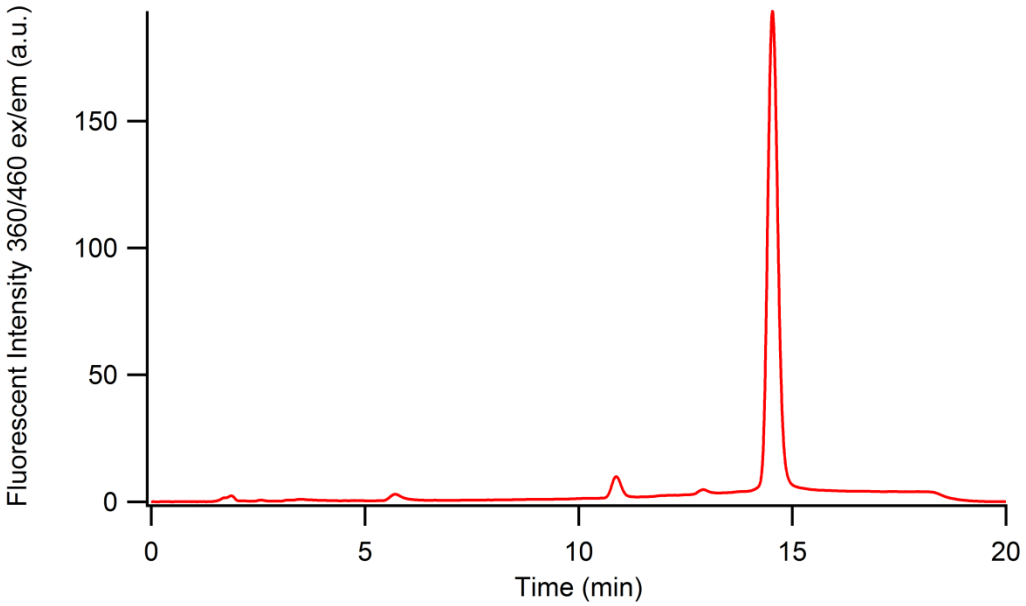

Figure 2-16. Derivatization of 4MC with BA in the presence of K3Fe(CN)6 to form 7a.

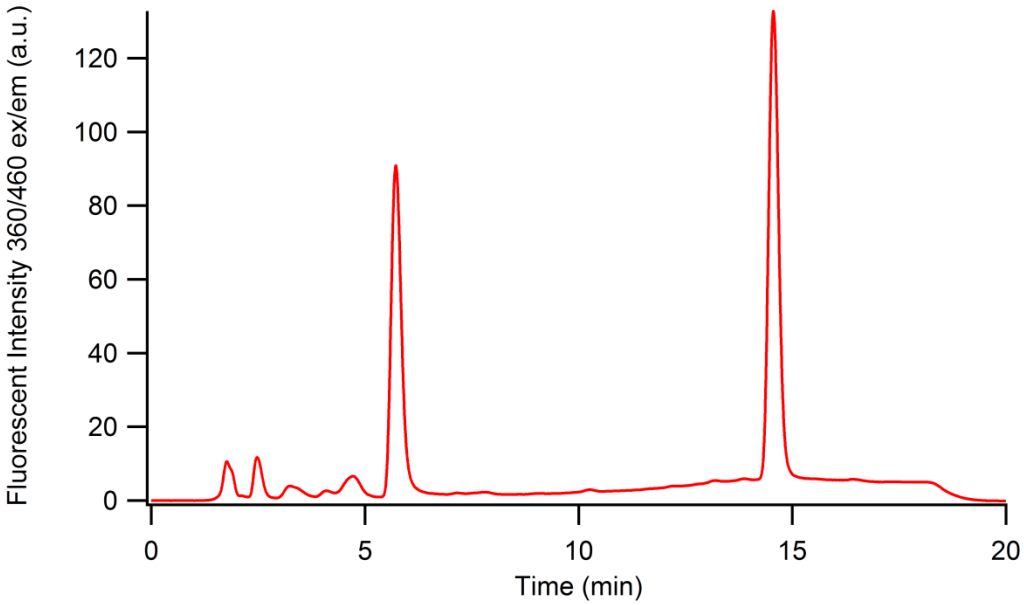

Figure 2-17. Derivatization of 4MC with DPE in the presence of K3Fe(CN)6, with standard 7a included for reference.

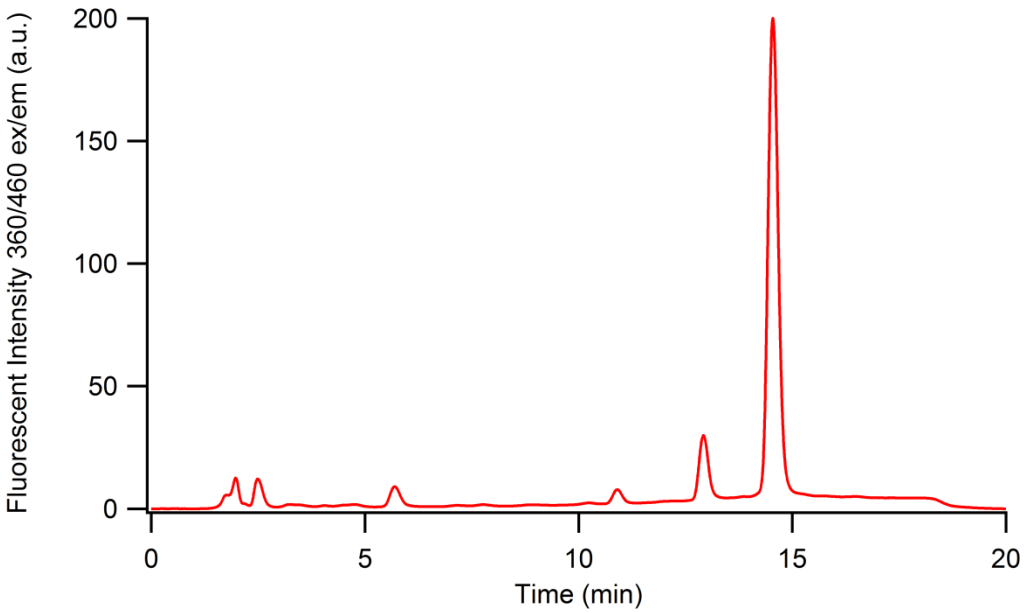

Figure 2-18. Derivatization of 4MC with BA and DPE in the presence of K3Fe(CN)6, with standard 7a present.

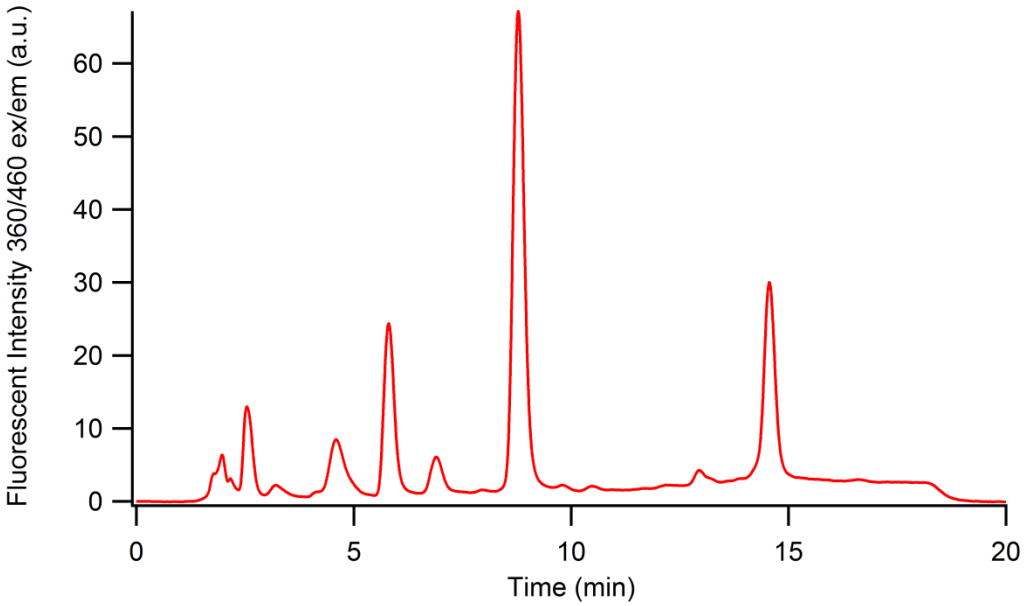

Figure 2-19 Derivatization of 4MC with DPE and BA in the presence of $K_3Fe(CN)_6$, and gly.

Analyte	Reagent	Gly Present	%Yield	%RSD*	Completion (min)
5HI-2-CAE	BA	no	33.2	0.9	20
5HI-2-CAE	DPE	no	34.2	0.7	50
5HI-2-CAE	DPE	yes	36.5	0.5	50
E	BA	no	45.1	1.2	30
E	DPE	no	48.3	0.8	30
E	DPE	yes	49.0	0.3	30
4MC	BA	no	88.2	1.7	30
4MC	DPE	no	73.9	4.5	75
4MC	DPE	yes	37.5	3.3	20

N = 3

Table 2-1. Summary of kinetic and yield experiments for model 5-HIs, CAs and Cs derivatized with BA, BA+DPE, and BA+DPE+gly.

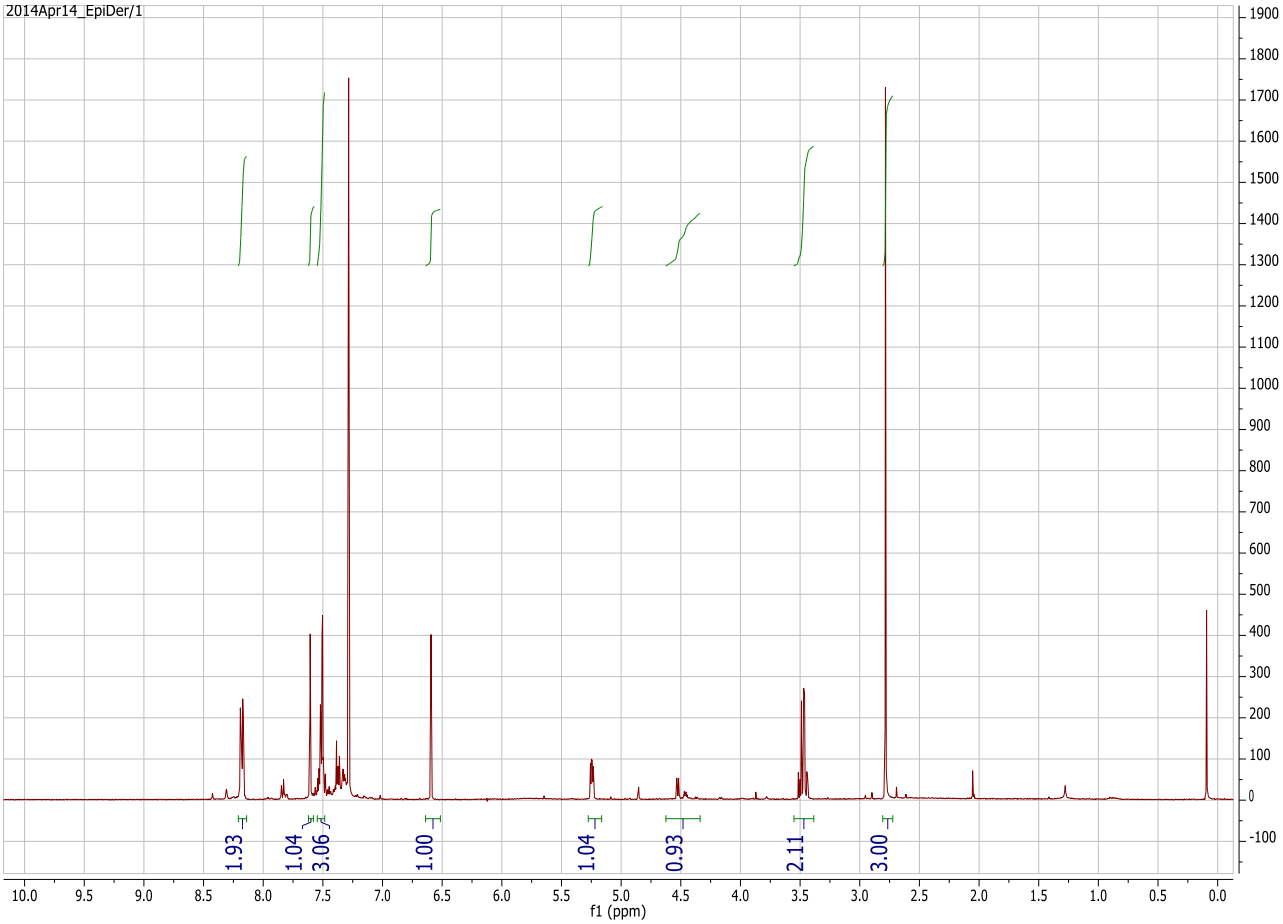

Figure 2-20. BA/Epi product spectra in deuterated chloroform. 1H NMR δ 8.2 (2H, m), 7.6 (1H, t, J = 0.7 Hz), 7.5 (3H, m), 6.6 (1H, s), 5.3 (1H, dd, J = 3), 4.5 (1H, dd, J = 5.8), 3.5 (2H, m), 2.8 (3H, s).

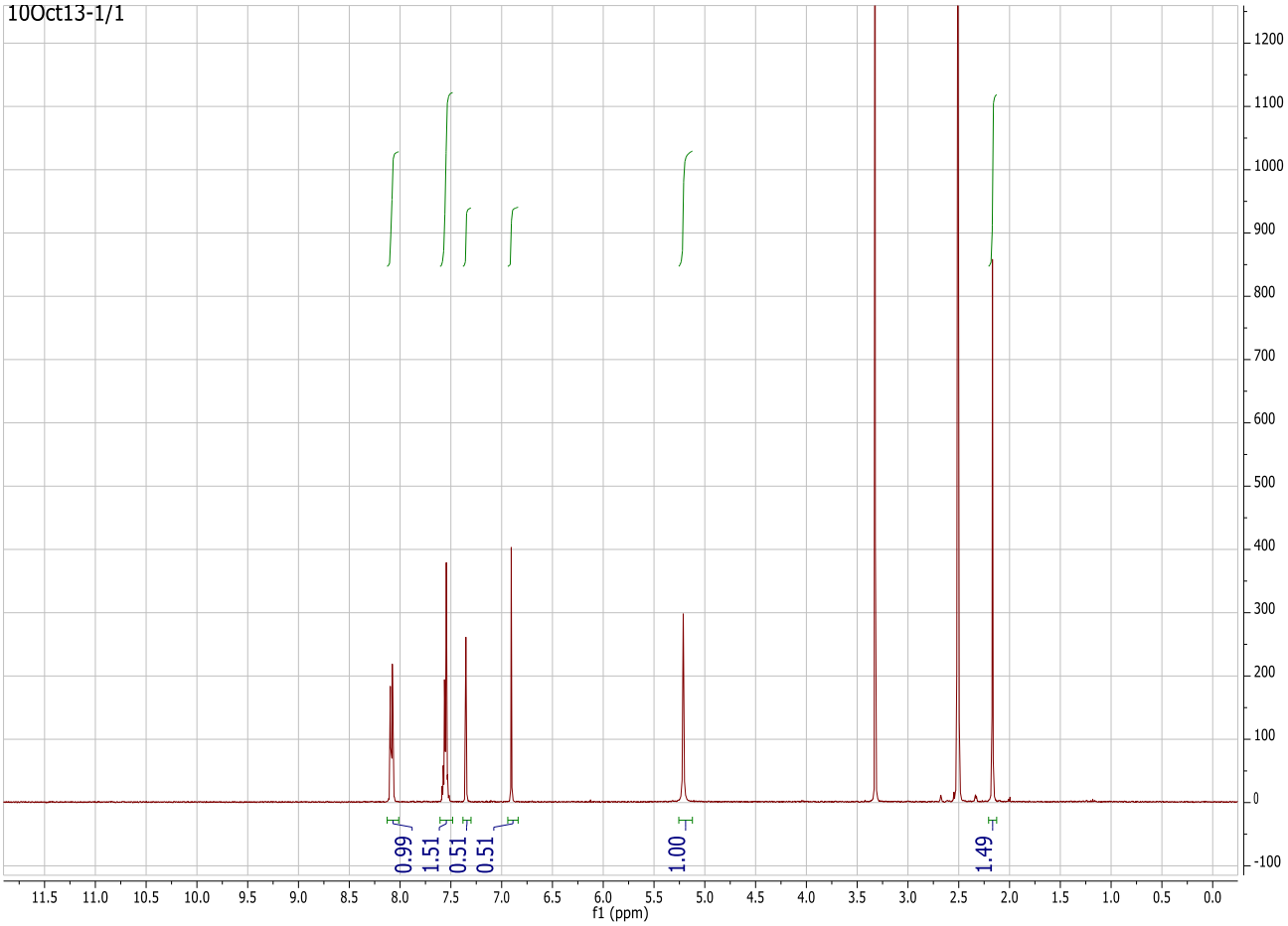

Figure 2-21. BA/DPE Product NMR Spectra. NMR Solvent DMSO. ^{1}H NMR ($CDCl_3$) δ 8.1 (2H, m), 7.55 (3H, tdd), 7.35 (1H, s), 6.9 (1H, s), 5.1 (2H, s), 2.2 (3H, s).

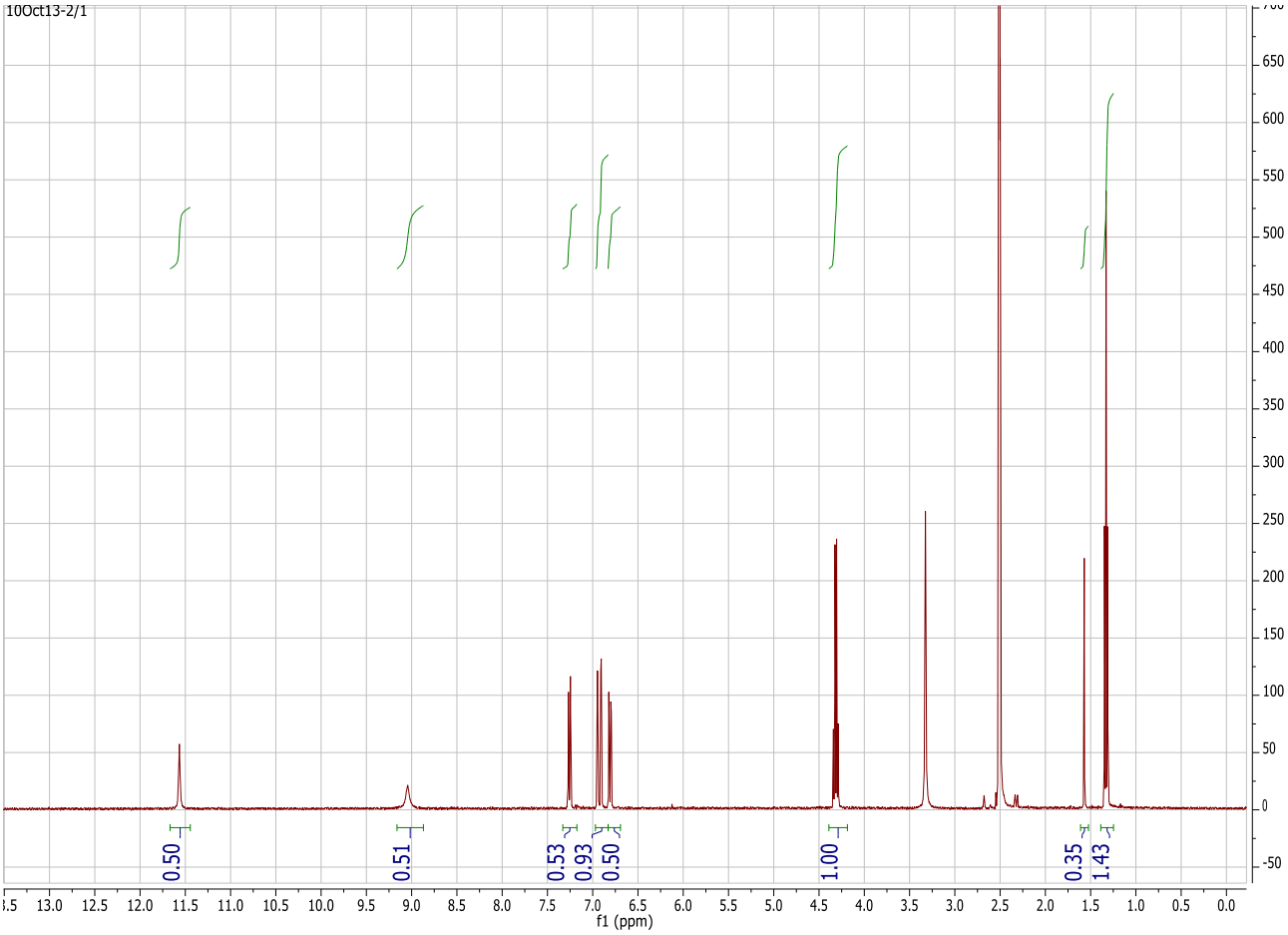

Figure 2-22. 5HI/BA Product Spectra. NMR Solvent DMSO. ^{1}H NMR ($CDCl_3$) δ 9.2 (1H, s), 8.35 (2H, m), 7.75 (1H, dd, J = 2.15 Hz, J = 0.95 Hz), 7.65 (1H, d, J = 8.85 Hz), 7.55 (3H, m), 7.45 (1H, dd, J = 9.0 Hz, J = 1.0 Hz), 4.45 (2H, q, J = 4.60 Hz), 1.5 (3H, t, 7.15 Hz).

2.6 Chapter 2 References

[1] Yoshitake T, Kehr J, todoroki K, Nohta H, Yamaguchi M (2006) Biomed Chromatogr 20:267-281
[2] Pennington JP, Schöneich C, Stobaugh JF (2007) Chromatographia 66:649-659
[3] Sharov V, Dremina E, Galeva N, Gerstenecker GS, Li X, Dobrowsky R, Stobaugh JF, Schöneich C (2010) Chromatographia 71:37-53
[4] Dremina E, Li X, Glaeva N, Sharov V, Stobaugh JF, Schöneich C (2011) Anal Biochem 418:184-196
[5] Davies MJ (2005) Biochim Biophys Acta 267:233-240
[6] Radi R (2013) Acc Chem Res 46:550-559
[7] Nichols DE, Nichols CD (2008) Chem Rev 108:1614-1641
[8] Kuhar MJ, Couceyro PR, Lamber PD (1999) Chap 12 Biosynthesis of Catecholamines. In: Basic Neurochemistry: Molecular, Cellular and Medical Aspects 6th ed, Philadelphia: Lippincott-Raven
[9] Some M, Helander A (2002) Life Sci 71:2341-2349
[10] Osborne NN (1982) Biology of Serotonergic Transmission. Chichester: Wiley
[11] Wang YL, Wei JW, Sun AY (1993) Neurochem Res 18:1293-1297
[12] Chaiyakul P, Reidman D, Pilipovic L, Maher T, Ally A (2001) Brain Res 900:186-194
[13] Lesage J, Bernet F, Montel V, Dupouy JP (1996) 21:87-96
[14] Nohta H, Mitsui A, Ohkura Y(1984) Anal Chim Acta 165:171-176
[15] Ishida J, Yamaguchi M, Nakamura M (1991) Analyst 116:301-304
[16] Nohta H, Lee M-K, Ohkura Y (1992) Anal Chim Acta 267:137-139
[17] Gouyette A, Auclair C, Paoletti C (1985) Biochem Biophys Res Commun 131:614-619
[18] Sundaramoorthi R, Kansal VK, Bhupesh C, Potier P (1986) J Chem Soc Chem Commun 371-372
[19] Yamaguchi M, Yoshitake T, Fujino K, Kawano K, Kehr J, Ishida J (1999) Anal Biochem 270:296-302
[20] Nohta H, Yukizawa T, Ohkura Y, Yoshimura M, Ishida J, Yamaguchi M (1997) 344:233-240
[21] Fujino K, Yoshitake T, Kehr J, Nohta H, Yamaguchi M (2003) J Chromatogr A 1012:169-177
[22] Pennington JP (2007) Doctoral Dissertation, Development of fluorescent/stable isotope tagging stragegies for proteins containing DOPA; University of Kansas, Lawerence, KS
[23] Mitsui A, Nohta H, Ohkura Y (1985) J Chromatogr 344:61-70
[24] Ling K-Q, Kim J, Sayre LM (2001) J Am Chem Soc 123:9606-9611
[25] Wu Y-B, Wu J-H, Shi Z-G, Feng Y-Q (2009) J Chromatogra B 877:1847-1855
[26] Nohta H, Mitsui A, Ohkura Y (1984) Bunseki Kagaku 33:E262-E269

Chapter 3

Synthetic Approaches Towards Improving Existing Derivatization Reagents

3.1 Introduction

3.1.1 General Goals of Derivatization

The goal of derivatization is to improve the detectability of an analyte through chemical modification. More broadly, the focus is to improve solubility, stability, chromatographic properties, and sensitivity at the time of detection for the analyte of interest[1]. In order to assess the importance of each of these attributes they should first be considered individually. Solubility can be a concern within the context of amino acid and peptide derivatization as there is a need for water-soluble derivatization reagents that can produce water soluble products. In turn, this concern can be extended towards chromatographic performance as hydrophobic products within a sample can result in chromatographic challenges. Typically, when groups of analytes exhibit physical properties that are extremely hydrophilic or hydrophobic, it is challenging to produce an acceptable separation. Chromatographic property concerns can further be extended towards the goal of sample cleanup as inclusion of a tag for sample enrichment and purification via affinity chromatography is a common goal for derivatization[2].

Stability is important both for derivatization reagent and derivatization product relevant to the time scale within the reaction time and detection time. Finally, the derivatization reagent should carry properties that enhance sensitivity at the time of product analysis, whether this involves functional groups, which can enhance ionization during mass spectrometry analysis, or produce a product, which can be measured using sensitive methods such as fluorescence that has inherently low limits of detection. With those objectives in mind, creating a reagent that not only accomplishes those goals, but also is uniquely reactive towards the analyte and produces a product in high yields, can provide a unique analytical challenge.

3.1.2 Derivatization Reagents for Protein-Bound 3-Nitrotyrosine

An early approach towards derivatization of protein-bound 3-nitrotyrosine focused on using a reagent containing a biotin tag [3]. The Tannenbaum strategy, which serves as a starting point for all derivatization strategies for protein bound 3-nitrotyrosine derivatizations, begins by reduction of the nitro group on tyrosine to an amine in order to create a reactive site for derivatization. After chemically modifying the newly formed amine by covalently attaching the biotin reagent, the tag served as a means for sample purification and enrichment through capture on streptavidin beads. The biotin reagent was the first exhibiting desired attributes for 3-nitrotyrosine derivatization, namely sensitivity through enrichment. However, as it depended upon pH control as a means of achieving selectivity, its ability to successfully enrich 3-nitrotyrosine from a biological matrix has been dismissed[4]. In a similar approach, Zhang et al. reported the successful derivatization of 3-nitrotyrosine using NHS S-acetylthioacetate[5]. The disadvantage of their methodology lies in the required sample preparation in which peptides were acetylated prior to nitro reduction in order to mask reactive amines. While this approach was successful in achieving selectivity by masking non-target amines, a reagent which imparts selectivity independent of sample preparation is inherently more valuable[6].

Within the scope of the current project, the goal was to build upon previously described work to produce a derivatization reagent that can be used to enhance detection of protein-bound 3-nitrotyrosine through HPLC coupled with either fluorescence detection or MS detection. To accomplish these objectives, our approach is to enhance existing derivatization reagents through structural modification. The reactions we are seeking to enhance are the derivatization reactions of pro-quinones by either BA or DPE. As benzylamine is structurally simpler, it was the focus of our initial attempts at modification. Although benzylamine itself is a water soluble compound, the product that results from its use in derivatization exhibits a high degree of hydrophobicity. While derivatizations described within this work occur on analytes dilute enough for the product solubility to not be an issue, we sought to create a more hydrophilic product to affect chromatographic properties during analysis. We also plan to include

a stable functional group on the reagent that can be used as a handle for either affinity chromatography, or ion exchange chromatography for the purpose of analyte purification and enrichment. Finally, we plan to create DPE based reagents that mirror the properties imparted to the BA counterparts.

3.2 Materials and Methods

3.2.1 Chemicals and Reagents

1R,2R-Diphenylethylenediamine, *meso*-1,2-diphenylethylenediamine,benzil, salicylaldehyde, ammonium hydroxide, acetic anhydride, 4-(dimethlamino)benzaldehyde, maleic anhydride, p-bromoaniline, ruthenium chloride, sodium metaperiodate, sodium thiosulfate, sodium chloride, magnesium sulfate, manganese perchlorate, pyridine-2-carboxylic acid, dioxane, 50% hydrogen peroxide, sodium acetate, sodium bisulfite, 2,2-dimethoxypropane, p-toluenesulfonic acid, cyclohexane, and *meso*-1,2-bis(2-hydroxyphenyl)ethylenediamine were purchased from Sigma Aldrich (St. Louis, MO). Tetrahydrofuran, ethyl acetate, hexanes, acetone, acetonitrile, benzene, chloroform, methylene chloride, and ethanol were purchased from Fisher Scientific (Waltham, MA).

3.2.2 Instrumentation

All NMR Spectra were obtained on a Bruker (Billerica, MA) Avance 400 MHz spectrometer. HPLC data was obtained on a Shimadzu (Kyoto, Japan) LC-10 series HPLC consisting of an SLC-10A vp system controller, two LC-10AD vp pumps, an SIL-10AD vp auto-injector and a SPD-10A vp UV detector. Mass spectra was recorded on a Waters (Milford, MA) MICROMASS QUATTRO *micro* triple quadrupole mass spectrometer.

Chromatographic separations to determine purity of synthetic products were carried out using a phenomenex (Torrance, CA) column measuring 150 x 4.6 mm packed with Inertsil 5 µm ODS-3 100 A particles. Mobile phase A was composed of 90:10 water:methanol with 0.1% formic acid and mobile

phase B was composed of 10:90 water:methanol with 0.1% formic acid. A gradient elution program was applied consisting of a linear change from 0% B to 100% B over 10 minutes, followed by holding 100% B for 7 minutes. The column was equilibrated for 7 minutes prior to an injection.

Preparative scale chromatography for isolation of sulfonic acid analogs was performed on a phenomenex 250 x 10 mm column packed with 10 µm LUNA ODS-3 particles. The mobile phase consisted of 20 mM ammonium bicarbonate buffer in water. The column was washed with for 10 minutes using a linear gradient program from 0 to 100% B with a mobile phase of 0.1% formic acid in water for mobile phase A and 0.1% formic acid in methanol for mobile phase B between injections.

3.2.3 Sulfonic Acid Modification

4-(Aminomethyl)benzenesulfonic acid (ABS). ABS was synthesized according to a previously published procedure[7]. To a 100 mL round bottom flask, 30 mL of oleum was added with a magnetic stir bar. The liquid was cooled 0°C on an ice bath upon which 10 mL of benzylamine was slowly added. After the addition was completed, the solution was removed from the ice bath, allowed to warm to room temperature, and then heated to 80°C on a water bath. After stirring for an hour, the solution was allowed to cool to room temperature and was subsequently poured into 300 mL of dioxane. The precipitate that forms is collected by suction filtration through a paper pad in a Buchner funnel and is washed with 50 mL addition dioxane. The collected solid is dissolved in a minimal amount of ammonium hydroxide. Slow and careful addition of concentrated hydrochloric acid affords 5 grams of product as a white precipitate.

3,3'-(1,2-diaminoethane-1,2-diyl)dibenzenesulfonic acid (DPE-SA). DPE-SA was synthesized according to previously published procedures[8] with slight modifications. Five grams of (1R,2R)-1,2-diphenylethane-1,2-diamine are slowly added to 25 mL of fuming sulfuric acid in a 100 mL round bottom flask equipped with a magnetic stir bar. The solution is heated to 100° C for 3 hours while stirring. After

cooling, the solution is cautiously added to 150 mL of cool THF. The product precipitates as a mixture of isomers which is isolated by filtration. Isomers are separated on a phenomenex Luna 10 µm-PREP C18(2) column measuring 250 x 21.20 mm using a 20 mM ammonium bicarbonate mobile phase. Solvent was removed from the collected product fraction by rotary evaporation leaving a white solid. ^{1}H NMR δ 7.5 (4H, m), 7.2 (4H, m), 4.3 (2H, m) (Figures 5 and 21).

3.2.4 Meso-1,2-bis(2-hydroxyphenyl)ethylenediamine (HPED)

The following syntheses for the formation of HPED were reproduced from previously published procedures by Vogtle and Goldschmitt[9] with minor variations throughout (Figure 3-2).

N,N'-((1R,2S)-1,2-bis(2-hydroxyphenyl)ethane-1,2-diyl)dibenzamide. In a 250 mL 3-necked round-bottom flask, 1.05 g of benzil was added to 1.06 mL of salicylaldehyde dissolved in 75 mL of ethanol. The flask was equipped with a condenser, a dropping flask, and a thermometer. One (1) mL of ammonium hydroxide dissolved in 20 mL of ethanol is added to the dropping funnel. The ammonium hydroxide solution is added over one hour. The solution was then heated to reflux and allowed to cool after 3 hours. The product crystallizes as a yellow powder and used without further purification in the next step. TLC analysis using a 75:25 ethyl acetate:hexanes produces a spot with an R_f of 0.8. ^{1}H NMR δ 10.0 (2H, s), 8.6 (2H, d, J = 8.6), 7.6 (4H, m), 7.5 (8H, m), 7.0 (2H, m), 6.8 (4H, m), 5.9 (2H, s) (Figure 3-6).

((1R,2S)-1,2-diacetamidoethane-1,2-diyl)bis(2,1-phenylene) diacetate. Ninety (90) grams of N,N'-((1R,2S)-1,2-bis(2-hydroxyphenyl)ethane-1,2-diyl)dibenzamide from the previous reaction are suspended in 250 mL of acetic anhydride in a 500 mL round bottom flask. A magnetic stir bar is added and the suspension is equipped with a condenser. The suspension is heated to reflux for 24 hours upon which it will turn dark brown and then black. Upon cooling, the product crystallizes as a white powder. The product is isolated by filtration and washed with additional acetic anhydride (40% yield) and used immediately in the next step.

1,2-bis(2-hydroxyphenyl)ethylenediamine. Thirty (30 g) of ((1R,2S)-1,2-diacetamidoethane-1,2-diyl)bis(2,1-phenylene) diacetate is suspended in a 1:1 solution of 48% hydrobromic acid: glacial acetic acid in a 250 mL round bottom flask. The flask is equipped with a condenser and heated to 90° C for 3 hours. After the solution is allowed to cool to room temperature, the solid is collected by filtration and dissolved into 200 mL of warm water. The solution is brought to neutral pH by 20% sodium hydroxide and a flaky white solid precipitates as the product. The product is recrystallized from either acetonitrile or benzene. Melting point 184-186 °C. ^{1}H NMR δ 7.3 (2H,m), 7.2 (2H, m), 6.9 (4H, m), 4.3 (1H, s) (Figure 3-7). ^{13}C NMR δ 129.8 (2C, d), 119.3 (1C, s), 118.0 (1C, s), 59.2 (1C, s) (Figure 3-8). MS (M+1) 245 (Figure 3-9).

3.2.5 Dimethylamine Modification

1,2-bis(4-(dimethylamino)phenyl)ethane-1,2-diamine (DMA-DPE) synthesis was reproduced from previously published procedures[10] (Figure 3-3).

2,2'-((1E,1'E)-((1,2-bis(4-(dimethylamino)phenyl)ethane-1,2-diyl)bis(azanylylidene))bis(methanylylidene))diphenol. Meso-1,2-bis(2-hydroxyphenyl)ethylenediamine (2.2 g) is suspended in 33 mL of ethanol in a 100 mL round bottom flask. The flask was equipped with a magnetic stir bar and 3.5 g of 4-(dimethylamino)benzaldehyde was slowly added to the suspension upon stirring. Within 30-60 minutes the suspension slowly turns clear. The solution is stirred for an additional 3 hours upon which the product slowly crystallizes as a yellow solid which is dried in an oven at 60 °C and subsequently used without further purification.

1,2-bis(4-(dimethylamino)phenyl)ethane-1,2-diamine. 2.5 grams of 2,2'-((1E,1'E)-((1,2-bis(4-(dimethylamino)phenyl)ethane-1,2-diyl)bis(azanylylidene))bis(methanylylidene))diphenol from the previous reaction were dissolved in 100 mL of THF in a 250 mL round bottom flask. The solution was

stirred vigorously as 3 mL of concentrated hydrochloric acid were slowly added. A white precipitate forms upon addition of the acid producing the product as a dihydrochloride salt.

3.2.6 Cis-Diol Functionalized Pyrrolidines

(3R,4S)-1-(4-bromophenyl)-3,4-dihydroxypyrrolidine-2,5-dione via tartaric acid. This synthesis was reproduced from previously published procedures with minor deviations[11]. To a 250 mL round bottom flask was added 2 g of meso-tartaric acid followed by 100 mL of xylenes. 2 g of p-bromoaniline was added and flask was equipped with a Dean-Stark apparatus. The solution was then heated to reflux until the reaction was complete (approx. 10 hours). Upon cooling, the product precipitates and is collected by filtration. The product is recrystallized from ethanol.

N-(4-bromophenyl) maleanilic acid[12]. In a 250 mL round bottom flask equipped with a reflux condenser, 18 g of maleic anhydride are dissolved into 150 mL of MTBE. To this, 31 g of 4-bromoaniline dissolved in 60 mL of MTBE are added over 30 min. After stirring the solution for an additional hour a white solid crystallizes. The solid maleanilic acid is collected by filtration, washed with 10 mL of MTBE and used in the next step without further purification. ^{1}H NMR δ 13.0 (1H, s), 10.5 (1H,s), 7.6 (2H, d, J = 8.7), 7.5(2H, d, J = 8.7), 6.5 (2H, d, J = 12), 6.3 (2H, d, J = 12) (Figure 3-10)

N-(4-bromophenyl) maleimide [12]. In a 50 mL round bottom flask, 0.8 g of anhydrous sodium acetate was added to 20 mL of acetic anhydride. 5g of N-(4-bromophenyl maleanilic acid are added and the suspension is swirled on a steam bath for an hour resulting in a clear solution. The solution is cooled on an ice bath and 40 mL of cold water is added upon which yellow needles crystallize. The product is collected by filtration and dried in a vacuum oven at 40 °C. (Figure 3- 14) ^{1}H NMR δ 7.7 (2H, m), 7.3(2H, m), 7.2 (2H, s) (Figures 11, 14)

Meso-N-(4-bromophenyl)-3,4-dihydroxy-2,5-pyrrolidinedione via ruthenium catalyzed hydroxylation. The following ruthenium catalyzed hydroxylation reaction was reproduced from a publication by Couturier[13].To a stirred solution of 0.020 g of ruthenium chloride hydrate in 10 mL of water was added a solution of 2 g N-(4-bromophenyl)maleimide dissolved in 5 mL ethyl acetate and 5 mL acetonitrile. The solution is cooled to 0° C and then 12 equal portions of 0.25 g sodium periodate were added to the solution. The slurry was allowed to cool between additions. Upon reaction completion, the slurry was quenched with a solution of 1.8 g sodium thiosulfate dissolved in 5 mL water. The slurry was filtered to remove solids and the solids were rinsed with 5 mL of ethyl acetate. The filtrate was transferred to a separation funnel and after the organic and aqueous layers separate, the aqueous layer was discarded. The organic layer was washed three times with a 2 M sodium chloride solution. After washing, the organic was dried with magnesium sulfate and concentrated by rotary evaporation to 1 mL. The flask was then cooled to 5° C and 5 mL of hexanes were added. The product crystallized as a white solid. ^{1}H NMR δ 7.7 (2H, m), 7.2(2H, m), 6.1 (2H, s), 4.5 (2H, s) (Figure 3-12, 15)

Meso-N-(4-bromophenyl)-3,4-dihydroxy-2,5-pyrrolidinedione via manganese catalyzed hydroxylation. The following manganese catalyzed hydroxylation was reproduced from previous published work by Saisaha et al[14]. In a 100 mL round bottom flask equipped with a magnetic stir bar, 0.03 g of manganese perchlorate, 0.03 g of pyridine 2-carboxylic acid and 2 g of N-(4-bromophenyl)maleimide are dissolved into 25 mL of acetone and cooled to 0° C. 167 µL of 6 M sodium acetate are added followed immediately by 1 mL of 50% hydrogen peroxide solution. The mixture is allowed to warm to room temperature and stirred for an additional 16 hours. Sodium bisulfite is added to the solution until excess peroxide is destroyed (checked by peroxide strip indicator). The suspension is filtered and solvent is removed by rotary evaporation producing the product as a white solid. (Figure 3-17)

(3aR,6aS)-5-(4-bromophenyl)-2,2-dimethyldihydro-4H-[1,3]dioxolo[4,5-c]pyrrole-4,6(5H)-dione[15]. To a 100 mL dry round bottom flask under argon is added 2 g of Meso-N-(4-bromophenyl)-3,4-dihydroxy-2,5-pyrrolidinedione from the previous reaction and a magnetic stirring bar. 25 mL of 2,2-dimethoxypropane, 25 mL of cyclohexane, and 0.1 g of p-toluenesulfonic acid are added and the flask is equipped with a dry vigruex column attached to a dry condenser and receiving flask. The mixture is heated to reflux to remove azeotropes and the solution will turn a dark red. The solution is kept under argon and heat for 1-2 days until the reaction reaches completion as checked by HPLC. (Figure 3-18) ^{1}H NMR δ 7.7 (2H, m), 7.3(2H, m), 5.1 (2H, s), 1.47 (6H, d, J = 3.8) (Figure 3-13)

(3aR,6aS)-5-(4-bromophenyl)-2,2-dimethyltetrahydro-4H-[1,3]dioxolo[4,5-c]pyrrole via Lithium Aluminum Hydride Reduction[11]. All glassware for this reaction was dried in an oven at 150°C for at least 24 hours prior to reaction and the reaction was kept under argon until workup. To a 250 mL round bottom flask was added 100 mL of dry THF under a stream of argon. 0.3 g of (3aR,6aS)-5-(4-bromophenyl)-2,2-dimethyldihydro-4H-[1,3]dioxolo[4,5-c]pyrrole-4,6(5H)-dione from the previous reaction was dissolved and the solution was cooled on an ice bath. 0.1 g of lithium aluminum hydride was added in small portions to the reaction. The flask was equipped with a reflux condenser and was heated to reflux for 24 hours while stirring. After the solution was allowed to cool, the vessel was placed on an ice bath and sequential additions of water (2 mL), 15% NaOH (2 mL), and water (6 mL) were added. The solution was extracted with ethyl acetate and the solvent evaporated. The resultant residue was analyzed by HPLC-UV showing severe product degradation (Figure 3-19).

(3aR,6aS)-5-(4-bromophenyl)-2,2-dimethyltetrahydro-4H-[1,3]dioxolo[4,5-c]pyrrole via $NaBH_4/I_2$[16]. All glassware for this reaction was dried in an oven at 150°C for 24 hours prior to use. To a 250 mL round bottom flask under argon is added 0.3 g of (3aR,6aS)-5-(4-bromophenyl)-2,2-dimethyldihydro-4H-[1,3]dioxolo[4,5-c]pyrrole-4,6(5H)-dione dissolved in 30 mL of dry THF. 0.3 g of

$NaBH_4$ is added under an argon stream. The solution is stirred and put on an ice bath and 0.2 g of starting material is added. The flask is equipped with a dropping funnel and 0.5 g of I_2 dissolved in 30 mL of dry THF are added over 30 minutes. The flask is then equipped with a reflux condenser and the solution is refluxed for over 18 hours. After the solution is allowed to cool, 5 mL of methanol is cautiously added. As HPLC-UV analysis shows a chromatogram more complicated than expected, the solution was not worked up.

3.3 Results and Discussion

3.3.1 Sulfonic Acid Modification of Benzylamine and Diphenylethylenediamine

In order to achieve a reagent that fulfills the previously described objectives, we sought to create modified versions of BA and DPE, which possesses a sulfonic acid substituent. p-Aminomethylbenzene sulfonic acid (ABS) was a relatively easy reagent to produce using slightly modified procedures which have previously been published. Sharov et al. have shown that this reagent accomplishes many of the goals we had hoped to accomplish with reagent modification[7]. Chief among these goals were the additional hydrophilicity the sulfonic acid adds to the product upon completion of derivatization and a longer stokes shift seen in the product fluorescence. In addition, we also show how it can be used for analyte purification using the sulfonic acid as an affinity handle for ion exchange chromatography (see chapter 4). Due to its ease of acquisition and utility in derivatization reactions, we sought to produce a similar analog based upon DPE.

The approach to create a sulfonic acid modified DPE was expected to be as straight forward as ABS synthesis (Figure 3-1). However, a publication from 2013 revealed a series of isomers is created when DPE is heated in fuming sulfuric acid[8]. Moreover, this series of isomers has the potential to create a needlessly complicated product distribution when used for derivatization. The same publication provided a means of product purification (detailed description of a preparative HPLC column and mobile

phase) that were not reproducible in our laboratories. Their methodology utilized an isocratic separation by preparative HPLC using a 20 mM potassium chloride mobile phase on a Varian Dynamax column measuring 250 X 10 mm. No further information was reported in that publication about particle dimensions, mobile phase velocity, or injection size. Through discussions with technical personnel from Agilent (Varian products were acquired by Agilent in 2009) the 5µm Zorbax C18 phase was claimed to be the same phase as previously supplied by Varian. As a result the Agilent preparative column (9.4 mm x 250 mm) was acquired for purification of the sulfonated DPE product mixture. Unfortunately baseline resolution of the three isomers could not be achieved with the so-called equivalent phase. Examination of other phases next turned to the evaluation of a Phenomenex Luna 10 µm-PREP C18(2) column measuring 250 x 21.20 mm. The Luna column did not resolve the two minor product isomers, but provided baseline resolution of the major product isomer we sought to isolate (Figure 3-20). As the different column provided a means of product isolation, it was used in subsequent separations with further modifications to chromatographic conditions.

During testing of column selectivity, we decided to see if diamine stereochemistry was important to the separation. To test this, we conducted the sulfonation reaction with S,S-1,2-diphenylethylenediamine, and then separately with meso-1,2-diphenylethylenediamine. Previous work had shown that diamine stereochemistry did not affect the derivatization reaction. There was an interest to see if meso-1,2-diphenylethylenediamine could be used instead of the published S,S-1,2-diphenylethylenediamine as the meso isomer is only 25% the cost of the S,S isomer. By using a cheaper version, we could accomplish our goal of producing higher quantities of the reagent in a cost efficient manner. Unfortunately, the product mixture obtained from sulfonation of the meso-diamine exhibited a much different separation selectivity than those of the other optical isomer, which was used in the previously noted publication, so efforts utilizing it were halted.

The next obstacle to overcome with regards to DPE-SA purification arose due to the nature of the isomer separation. The published method utilized a 20 mM KCl mobile phase. Upon collection of the desired isomer and subsequent solvent evaporation, the resulting solid consisted of a majority salt with a minor amount of desired sulfonic acid. To find an easy way to desalt the collected isomer, we hypothesized that an SPE separation could provide an easy means of capturing the product while washing away the salt. A phenomenex Strata X-AW 33 µm polymeric weak anion exchange cartridge was used to see if the product could be easily purified through anion exchange. Initial attempts failed to retain the product within the salty solvent composition.

In tandem with testing purification by extraction, we also hypothesized that the purification could proceed in a much easier fashion if there was a way to remove the high salt content from the chromatography. During test separations involving different mixtures of water, methanol, and acetonitrile as mobile phases, it became rapidly apparent that separation of the different isomers was dependent upon the presence of the potassium chloride. With the need for salt to achieve separation, it was then hypothesized that if the salt content was switched from a non-volatile mobile-phase additive to a salt that could be evaporated during subsequent solvent removal, the isomer purification could be completed in a one-step separation. Towards this end, the 20 mM potassium chloride mobile phase was exchanged for a 20 mM ammonium bicarbonate mobile phase (Figure 3-21) which achieved the goal of separating the different isomers using a volatile buffer providing pure reagent for use in derivatization.

3.3.2 Dimethylamine Modification of BA and DPE

During our work producing sulfonic acid modified derivatization reagents, we also sought to elaborate the base structure of BA and DPE by providing a basic substituent. Addition of a dimethylamino-substituent to the derivatization reagents fit the profile of a functional group that would accomplish these goals along with the objectives we sought to accomplish for general derivatization

reagent previously described. It was proposed that a tertiary amine could be used as an affinity handle, would aid in ionization during mass spectrometry analysis, and would influence fluorescence emission. Fortunately, p-dimethylaminobenzylamine (DMA-BA) was commercially available and did not require synthesis. A DPE analog was not commercially available and required synthesis.

A 2008 publication which describes the creation of functionalized DPE analogs reported the synthesis of the desired 1,2-bis(4-(dimethylamino)phenyl)ethylenediamine (DMA-DPE) (Figure 3-3). Such synthesis required benzaldehyde with the desired functional group modification and 1,2-bis(2-hydroxyphenyl)ethylenediamine (2HPED) that is used as a templating reagent for creation of new DPE analogs[10]. The required starting materials, benzaldehyde for DMA-DPE synthesis and 2HPED, are commercially available; however, 2HPED is used as a starting material for synthesis of certain cisplatin[17] anticancer drugs, and it was found to be both expensive and frequently of limited supply. To address these issues, its preparation was undertaken.

The synthesis of 2HPED was first reported in an 1884 publication by Japp and Hooker[18]. The reaction involves benzil in the presence of ammonium hydroxide and salicylaldehyde to form an intermediate diimine. This complex rapidly undergoes a diazo-Cope rearrangement as characterized by Vogtle and Goldschmitt[9]. Subsequent acetylation of both the alcohols and amines creates a tetra-acetyl compound, which was hydrolyzed using strong acid at high temperature (Figure 3-2), to provide the desired meso-2HPED, the critical template for the preparation of various DPE analogs. In the present case, 2HPED was used for preparation of DMA-DPE.

As meso-2HPED was the most straightforward template diamine to prepare, it was used in subsequent diazo-cope rearrangements and caused the synthesis of the desired DMA-DPE to proceed slowly, as compared to the previously noted required reaction times. The reference procedure used R,R-HPED as opposed the meso isomer we produced. Previous publications from the same group confirmed

that the meso isomer undergoes rearrangement up to 30 times slower. The reason for this is the R,R isomer is “pre-organized” so that its transition state can more easily form hydrogen bonds between the phenolic hydrogens and bridging amines that aid in driving the reaction towards completion[19]. Subsequently, we altered the reaction times of the critical steps (aided by monitoring reaction progress by HPLC) and developed appropriate overall procedures for the synthesis and obtained the desired DMA-DPE product. Of note, shortly after our successful synthesis of the meso-DMADPE, the R,R-DMADPE became commercially available, thus mitigating against the need for further synthesis of this particular product.

3.3.3 Cis-diol Functional Group as a Desired Analog

Following the successful synthesis of DMA-DPE, steps were taken to produce a DPE analog that possessed a cis-diol functional group. Incorporation of this specific functional group not only imparts needed hydrophilicity onto DPE but also has been shown to be valuable as an affinity handle for boronate affinity chromatography. A BA version of this derivatization reagent, which incorporated a cis-diol attached through a pyrrolidine ring, had been successfully synthesized and used for 3-nitrotyrosine purification, enrichment, and analysis [20].

Our approach in synthesizing a DPE based derivatization reagent that incorporated a cis-diol was the same approach used for synthesizing DMA-DPE, except in place of the simple tertiary amine, we sought to replace the dimethylamine with a pyrrolidine ring containing a cis-diol. To achieve this, we sought to create 4-((3S,4R)-3,4-dihydroxypyrrolidin-1-yl)benzaldehyde. We could then use the newly created benzaldehyde in the previously described diaza-cope rearrangement to produce the desired cis-diol-DPE (Figure 3-4).

Our first priority in producing the desired benzaldehyde was a facile way of generating a cis-diol substituted pyrrolidine. In what appeared to be an easy way to accomplish this goal, we pursued the

reaction of aniline with meso-tartaric acid in xylenes at elevated temperatures following a related preparation which used benzylamine instead of aniline[21]. While this reaction successfully generates the expected cis-diol pyrrolidine dione, at the high temperatures necessary to generate the pyrrolidine dione, the diol found on meso-tartaric acid racemizes creating a mixture of the desired cis-diol and an undesired trans-diol. As this finding is supported by literature[22], a different approach was explored for cis-diol formation.

In order to generate the pure cis-diol pyrrolidine dione, an approach similar to previously synthesized pyrrollidine diol derivatization reagents was used [20]. This involved the well-established formation of N-phenyl maleimide[12] followed by oxidation to create the desired cis-diol. In an effort to avoid the use of highly toxic osmium tetroxide, which had been previously used for the formation of the cis-diol, ruthenium chloride was first used for oxidation as it had been well established as a means to generate the desired diol stereochemistry[13]. While we were successful in synthesis of the desired cis-diol pyrrolidine dione, the reaction was not reliably reproducible. The main issue with the reaction is the need to control reaction temperature. The reference procedure used cautioned against allowing the temperature to rise above 5° C, as this can lead to over-oxidation and oxidative scission[23]. We found that over-oxidation occurs when the temperature rises above 0 °C (Figures 15, 16). An alternative cis-hydroxylation procedure that uses manganese as a catalyst in the presence of hydrogen peroxide[14] was chosen as a superior route, as it not only avoids the previously encountered problems with over-oxidation (Figure 3-17), but avoids tedious cleanup of periodate salts generated in the ruthenium chloride reaction.

The next step in producing the desired benzaldehyde was the reduction of acquired pyrrolidine dione to pyrrolidine. It has been reported that reduction of pyrrolidine dione can be accomplished by using lithium aluminum hydride[11]. Problems with this approach became readily apparent while the

reaction was monitored. In several attempts to effect the reduction, it was found that several side products were generated (Figure 3-18). While such reductions have previously been reported as successful, a critical review of the literature reveals that for this particular substrate type that undesired side products are frequently encountered[11, 24]. In an effort to avoid side product formation, we attempted to reduce the n-phenylpyrrolidinedione with sodium borohydride in the presence of iodine. This approach was based on prior successful reports of very similar substrates. Although the reaction proceeded in a cleaner fashion than the previously explored lithium aluminum hydride reaction, side product generation was still an issue, as reductive cleavage of carbon-carbon bonds is reported as a problem with this route of reduction [25]. As considerable effort had been put forth to produce cis-diol pyrrolidine benzaldehyde without success, efforts were redirected towards development of other successfully synthesized derivatization reagents and pyrrolidinedione reduction was no longer pursued.

3.4 Conclusions

The goal of the current work was creation of novel derivatization reagents through synthetic modification of existing derivatization reagents in an effort to improve solubility, stability, chromatographic properties, and sensitivity at the time of detection. BA and DPE provided the base reagents for modification. The attempted modifications included addition of sulfonic acid, addition of a tertiary amine, and addition of a cis-diol.

Addition of sulfonic acid to BA to produce ABS had been previously accomplished. The same approach was used to successfully produce the sulfonic acid modified DPE and the product was purified for use by preperative chromatography. Acquisition of BA and DPE modified by addition of a tertiary amine was accomplished as the desired DMA-BA was commercially available and published procedures to produce DMA-DPE via diaza-cope rearrangement were successfully utilized within our lab. Several different approaches to synthesize a DPE modified by addition of a cis-diol were taken. The

condensation reaction between meso-tartaric acid and aniline was found to produce an unusable racemic mixture. While two different oxidative approaches at cis-diol synthesis were successful, subsequent attempts at pyrrolodinedione reduction through utilization of both lithium aluminum hydride and sodium borohydride were not successful which halted any further pursuits of cis-diol modified DPE.

3.5 Chapter 3 Figures

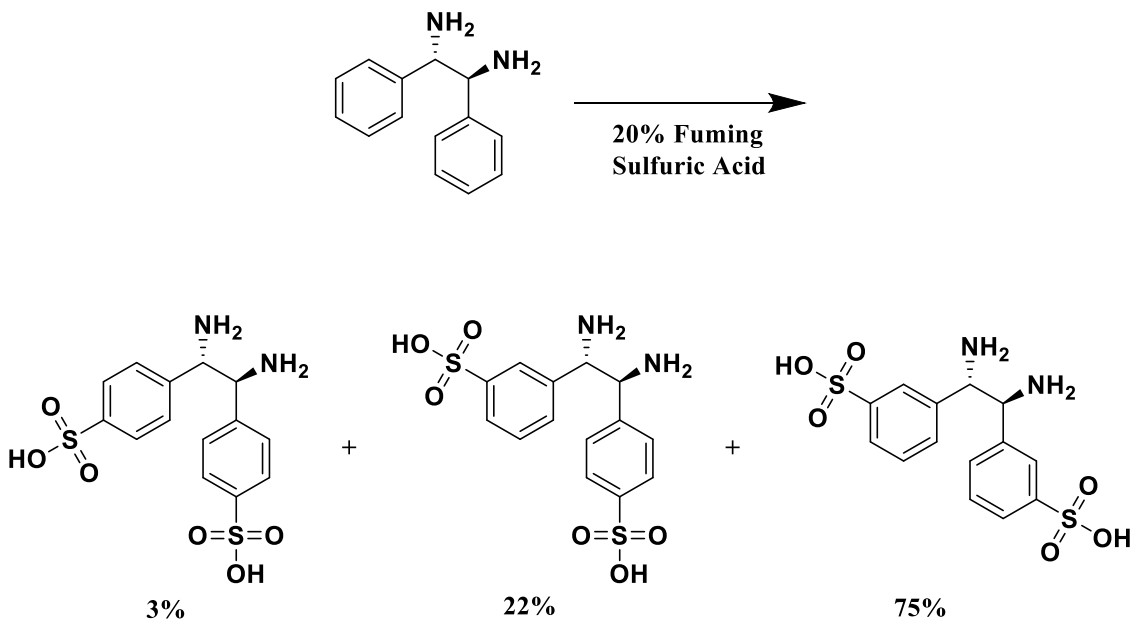

Figure 3-1. Reaction scheme showing distribution of isomers that result from the reaction of DPE with fuming sulfuric acid.

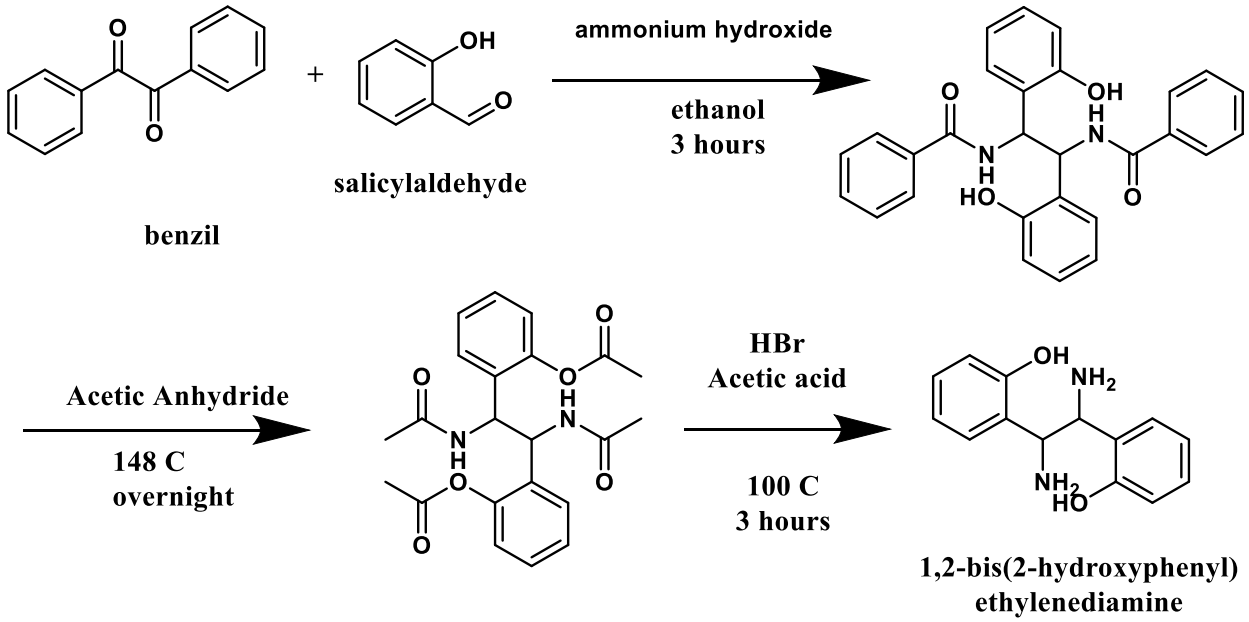

Figure 3-2. Reaction scheme used for the synthesis of template diamine 2HPED[9].

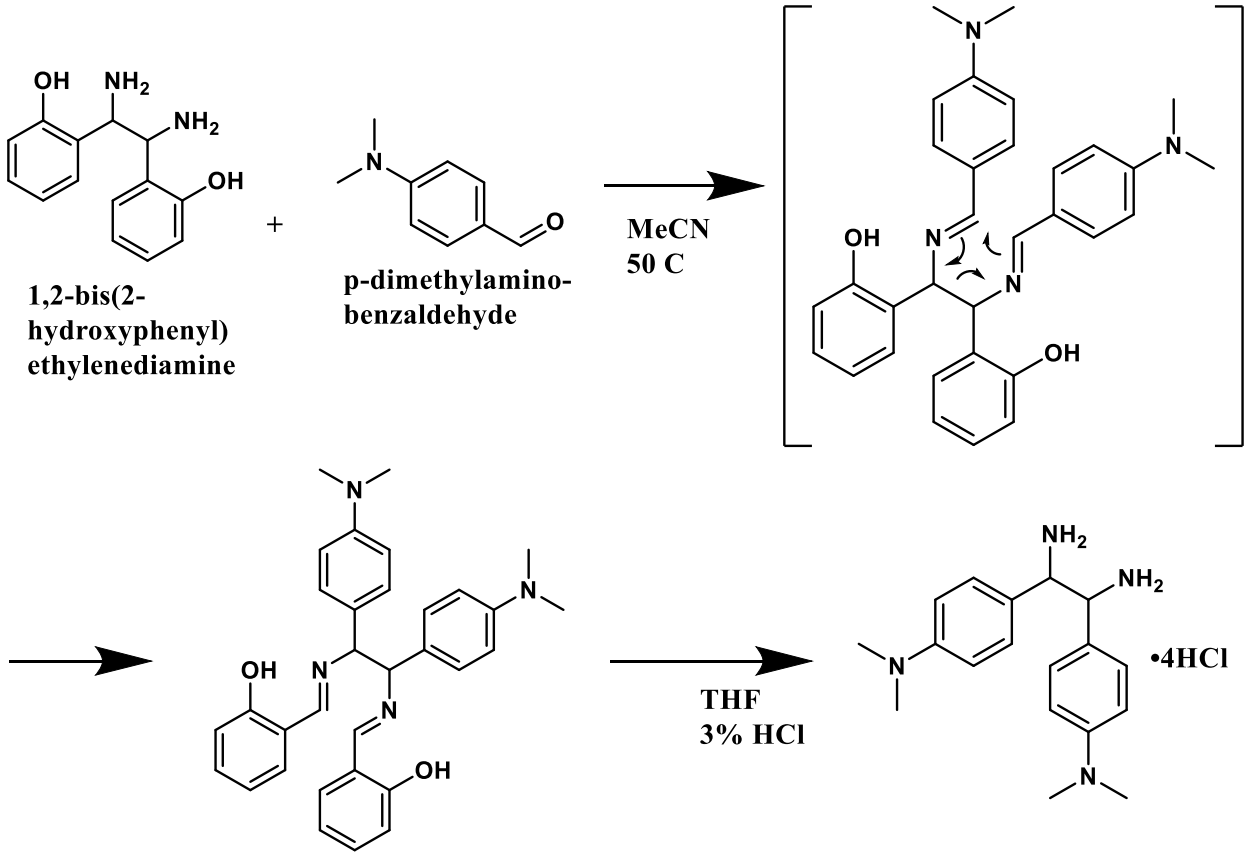

Figure 3-3. Diaza-Cope rearrangement utilizing p-dimethylaminobenzaldehyde to synthesize DMA-BA[10].

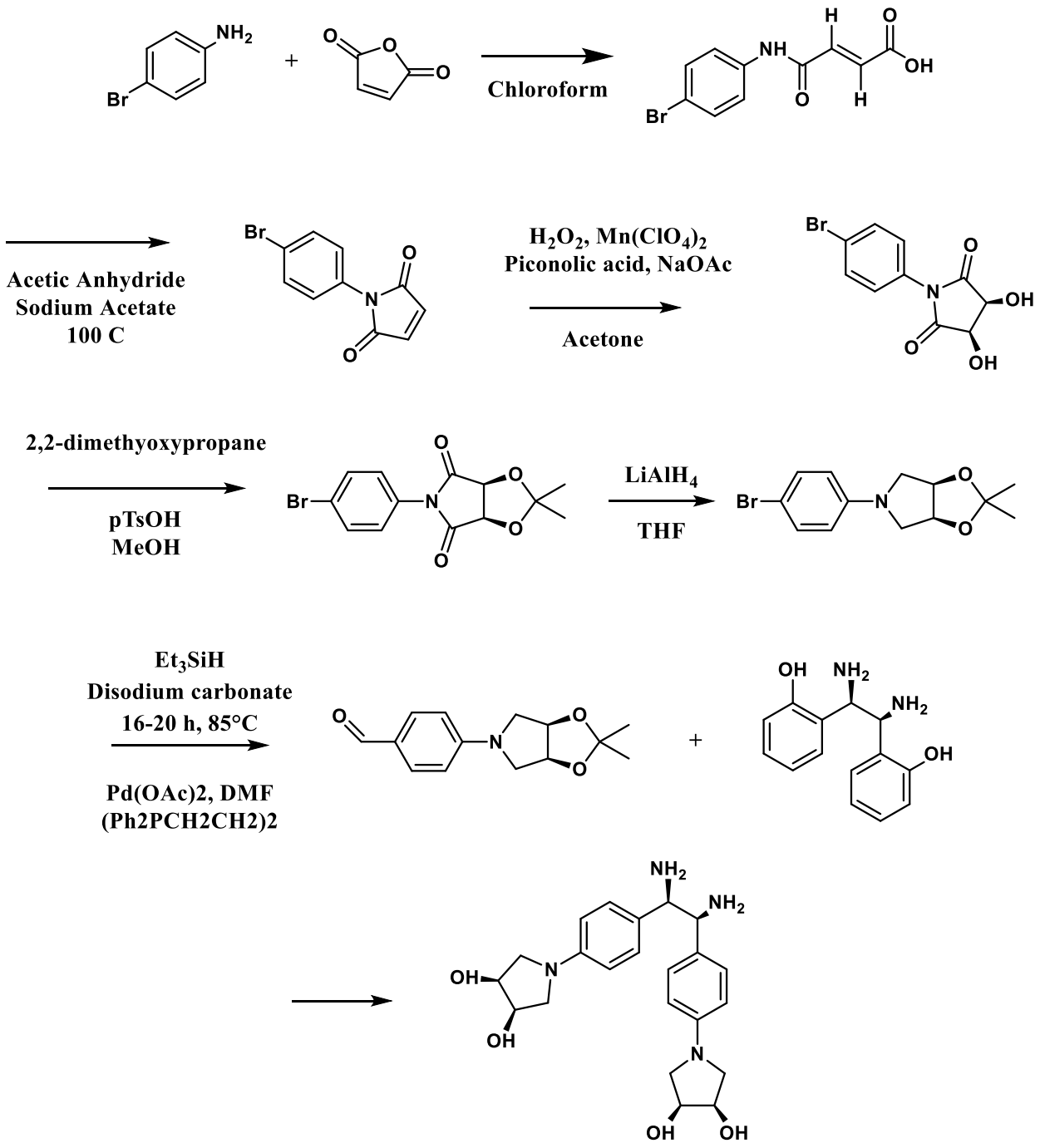

Figure 3-4. Proposed synthetic scheme for creation of a novel DPE analog from N-(p-bromophenyl)maleimide which incorporates a cis-diol functional group attached through a pyrrolidine ring.

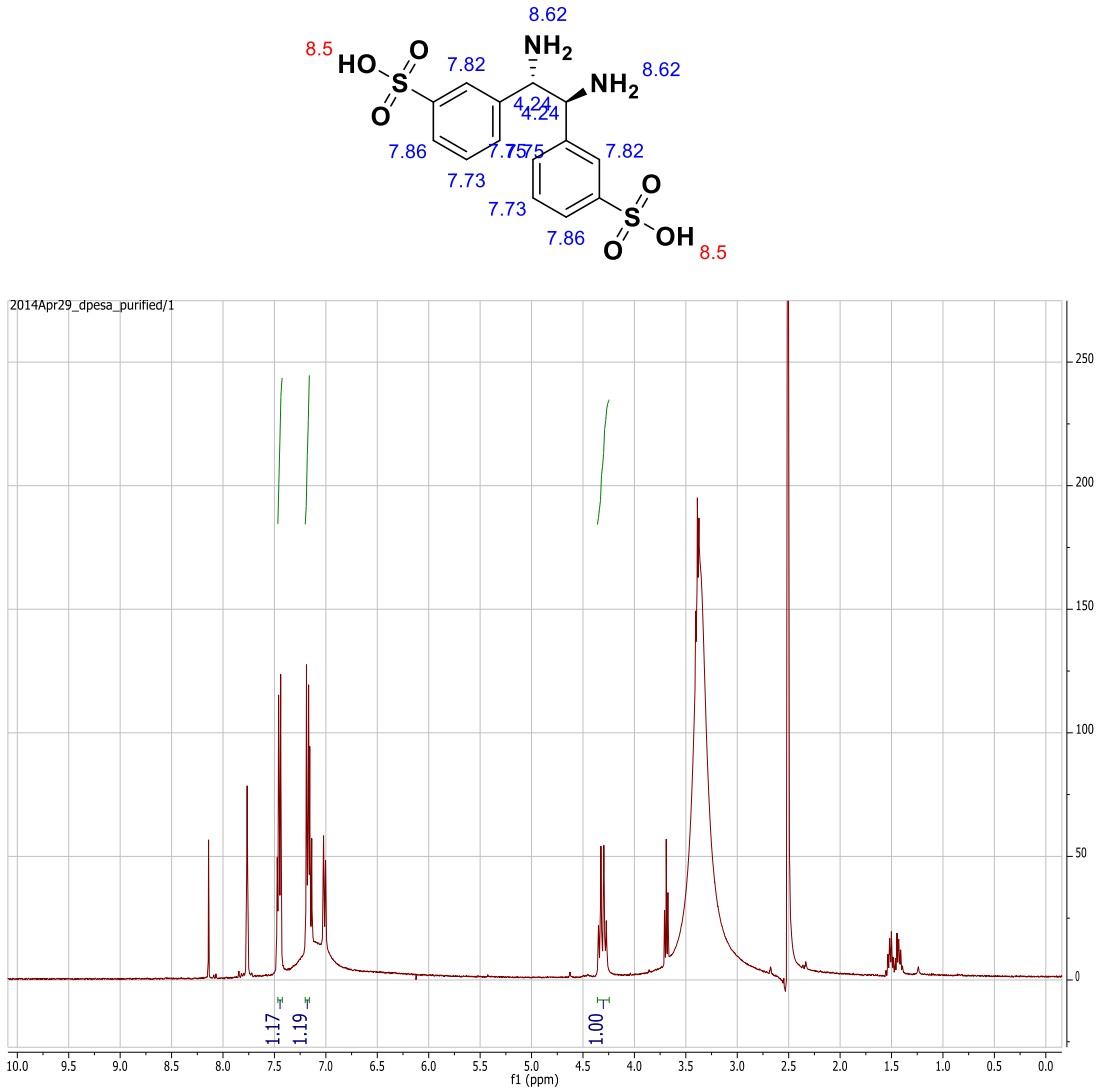

Figure 3-5. ^{1}H NMR spectra for DPE-SA.

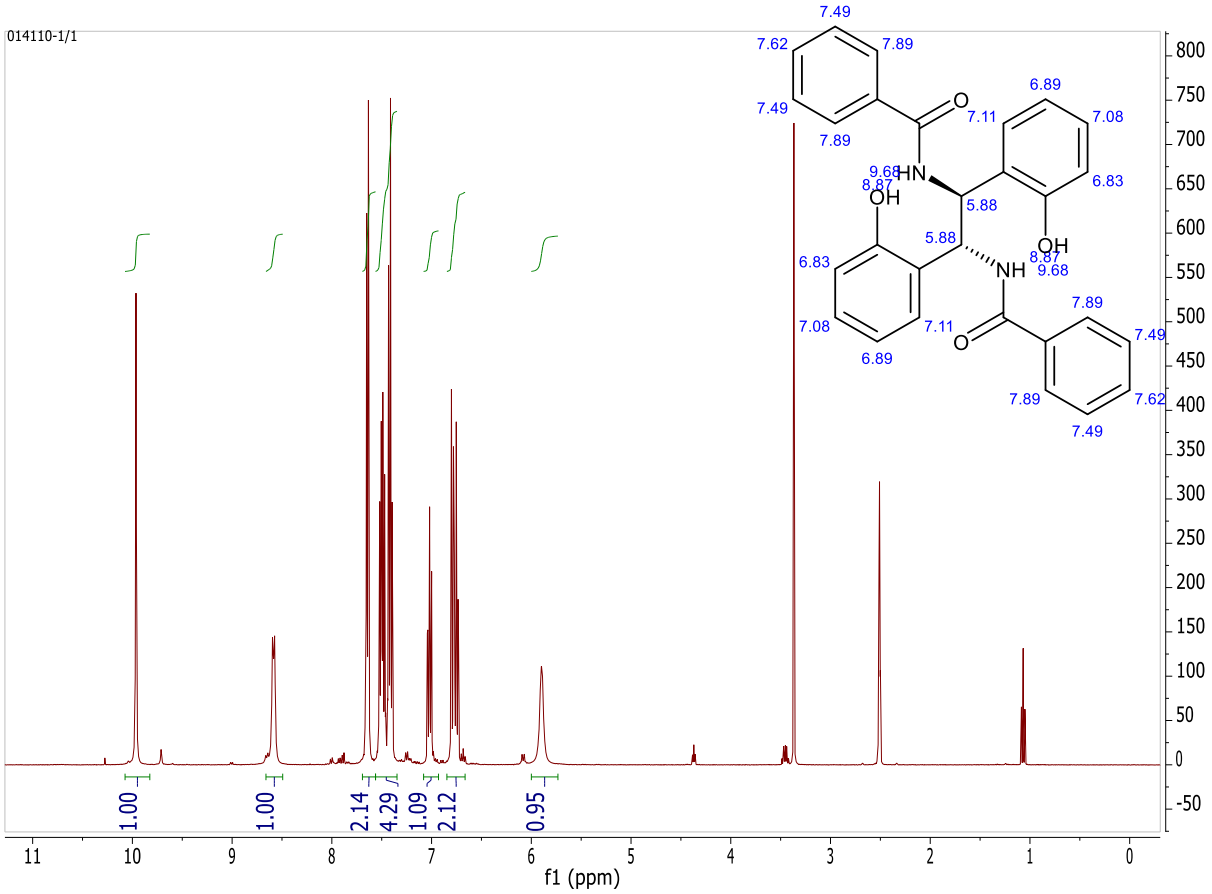

Figure 3-6. ^{1}H NMR Spectra for N,N'-(1,2-bis(2-hydroxyphenyl)ethane-1,2-diyl)dibenzamide.

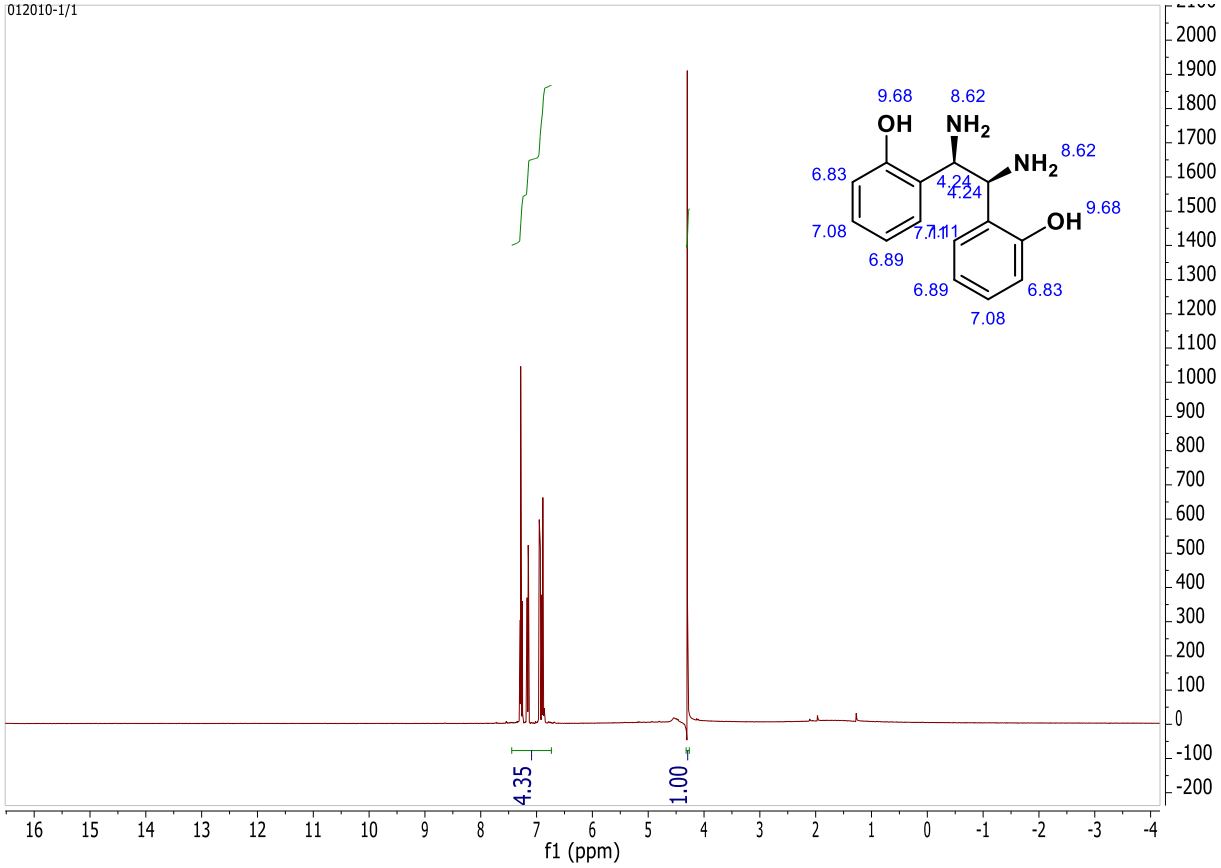

Figure 3-7. ^{1}H NMR for 1,2-bis(2-hydroxyphenyl)ethylenediamine

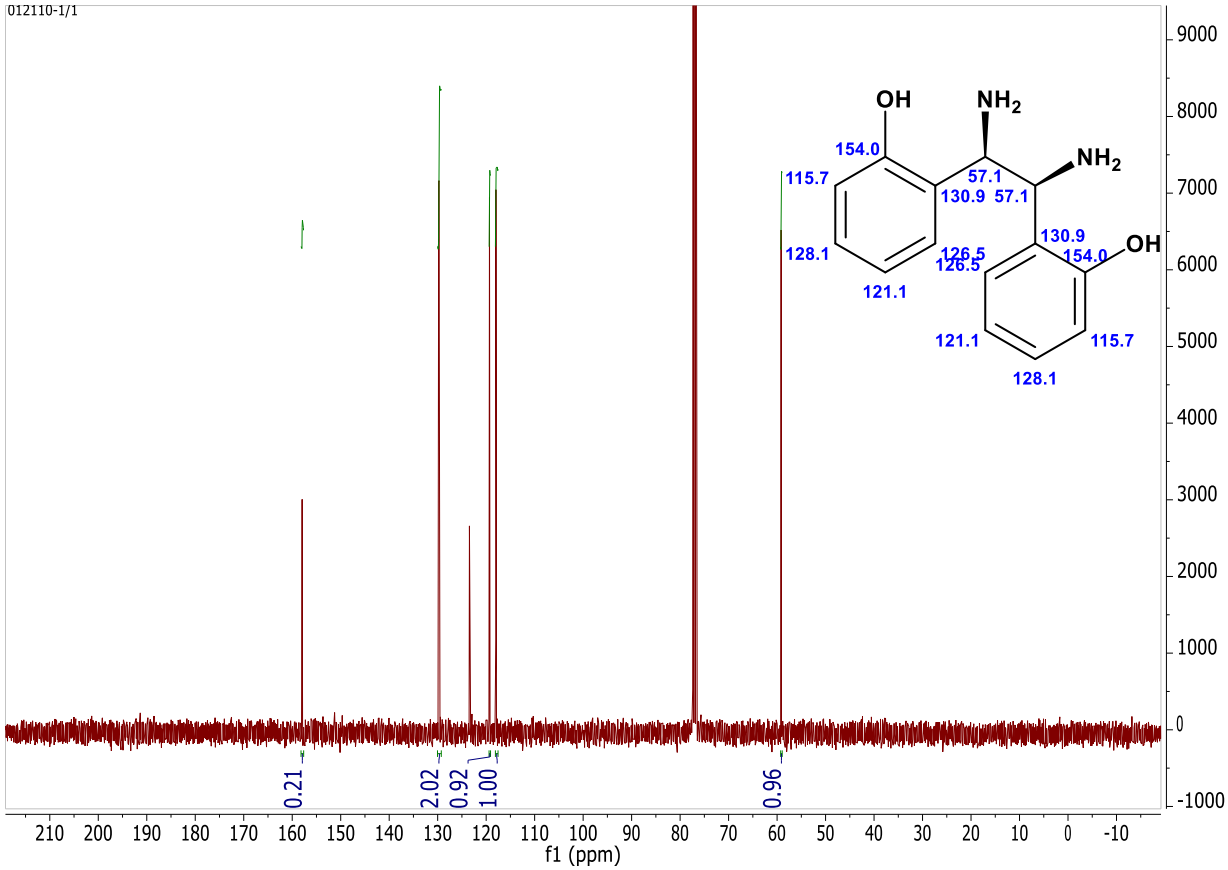

Figure 3-8. ^{13}C NMR for 1,2-bis(2-hydroxyphenyl)ethylenediamine.

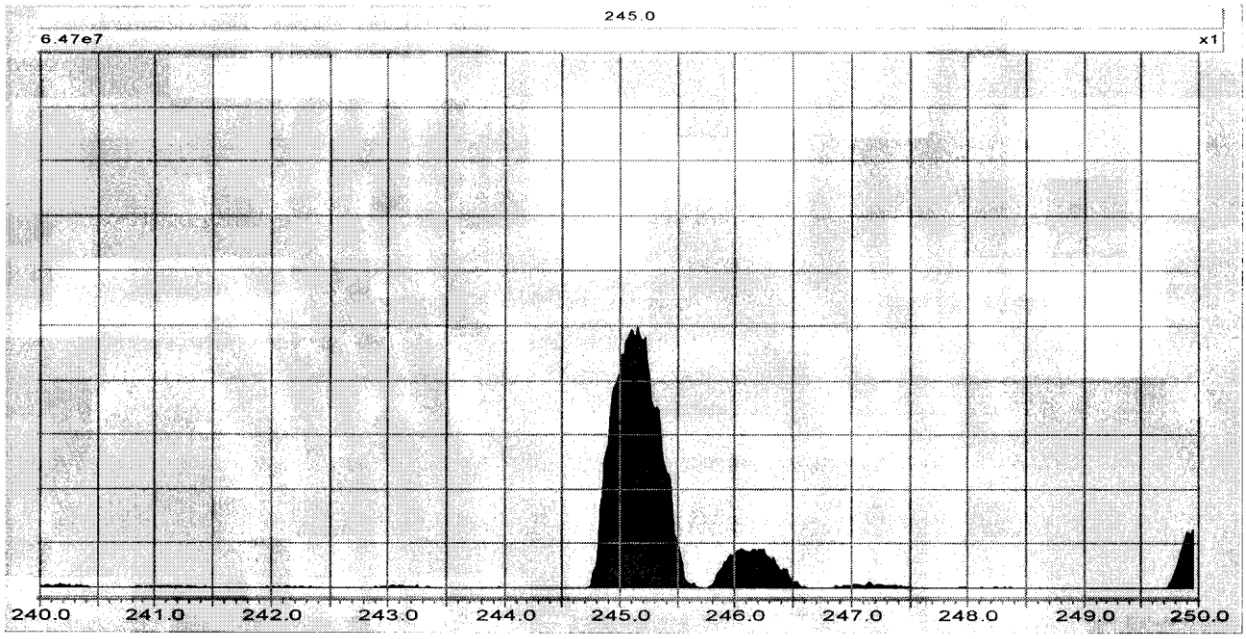

Figure 3-9. Mass spectra scan from 240 amu's to 250 amu's showing (M+1) for 1,2-bis(2-hydroxyphenyl)ethylenediamine.

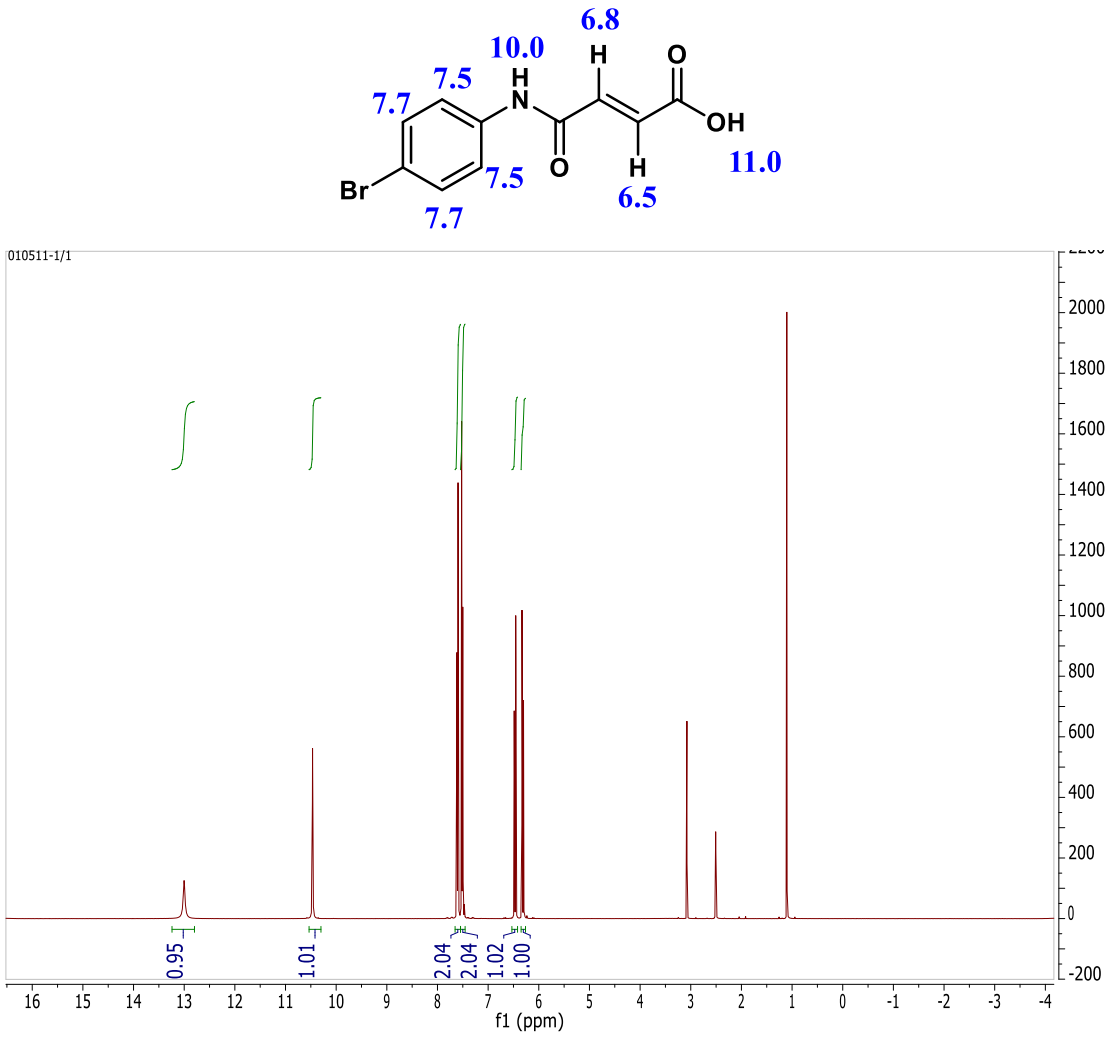

Figure 3-10. ^{1}H NMR for N-(4-bromophenyl)maleinilic acid.

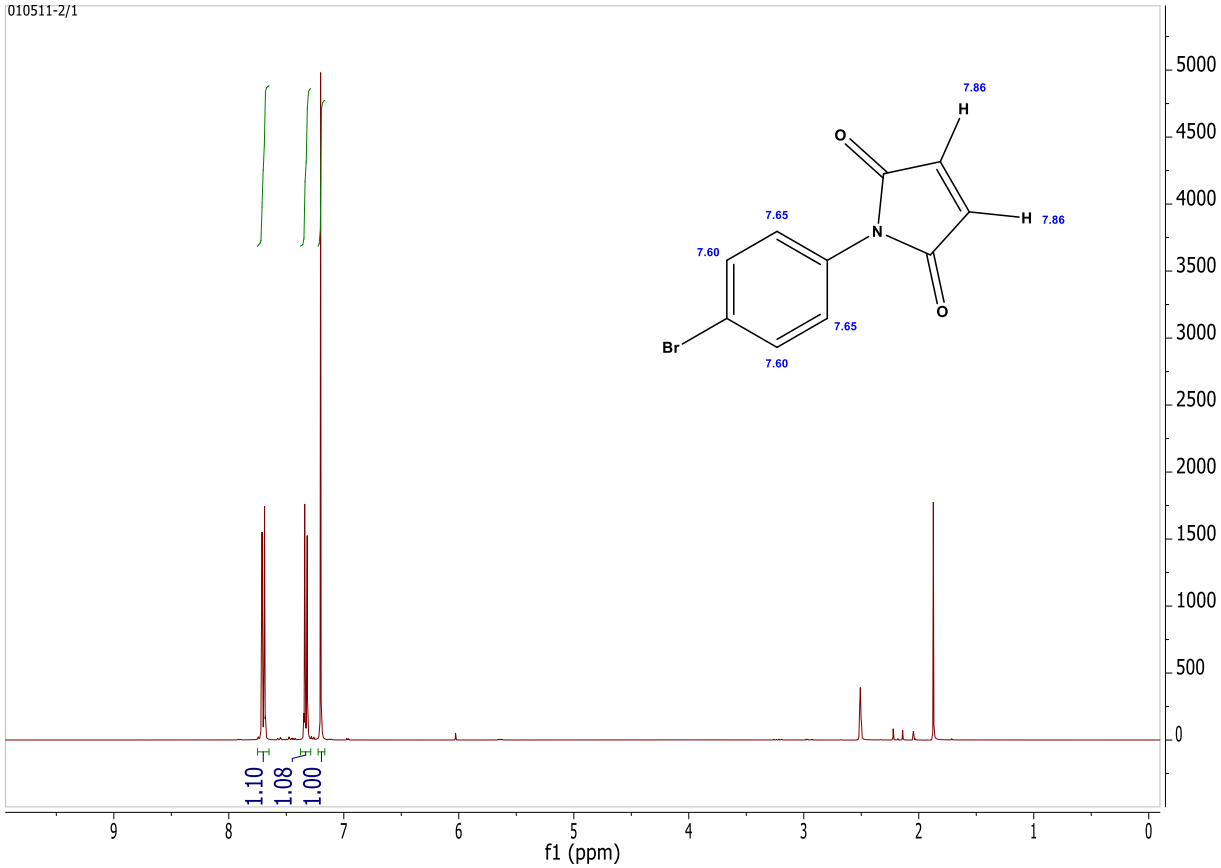

Figure 3-11. ^{1}H NMR for N-(4-bromophenyl)maleimide.

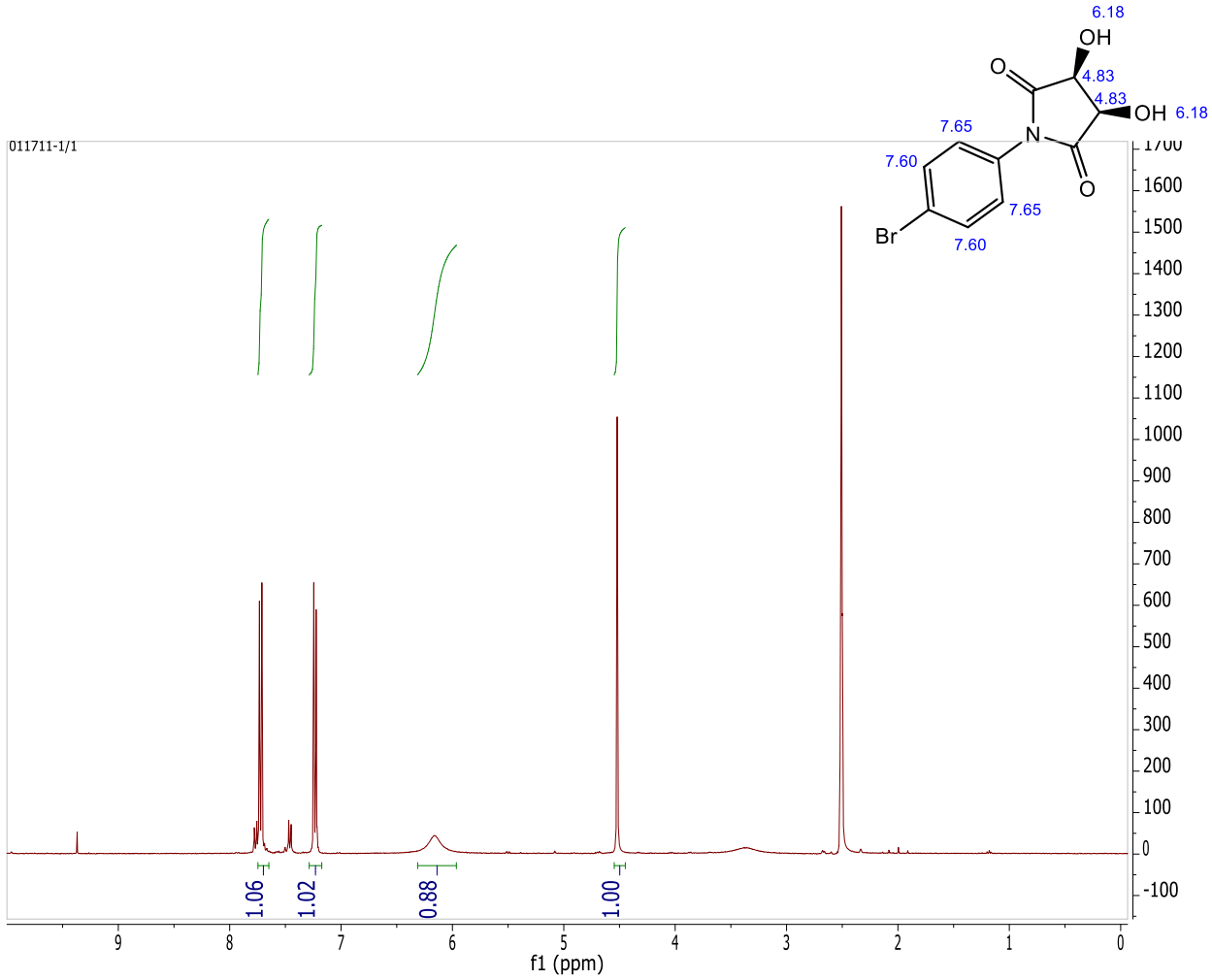

Figure 3-12. ^{1}H NMR for meso-n-phenyl-3,4-dihydroxy-2,5-pyrrolidinedione.

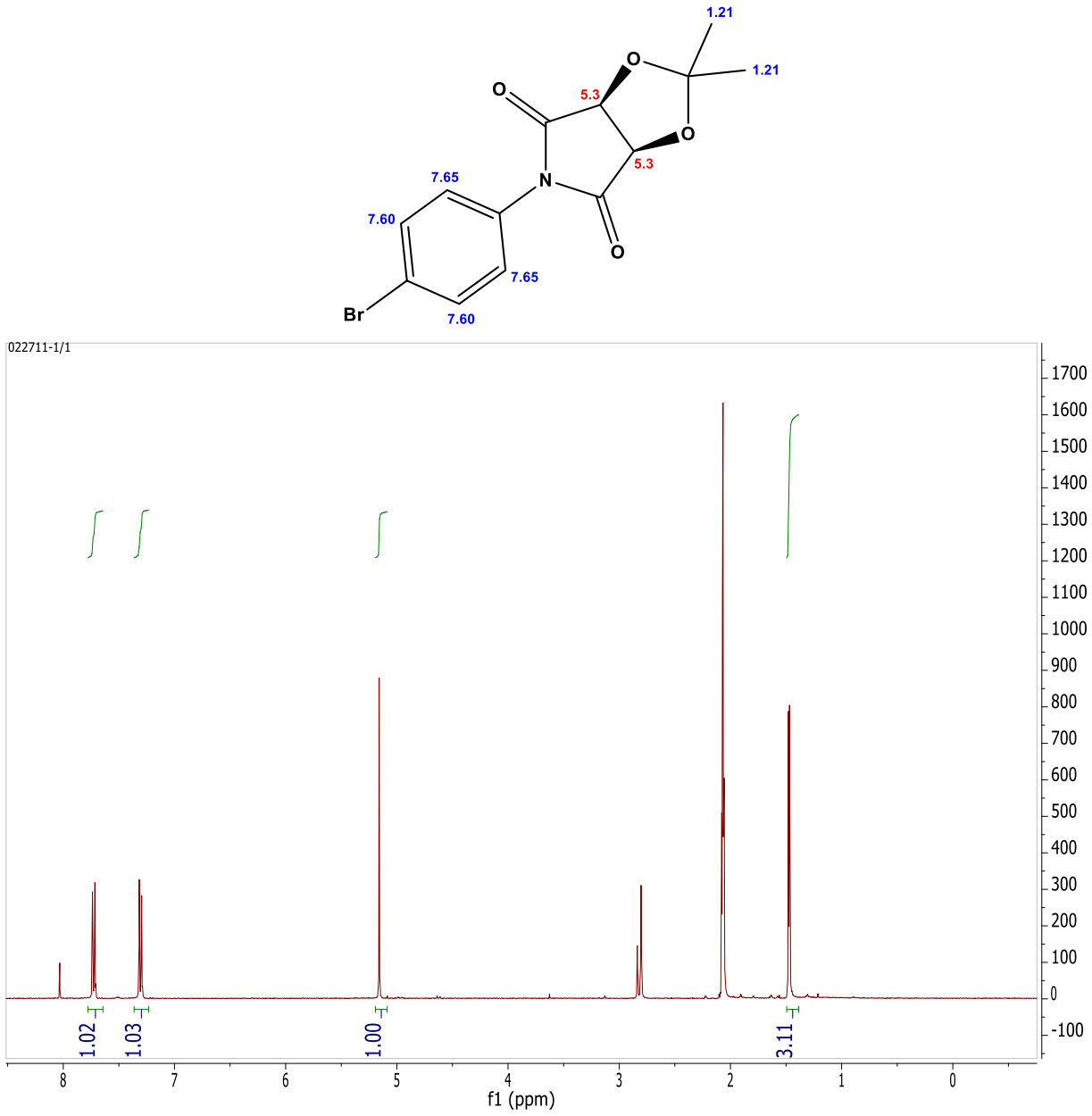

Figure 3-13. ^{1}H NMR for (3aR,6aS)-5-(4-bromophenyl)-2,2-dimethyldihydro-4H-[1,3]dioxolo[4,5-c]pyrrole-4,6(5H)-dione

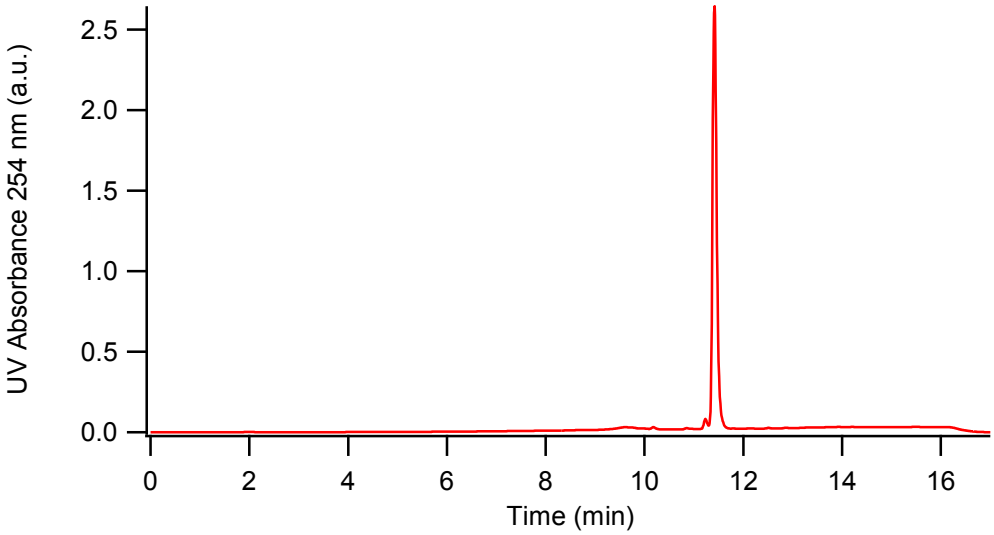

Figure 3-14. HPLC-UV chromatogram showing 99% purity for N-(4-bromophenyl)maleimide.

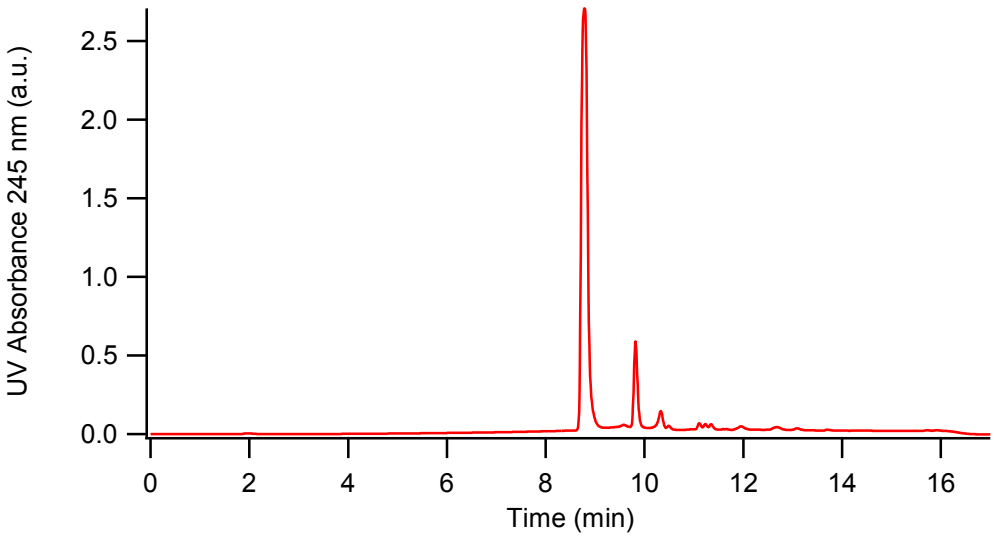

Figure 3-15. Reaction products from the ruthenium catalyzed hydroxylation reaction showing meso-n-phenyl-3,4-dihydroxy-2,5-pyrrolidinedione eluting at 8.9 min with side product from over oxidation showing at 9.8 min.

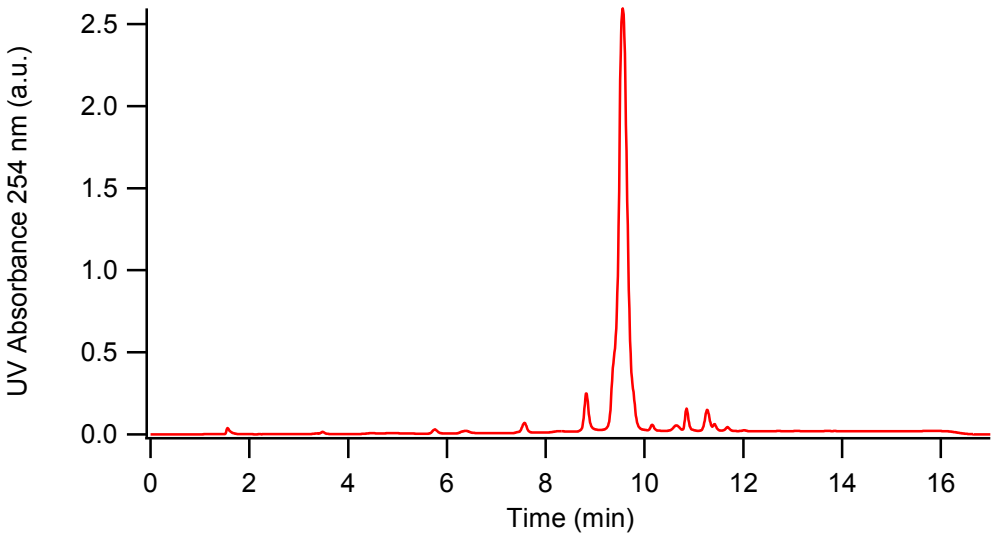

Figure 3-16. Ruthenium catalyzed hydroxylation showing over oxidized product from the ruthenium hydroxide catalyzed oxidation of N-(4-bromophenyl)maleimide which occurs when temperature rises above 0°C.

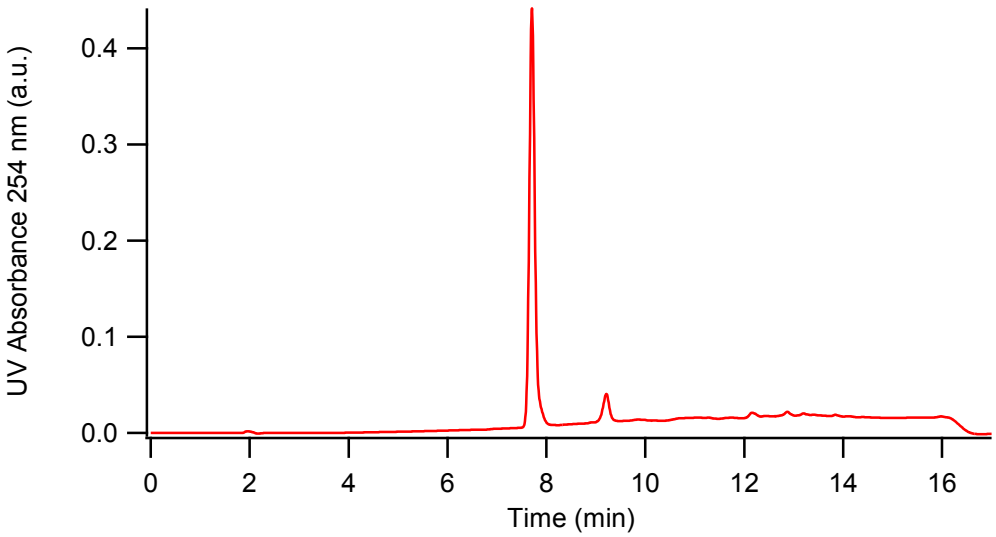

Figure 3-17. Product from the manganese catalyzed hydroxylation reaction showing product meso-n-phenyl-3,4-dihydroxy-2,5-pyrrolidinedione exhibiting 96% purity.

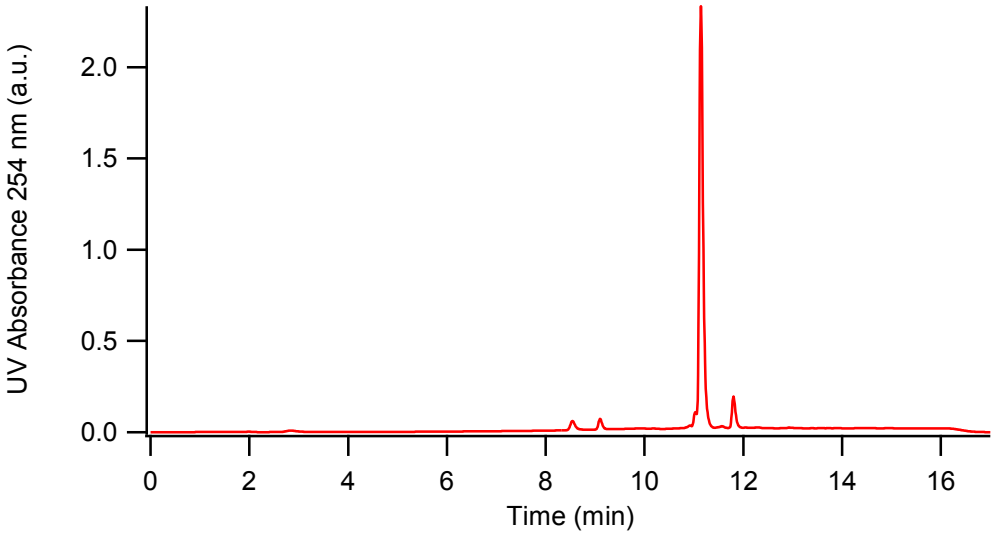

Figure 3-18. Pure (3aR,6aS)-5-(4-bromophenyl)-2,2-dimethyldihydro-4H-[1,3]dioxolo[4,5-c]pyrrole-4,6(5H)-dione product from the cis=diol protection reaction.

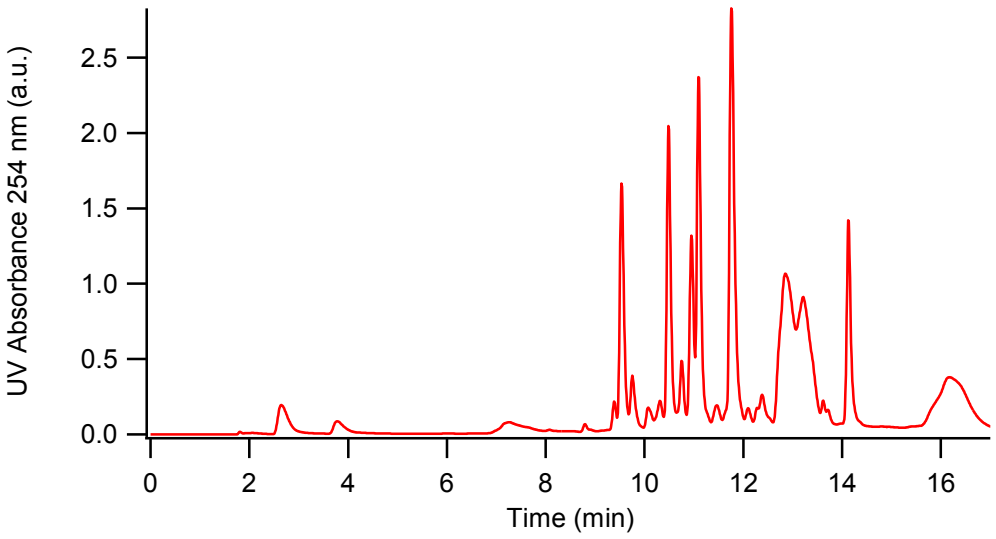

Figure 3-19. HPLC-UV chromatogram of the solid residue produced from the lithium aluminum hydride reduction of (3aR,6aS)-5-(4-bromophenyl)-2,2-dimethyldihydro-4H-[1,3]dioxolo[4,5-c]pyrrole-4,6(5H)-dione.

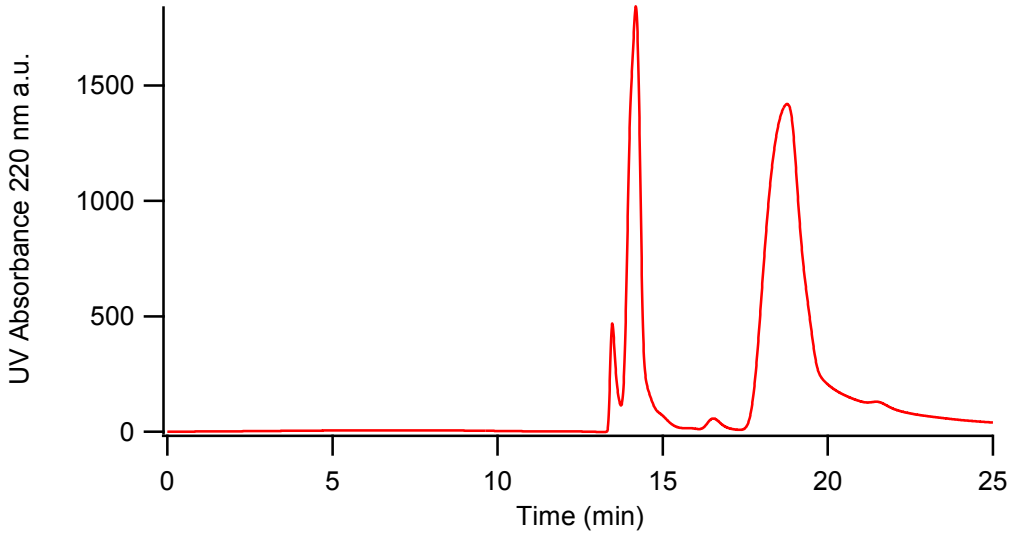

Figure 20. Separation of DPE-SA isomers on a phenomenex Luna 10 µm C18-2 250 X 21.20 mm column using 20 mM KCl mobile phase DPE with fuming sulfuric acid.

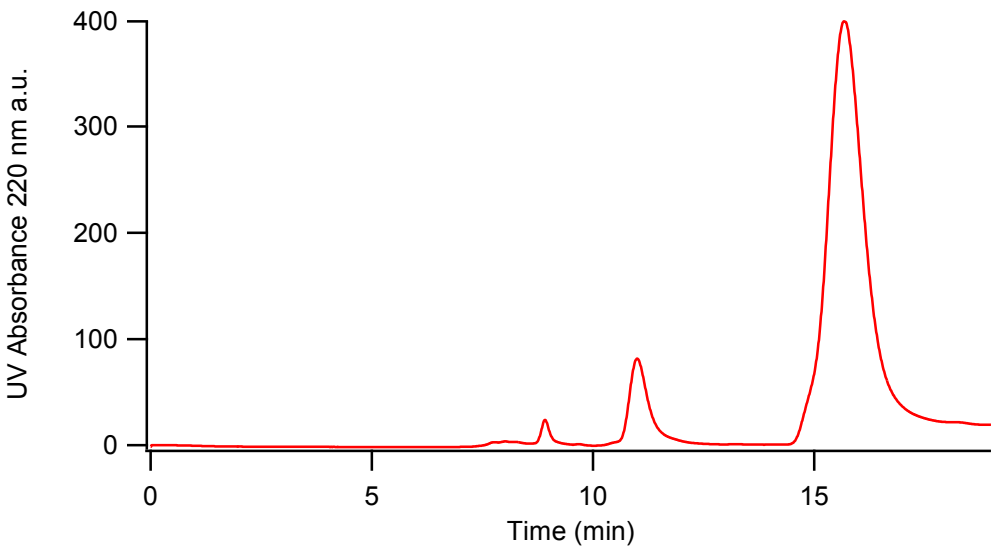

Figure 3-21. HPLC-UV chromatogram showing baseline resolution of all three isomers resultant from the reaction of DPE in fuming sulfuric acid on a phenomenex Luna 10 µm C18-2 250 X 21.20 mm column using 20 mM ammonium bicarbonate buffered mobile phase of which the major peak was collected for future derivatization reactions.

3.6 Chapter 3 References

[1] J. A. Field, *Journal of Chromatography A* **1997**, *785*, 239-249.
[2] J. M. Rosenfeld, *Journal of Chromatography A* **1999**, *843*, 19-27.
[3] G. Nikov, V. Bhat, J. S. Wishnok and S. R. Tannenbaum, *Anal Biochem* **2003**, *320*, 214-222.
[4] N. Abello, H. A. Kerstjens, D. S. Postma and R. Bischoff, *J Proteome Res* **2009**, *8*, 3222-3238.
[5] Q. Zhang, W. J. Qian, T. V. Knyushko, T. R. Clauss, S. O. Purvine, R. J. Moore, C. A. Sacksteder, M. H. Chin, D. J. Smith, D. G. Camp, 2nd, D. J. Bigelow and R. D. Smith, *J Proteome Res* **2007**, *6*, 2257-2268.
[6] S. A. Margolis, *Applied Biochemistry and Biotechnology* **1993**, *43*, 161-161.
[7] V. S. Sharov, E. S. Dremina, N. A. Galeva, G. S. Gerstenecker, X. Li, R. T. Dobrowsky, J. F. Stobaugh and C. Schoneich, *Chromatographia* **2010**, *71*, 37-53.
[8] J. Li, X. Li, Y. Ma, J. Wu, F. Wang, J. Xiang, J. Zhu, Q. Wang and J. Deng, *RSC Advances* **2013**, *3*, 1825-1834.
[9] F. Vögtle and E. Goldschmitt, *Chemische Berichte* **1976**, *109*, 1-40.
[10] H. Kim, Y. Nguyen, C. P. Yen, L. Chagal, A. J. Lough, B. M. Kim and J. Chin, *J Am Chem Soc* **2008**, *130*, 12184-12191.
[11] A. M. d. A. Rocha Gonsalves, M. E. S. Serra, D. Murtinho, V. F. Silva, A. Matos Beja, J. A. Paixão, M. Ramos Silva and L. Alte da Veiga, *Journal of Molecular Catalysis A: Chemical* **2003**, *195*, 1-9.
[12] A. A. D. M. P. Cava, K. Muth, and M. J. Mitchell, *Organic Synthesis* **1961**, *41*.
[13] M. Couturier, B. M. Andresen, J. B. Jorgensen, J. L. Tucker, F. R. Busch, S. J. Brenek, P. Dubé, D. J. am Ende and J. T. Negri, *Organic Process Research & Development* **2001**, *6*, 42-48.
[14] P. Saisaha, D. Pijper, R. P. van Summeren, R. Hoen, C. Smit, J. W. de Boer, R. Hage, P. L. Alsters, B. L. Feringa and W. R. Browne, *Organic & Biomolecular Chemistry* **2010**, *8*, 4444-4450.
[15] K. A. N. Eugene A. Mash, Shawne Van Deusen, and Susan B. Hemperly, *Organic Synthesis* **1990**, *68*, 92.
[16] M. J. M. McKennon, A. I.; Drauz, Karlheinz; Schwarm, Michael, *Journal of Organic Chemistry* **1993**, *58*, 3568-3571.
[17] a) G. Bernhardt, R. Gust, H. Reile, H. D. vom Orde, R. Muller, C. Keller, T. Spruss, H. Schonenberger, T. Burgemeister, A. Mannschreck and et al., *J Cancer Res Clin Oncol* **1992**, *118*, 201-208; b) R. Muller, R. Gust, G. Bernhardt, C. Keller, H. Schonenberger, S. Seeber, R. Osieka, A. Eastman and M. Jennerwein, *J Cancer Res Clin Oncol* **1990**, *116*, 237-244.
[18] F. R. Japp and S. C. Hooker, *Journal of the Chemical Society, Transactions* **1884**, *45*, 672-685.
[19] a) H.-J. Kim, H. Kim, G. Alhakimi, E. J. Jeong, N. Thavarajah, L. Studnicki, A. Koprianiuk, A. J. Lough, J. Suh and J. Chin, *Journal of the American Chemical Society* **2005**, *127*, 16370-16371; b) H. Kim, Y. Nguyen, A. J. Lough and J. Chin, *Angew Chem Int Ed Engl* **2008**, *47*, 8678-8681.
[20] E. S. Dremina, X. Li, N. A. Galeva, V. S. Sharov, J. F. Stobaugh and C. Schoneich, *Anal Biochem* **2011**, *418*, 184-196.
[21] D. Rejman, P. Kočalka, M. Buděšínský, R. Pohl and I. Rosenberg, *Tetrahedron* **2007**, *63*, 1243-1253.
[22] Y. Fricke, N. Kopp and B. Wünsch, *Synthesis* **2010**, *2010*, 791-796.
[23] a) B. Plietker, *Tetrahedron: Asymmetry* **2005**, *16*, 3453-3459; b) B. Plietker, *J Org Chem* **2004**, *69*, 8287-8296; c) B. Plietker and M. Niggemann, *Org Biomol Chem* **2004**, *2*, 2403-2407; d) T. K. M. Shing, E. K. W. Tam, V. W. F. Tai, I. H. F. Chung and Q. Jiang, *Chemistry – A European Journal* **1996**, *2*, 50-57.
[24] A. M. d. A. R. Gonsalves, M. E. d. S. Serra, M. R. Silva, A. M. Beja, J. A. Paixão and L. A. d. Veiga, *Journal of Molecular Catalysis A: Chemical* **2001**, *168*, 53-59.
[25] E. R. Burkhardt and K. Matos, *Chem Rev* **2006**, *106*, 2617-2650.

Chapter 4

Comparison of Derivatization Reagent Analogs towards Protein-Bound 3-Nitrotyrosine Analysis

4.1 Introduction

4.1.1 Protein Bound 3-Nitrotyrosine as an Analytical Target

Protein bound 3-nitrotyrosine (P3NY) is a post-translation modification that results from nitroxidative stress. Its formation and accumulation have been related to several age related diseases such as cancer, Parkinson's, and ALS[1]. As this specific modification is an established biomarker of said disease states, analytical strategies which take advantage of this knowledge for diagnostic purposes are just becoming available. Additionally, while P3NY has been shown to form through several different nitrosative pathways, the protein structural features that are responsible for increased susceptibility to nitration have not been conclusively defined[2].

Analysis of P3NY is complicated by several factors. First among these is the low abundance of the modification. With respect to plasma proteins subjected to inflammatory conditions, approximately one in 10,000 tyrosine residues are nitrated [3]. Within the context that tyrosine residues constitute only three to four molar percent of proteins[2], any technique that attempts P3NY detection needs to exhibit inherently low detection limits. The sample matrix further complicates the challenge of low abundance determinations of 3NY. Analysis of biological tissues requires expertise beyond standard analytical techniques[4]. Favored methodology for identification of post-translational modifications involves protein isolation, protein digestion, and detection by LC-MS/MS. However, within the field of proteomics, robust methodologies for analysis of P3NY do not exist. In order to better understand the nature of P3NY formation, and more importantly what conditions lead to formation in vivo, better analytical strategies need to be developed. Such strategies must have low limits of detection, specificity towards the analyte, and compatibility towards the matrix where the analyte resides. These requirements can be met through chemical derivatization, post-derivatization extraction for sample enrichment, and analysis by LC-MS/MS.

An early example of the use of chemical modification for enhancement of detectability in the amino acid and protein chemistry analysis was the 1963 publication where investigators derivatized amino acids, which allowed for their determination by GC/MS [5]. Through chemical modification, sufficient volatility and thermal stability was imparted to the analyte to allow for determination by GC/MS, which provided for high sensitivity detection. In a similar fashion, our labs strategy to enhance the detectability of P3NY began by creating a fluorescent reporter molecule using derivatization. We have shown that we can increase the detectability of P3NY by first reducing the nitro group on tyrosine to a reactive amine, and subsequently reacting the new species with either benzylamine (BA) or *meso*-1, 2-diphenylethylenediamine (DPE) to form a 6-substitued 2-phenylbenzoxazole[6]. This chemical transformation results in imparting desirable physical properties, namely fluorescence, which improves detectability along with the inherently low detection limits of fluorescence (sub nano-molar in this specific case). Additionally, reaction specificity that only targets ortho aminophenols imparts a high degree of selectivity with regards to proteomic analysis.

4.1.2 Specific goals of recently synthesized reagents

An original objective of the new class of derivatization reagents was improvement of existing fluorescent profiles through modification of the molecule so that the emmission wavelength were longer. BA and DPE derivatization products have been previously shown to display excitation/emission profiles of 360/460 respectively[6]. While such fluorescent properties exhibit a relatively large stokes shift of 100 nm putting this particular profile outside of amino acid fluorescence, there is still enough auto-fluorescence within a biological sample to exhibit a need for longer excitation/emission wavelengths. The modified benzylamine, 4-aminomethylbenzenesulfonic acid (ABS), had been shown to increase the emission wavelength from 460 nm to 490 nm[7]. Encouraged by wavelength changes

through functional group manipulation, we sought to utilize the dimethylamino-substituent as an alternative functional group, which had potential to affect fluorescence in a positive way.

Despite the positive gains in fluorescence attributed to use of ABS, it has been shown during ABS reaction characterization that side product formation can be a concern from BA based derivatization reagents[7a, 8]. As shown in Figure 4-4, two known side products are formed from this derivatization reaction. While it may be impossible to avoid the formation of the minor intra-molecular side product, the issue of the major side product can potentially be addressed. The expected product from DPE based reactions is the same as the major side product from the BA reactions. Moving from BA based reagents to DPE based reagents shifts the product distribution to the major side product from the BA reaction and eliminates the expected BA product. This shift is expected to lead to an inherent increase in reaction yield.

In addition to improving P3NY detection through fluorescence, we also hope to accomplish increased detectability by mass spectrometry. Adding basic functionality to peptides through derivatization has the potential to enhance ionization during positive mode mass spectrometry by adding additional sites that can carry charge. While many derivatization strategies seek to improve ionization through addition of a quaternary amine[9], incorporation of secondary or tertiary amines has been used effectively to increase ionization efficiency in peptides by providing addition basic sites for protonation[10]. Following from these established gains in ionization efficiency, we have incorporated a tertiary amine onto our derivatization reagents with the expectation of increased ionization efficiency during positive mode analysis.

Finally, we hope to incorporate chemical handle for extraction and enrichment of P3NY as a means of increasing detectability. To do so, we looked at ion exchange chromatography as a means of extraction. Extraction of peptides through ion exchange has been previously accomplished by attaching

a quaternary amine through derivatization. The quaternary amine with peptide attached could then be captured by strong cation exchange chromatography[9]. As we already had access to a reagent containing a sulfonic acid, we pursued analyte purification through weak anion exchange solid phase extraction.

The overall goal of the present work was utilization of newly synthesized derivatization reagents that have potential to further enhance detectability of P3NY. Presented here is the work showing the feasibility of the six different reagents produced (previously described in Chapter 3) for derivatization of P3NY and subsequent evaluation to determine which reagent would be the best candidate for further pursuit. The base reagents used for comparison are BA and DPE. Both have been modified by incorporation of a dimethyl amine producing two additional reagents, 4-dimethylaminobenzylamine (DMA-BA) and meso-1,2-bis(4-(dimethylamino)phenyl)ethylenediamine (DMA-DPE). The final two reagents are sulfonic acid modified BA and DPE, ABS and 3,3'-((1R,2R)-1,2-diaminoethane-1,2-diyl)dibenzenesulfonic acid (DPE-SA). Within this work, we show relative fluorescent yields among the six different reaction products. We also compare relative detectability of the six reaction products by mass spectrometry. Results from mass spectrometry also show how product distributions can complicate chromatography from BA based reactions. Finally we show how sulfonic acid modified reagents can be used for ion exchange extraction and enrichment of P3NY.

4.2 Experimental

4.2.1 Reagents and Materials

N-cyclohexyl-3-aminopropanesulfonic acid (CAPS), potassium ferricyanate, benzylamine, meso-1,2-diphenylethylenediamine, and ammonium hydroxide were purchased and used as received from Sigma Aldrich (St. Louis, MO). Methanol, OPTIMA grade acetonitrile with 0.1% formic acid, OPTIMA grade water with 0.1% formic acid were purchased and used as received from Fisher Scientific

(Waltham, MA). Nitrated peptide FSAY(NO_2)LER was purchased at 96% purity from BioMatik and stored at -20° C until use. Purified water was obtained from a Labconco Water ProPS Filtration Apparatus (Labconco Corporation, Kansas City, MO, USA).

4.2.2 Buffers and solutions

A 0.3 M pH 10 CAPS buffer was used for all derivatization reactions. $K_3Fe(CN)_6$ was diluted to 10 mM in CAPS buffer. Stock derivatization solutions were prepared as follows: 0.3 M BA in water, 0.3 M DPE in methanol, 0.1 M p-dimethylaminobenzylamine in 1:1 0.1 M pH 3 acetic acid:methanol, 0.3 M ABS in 1:1 pH 10 CAPS:methanol, 0.1 M DMA-DPE in methanol, 0.1 M DPE-SA in CAPS buffer. 0.1 M pH 3 acetic acid buffer solution and 5% ammonium hydroxide in methanol was used for sulfonic acid extractions.

4.2.3 UPLC-MS/MS

Relative mass spectrometry measurements and derivatization extraction data were recorded on a Waters Synapt G2 quadrupole-tof hybrid mass spectrometer equipped with a nano-electrospray source. Separations carried out pre-ionization utilized a Waters nano-ACQUITY UPLC. The UPLC was set to a single pump-trapping configuration. The trap column used was an ACQUITY UPLC PST C18 nanoACQUITY Trap column measuring 180 µm x 20 mm packed with 5 µm particles. The analytical column was an ACQUITY UPLC HSS T3 nanoACQUITY Column measuring 75 µm x 150 mm packed with 1.8 µm particles. Fisher Scientific OPTIMA grade water with 0.1% formic acid was used for mobile phase A. Fisher Scientific OPTIMA grade acetonitrile with 0.1% formic acid was used for mobile phase B. Following a 1 µL injection, samples were loaded onto the trap column for four minutes with a flow rate of seven µL/min with a 97:3 A:B mobile phase composition. Following trapping operation, a linear gradient program of 3% B to 40% B over 60 minutes was used. A column wash cycle of 85% B for 5

minutes was used after each injection and the column was allowed to re-equilibrate for 10 minutes at 3% B between each injection cycle.

4.2.4 HPLC-FL Detection

Relative fluorescent comparisons of peptide derivatization products were performed on a Shimadzu LC-10 series HPLC consisting of an SLC-10A vp system controller, two LC-10AD vp pumps, and SIL-10AD vp auto-injector and a RXL-10A xl fluorescence detector. Separations were carried out on a Vydac Protein & Peptide C18 column measuring 150 x 2.1 mm packed with 5 µm particles. Mobile phase A contained 0.1% formic acid in water and mobile phase B contained 0.1% formic acid in acetonitrile. Peptides were eluted using a linear gradient program. The program begins at 0% B which is held for 2 minutes followed by a linear increase in B to 60%. The B concentration is then ramped to 100% for the remainder of the run. The column is equilibrated for eight minutes between injections. The fluorescence detector was set to record excitation/emission spectra at 360/475.

4.2.5 Protein Bound 3-nitrotyrosine Derivatization

FSAY(NO_2)LER Reduction. FSAY(NO_2)LER was dissolved in a 0.1% formic acid solution and diluted to 10 µM. The solution was diluted 1:10 into a 10 mM sodium dithionite solution for reduction of the nitro group. During reduction, an Oasis HLB solid phase extraction cartridge was prepared by rinsing with 2 mL methanol followed by 2 mL of 0.1% formic acid. After 5 minutes at room temperature, the peptide solution was loaded onto the Oasis SPE cartridge. The cartridge was washed by 1 mL of water and the peptide was eluted with two 1 mL volumes of methanol. The solvent was evaporated and the captured peptide was reconstituted in a buffer appropriate to derivatization at the same approximate concentration. An aliquot of sample was (20 µL) was injected onto an HPLC column pre and post-extraction to determine relative extraction recovery.

General derivatization scheme. FSAY(NH2)LER was dissolved into a 0.3 M pH 10 CAPS buffer and diluted to approximately 10 µM. 70 µL of pH 10 CAPS buffer, 10 µL of 10 mM K3Fe(CN)6, 10 µl of peptide solution, and 10 µL of 0.1 M derivatization reagent were added successively to a 1 mL autosample vial. The vial was then vortexed and allowed to incubate at room temperature for 2 hours. Vials were then stored at -10° C until analyzed.

4.2.6 ABS extraction

Reduced FSAY(NH_2)LER peptide was spiked into a BSA digest resulting in 1 pmol/µL peptide and 100 fmol/µL digest in a total volume of 100 µL. The solution was derivatized with ABS following the derivatization scheme described above. A 10 µL aliquot of derivatized peptide solution was taken and analyzed by UPLC-MSMS. Meanwhile, a Phenomenex Strata X-AW 33 u Polymeric Weak Anion Exchange cartridge was prepared by flushing with 2 mL of methanol followed by 2 mL of pH 3 acetic acid. The remaining derivatization solution was diluted into 10 mL of pH 3 acetic acid and subsequently loaded onto the SPE cartridge. The cartridge was then washed with 2 mL of pH 3 acetic acid and then 2 mL of methanol. Captured peptide was eluted with a 5% ammonium hydroxide solution in methanol. The solvent was evaporated on a water bath under a nitrogen air stream. The solid was reconstituted in either 100 µL or 1 mL of CAPS buffer and subjected to UPLC-MSMS analysis.

4.3 Results and Discussion

4.3.1 Relative Yields by HPLC-FL

Nitrated FSAY(NO_2)LER was reduced (Figure 4-1), derivatized by six different derivatization reagents (Figures 2 and 3), and analyzed by HPLC to determine relative detectability by fluorescence. The fluorescence detector was set to 360/475 ex/em based on upon previously recorded spectra as all derivatization products show excitation near 360. While 475 is not an emission maximum for any

product, it is an average emission where all products exhibit overlap for detection as BA/DPE products show maxima at 460 and sulfonic acid analogs show maxima at 490.

The first derivatization reagents (BA and DPE) to be compared provide the foundation for all analogs. What is seen in the BA chromatogram (Figure 4-6), which follows from previously published work with ABS[7a], is formation of the DPE product (Figure 4-3). Even though 22% of the BA reaction product is lost to this side product, the comparable DPE reaction only produces a 69% yield relative to the expected benzylamine product (Table 1). From this initial observation, BA could be considered a superior derivatization reagent of the two base reagents despite its potential to generate side products.

When examining the remaining LC-FL chromatograms, it becomes immediately obvious that dimethylamino-substituted products exhibit significantly lower fluorescence intensity when compared to other products (Figures 6 and 7). In initial scouting work using 2-amino-p-cresol as a model for P3NY, the DMA-BA derivatization reagent failed to produce a fluorescence product despite its formation as seen by mass spectrometry. In contrast to those initial results, the DMA-DPE analogue shows fluorescent character with excitation/emission profiles similar to that of DPE and BA (Figure 4-5). The utilization of these two reagents in peptide analysis follows this trend.

DMA-BA and DMA-DPE chromatograms resulting from derivatization at 1 μM peptide concentration show too little fluorescence to make a relevant comparison of the two different tertiary amine reagents. In order to have a more critical evaluation of the different tertiary amine analogs, peptide concentrations were increased 10-fold and derivatized according to the same procedures (Figure 4-8). Examining chromatograms from the DMA-BA reaction with increased concentration, we see no corresponding increase in observed fluorescence. This leads to the conclusion that observed peaks are not derivatization product peaks. This is contrary to the more concentrated DMA-DPE reaction in which an increase in analyte concentration is directly proportional to an increase in fluorescence

intensity as expected. These results show DMA-BA is a reagent not worth pursuing as it does not produce an expected fluorescent product. As DMA-DPE does produce expected fluorescence, it is the reagent worth pursuing of the tertiary amine derivatization analogs.

The remaining derivatization reagents for comparison are the sulfonic acid analogs of BA and DPE: ABS and DPE-SA. Both exhibit much lower fluorescence intensity than either BA or DPE. In the chromatogram for ABS derivatization, one observes the previously reported side products (Figure 4-6). The DPE-SA product is seen in the ABS chromatogram constituting 23% of the total product yield. At the wavelengths used for detection, the ABS total relative yield is only 40% of the BA product (Table 1).

Upon examination of the DPE-SA chromatogram, two peaks are seen (Figure 4-7). The chromatogram produced by UPLC-MS also shows two closely eluting peaks (Figure 4-11). It is possible that despite extensive work in DPE-SA purification that the purified derivatization reagent still exists as a mixture of isomers. With such a product distribution taken into account, DPE-SA still produces only 7% relative fluorescence intensity compared to BA and only 17% relative fluorescence intensity when compared to ABS. Due to the extensive difficulties from purification of DPE-SA and the less relative fluorescence intensity, ABS would be preferred reagent of the two sulfonic acid analogs.

4.3.2 Relative Detectability by UPLC-MS/MS

Over the course of this investigation, the proteomics field has evolved from its infancy to a more mature discipline. Mass spectrometers have progressed as the de facto detectors within this field when paired with soft ionization techniques such as ESI or MALDI, which as soft-ionization techniques result in minimal peptide fragmentation[11]. In 2010 the University of Kansas acquired a Syanpt G2 to further current research within proteomics. With the necessary technology in place, making enhancements to detectability via derivatization during mass spec analysis has become a primary goal in recent years. Adding basic functionality to peptides through derivatization has the potential to enhance ionization

during positive mode mass spectrometry by adding additional sites that can carry charge. While many derivatization strategies seek to improve ionization through addition of a quaternary amine[9], incorporation of secondary or tertiary amines has been used effectively to increase ionization efficiency in peptides by provide addition basic sites for protonation[10]. Following from these established gains in ionization efficiency, we have incorporated a tertiary amine onto our derivatization reagents with the expectation of increased ionization efficiency during positive mode analysis.

When evaluating relative yields by mass spectrometry, it must be mentioned that yields produced from such analysis are in no way quantitative. Further, several factors play into what determines analyte detectability by mass spectrometry. Mode of acquisition is important within the setting of these comparisons. Although positive mode ionization is generally seen as capable of producing better spectra, it may not be the case for analysis of sulfonic acids. Ionization efficiency must also be considered as a goal of conducting analyte derivatization. Within this context, it should be noted that ionization is a variable which changes during the course of a chromatogram causing as much as a 15% change in relative detectability. The typical means of mitigating such variability is through use of internal standards[12]. This was not done here as it falls beyond the scope of the current project. Finally, while peptide samples could be generated and analyzed repeatedly by HPLC-FL, instrument availability and time restraints for the UPLC-MS limited data collection to single runs per derivatization reagent.

With current limitations on how mass spectrometry data should be considered, some general conclusions and observations could be made about the relative detectability of the six-derivatization products. Upon initial comparison of BA product to DPE product, a 40% gain in ion counts is seen from the DPE product (Table 2). A possible reason for gains in DPE product detectability by mass spectrometry could be from the nature of sample ionization. The BA product requires a higher percentage of the organic modifier for elution. Higher organic composition is generally seen to enhance ionization

efficiency. Because of this, the reason for gains in DPE ionization must stem from structural attributes. When comparing the DPE product structure to the BA product structure, the difference lies at the 6-position of the benzoxazole ring. The BA product carries a benzylamine at said position where the DPE product has a primary amine at the same position. It is possible the primary amine is easier to charge during ESI than the secondary amine from the BA product.

A second surprise resulting from data generated during mass spectrometry analysis is the relatively high abundance of the ABS product when compared to the BA product. One might expect an analyte containing multiple sulfonic acids to be inhibited during positive mode ionization. However, as mobile phase pH has been shown not to affect positive mode ESI[13], such worries can be dismissed. Several possibilities exist for why an enhanced response is attained from ABS derivatization compared to BA derivatization. A direct increase in observable ions could arise if the ABS product has a higher potential to ionize more efficiently than the BA product. A second possibility for the enhanced ionization could be from less product loss due to side product generation. BA derivatization chromatograms reveal a higher percent of side product ions when compared to ABS derivatization from both fluorescent and mass spectrometry data. While mass spectra results are not quantitative, it could point to loss of relative yields because of side product formation.

4.3.3 Side Product Formation and Considerations

It has been previously reported through use of APPD and ABS that side product formation is a concern when BA is used as a derivatization reagent. A general observation from use of these reactions can be made when considering the reaction mechanism. For the reaction to proceed, a 2-aminophenol is placed in an oxidative environment to generate an ortho-quinone imine. This highly reactive intermediate is subject to nucleophile attack by any available nucleophile. In order to mitigate product

loss through side product formation, an unusually large excess of derivatization reagent is used. However, this approach at preventing side product formation is not completely successful.

In the case of the peptide FSAYLER, in addition to the expected 2-phenyl-6-benzylaminobenzoxazole, the N-terminal primary amine participates in an intra-molecular attack at position 6, which results in a cyclic side-product (Figure 4-4). Formation of this product cannot be prevented without previously blocking reactive amines. Within the current studies, the BA derivatization reaction produced 4.3% of the intra-molecular product, while the ABS reaction produced a negligible 0.3% relative ions of the analogous product as determined by mass spectrometry. As a goal of this research is to prevent the need for prior reactive site blocking, the observed 5% product loss is deemed acceptable.

Of higher concern when taking a critical look at peptide derivatization (FSAYLER) data, the product resulting from DPE based reactions is seen to form within BA reactions (Figures 2-4). The reason for the observed DPE product has been speculated to be from reaction with ammonia. While there is no ammonia initially present in the sample, it can be generated from BA oxidative degradation. A general trend for formation of the DPE product within BA based reactions is for 15% of product formation to proceed down this side path. When examining LC-FL chromatograms for both BA and ABS derivatization reactions, DPE side product formation is found to be consistent with the BA reaction producing 22% side product and the ABS reaction producing 23% side product (Table 1). While mass spectra for both of these reactions support correct product identification, the relative ion counts are much more conservative at 3% for BA and 5% for ABS (Table 2).

Examination of LC-FL chromatograms and mass spectra for DMA-BA derivatization reactions reveals no formation of the expected reaction product. Upon further examination of LC-MS chromatograms, masses corresponding to the expected potential side products are observed (Figure 4-

10). Both the DMA-DPE based reaction product and the intra-molecular product are observed to form within the DMA-BA derivatization. Unique to this reaction, the intra-molecular product is observed in higher ion counts than the DPE based product.

Unlike the BA based reactions, DPE based reactions have not been shown to produce side products. Examination of chromatograms produced by mass spectrometry reveals that an intra-molecular product can result from DPE based reactions. However, as the relative ion counts all fall below 0.1% of the expected products, such side product formations can be largely ignored.

4.3.4 ABS purification

As P3NY is an extremely low abundant post-translational modification, increasing detectability through extraction has become a prominent goal. Analyte extraction remains a sure way for sample purification and sample enrichment, both of which can lead to increased selectivity and increased sensitivity[14]. Several different extraction handles have been attempted for P3NY through derivatization reagents. Most recently APPD, a derivatization reagent that contains a cis-diol functional group, has been shown to be a capable derivatization reagent for P3NY. The cis-diol of APPD acts as a handle for extraction when paired with boronate-affinity chromatography[8]. Following the success of APPD, we sought to achieve a reagent capable of extraction with an additional goal of the reagent being easier to acquire.

At the time of this writing, ABS has become an established derivatization reagent for enhancing detectability of P3NY. ABS contains several features which make it attractive as a derivatization reagent[7a]. It is easy to acquire through a simple sulfonation reaction. Through control in reagent formation, stable heavy isotopes can be incorporated for relative quantitation. The products resulting from ABS derivatization exhibit fluorescence with ex/em of 460/490 nm. An aspect that not previously pursued was the evaluation of ABS derivatives as the basis of a sample preparation strategy utilizing the

sulfonic acid moiety of the product. The pKa of benzensulfonic acid is 0.7, which is substantially lower than the pKa of any expected carboxylic acids present on peptide analytes (expected pKa 4-5). This provides an opportunity for selective ionization of the sulfonic acid while maintaining peptide associated carboxylic acids as the neutral species through pH control.

Recognizing the potential for attaining selective functional group ionization (sulfonic acid versus carboxylic acid) via pH control, which will only occur for peptides that have undergone derivatization with ABS, one can envision the development of a selective solid-phase extraction procedure wherein the reduction of sample complexity while accomplishing sample enrichment is possible, if an appropriate extraction phase can be identified. To this end, anion exchange is an obvious choice for ABS derivative extraction. When choosing between strong anion exchange and weak anion exchange, we considered what different functional groups each different stationary phase contained. Strong anion exchange typically incorporates a quaternary amine. We were concerned that using a stationary phase of fixed positive charge would result in the product being irreversibly bound to the extraction phase. With this in mind, we found a weak anion exchange solid phase extraction cartridge, which contained a diamine bound to a polymeric support. In addition to the expected electrostatic interaction, the presence of an aromatic ring system provides the stationary phase with hydrophobic interactions and potential pi-pi stacking, which would provide for two separate retention mechanisms for the ABS derivatives.

To test the effectiveness of the strata x-aw cartridges, FSAY(NH2)LER was spiked into a bsa digest standard at an equimolar concentration (100 fmol/µL for each). The peptide mixture was then subjected to the established derivatization procedure. After completion of the derivatization reaction, the solution was adjusted to pH 3 and loaded onto the SPE cartridge (Figure 4-13). At this pH, the product is expected to be retained, with all other peptides flowing through the device to waste. As the primary retention process is through electrostatic interaction, this particular extraction allows for

washing by pure organic which is favorable to washing away all unwanted peptides. The extracted analyte is then subsequently released by washing with an ammonium hydroxide solution in methanol. The pH shift results in the de-protonation of the support, with the captured derivative being released and isolated as a substantially purified solution (Figure 4-14). The isolated extract can then be evaporated and reconstituted for an enhancement of analyte sensitivity (Figure 4-15).

4.4 Conclusions

Six different derivatization reagents were utilized in order to enhance the detectability of P3NY. BA has been previously reported as a reagent capable of chemically modifying ortho-aminophenol's under oxidative conditions in order to create a fluorescent reporter molecule. The inherently low detection limits of fluorescence detection makes BA a valuable and economical reagent for enhancing detection of P3NY. DPE is a structurally similar reagent that produces a slightly different reaction product when used for derivatization. Despite BA's potential for side product formation, it has been shown within this work to produce higher relative product yields by both fluorescence and mass spectrometry measurements.

The dimethylamino analogs of both BA and DPE were pursued as derivatization reagents. It was hypothesized that incorporation of a tertiary amine could positively affect fluorescence spectra and lead to increased ionization during mass spectrometry analysis. DMA-BA as a derivatization reagent was shown to be ineffective as the predicted reaction product failed to form. Despite this, side products related to other BA reactions were generated from this analogue; however, DMA-DPE did form the expected derivatization product. Relative fluorescence yields and relative ion counts from mass spectrometry were both lower than those produced by BA, thus negating the usefulness of this DPE analog.

ABS proved to be a very useful modification of BA, with properties that possessed advantageous physical-chemical properties. Despite moderately lower relative fluorescent yields, ion counts by mass spectrometry were shown to be higher. In addition, side product formation from ABS compared to BA was shown to be lower. Additionally, ABS was shown to provide further utility through use in weak anion exchange solid phase extraction. DPE-SA as a derivatization reagent proved to be disappointing providing lower product yields compared to other reagents. Despite extensive reagent purification, evidence of reagent isomers can be seen through split product peaks. With the difficulties involved in obtaining pure reagent, DPE-SA does not appear to be a derivatization reagent of value. With the ease of acquisition, relatively high product yields, and its ability to be used in solid-phase extraction, ABS was shown to be the reagent of highest utility amongst the six reagents tested within this work.

4.5 Chapter 4 Figures

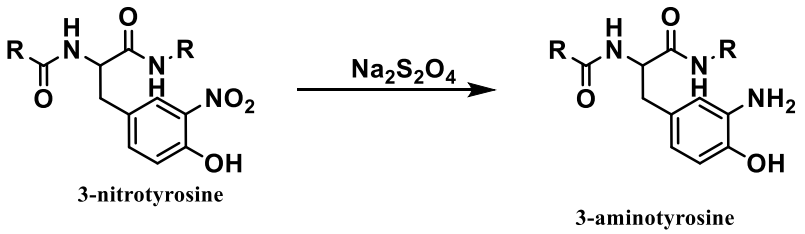

3-nitrotyrosine

3-aminotyrosine

Figure 4-1. Sodium dithionite reduction of protein bound 3-nitrotyrosine to 3-aminotyrosine

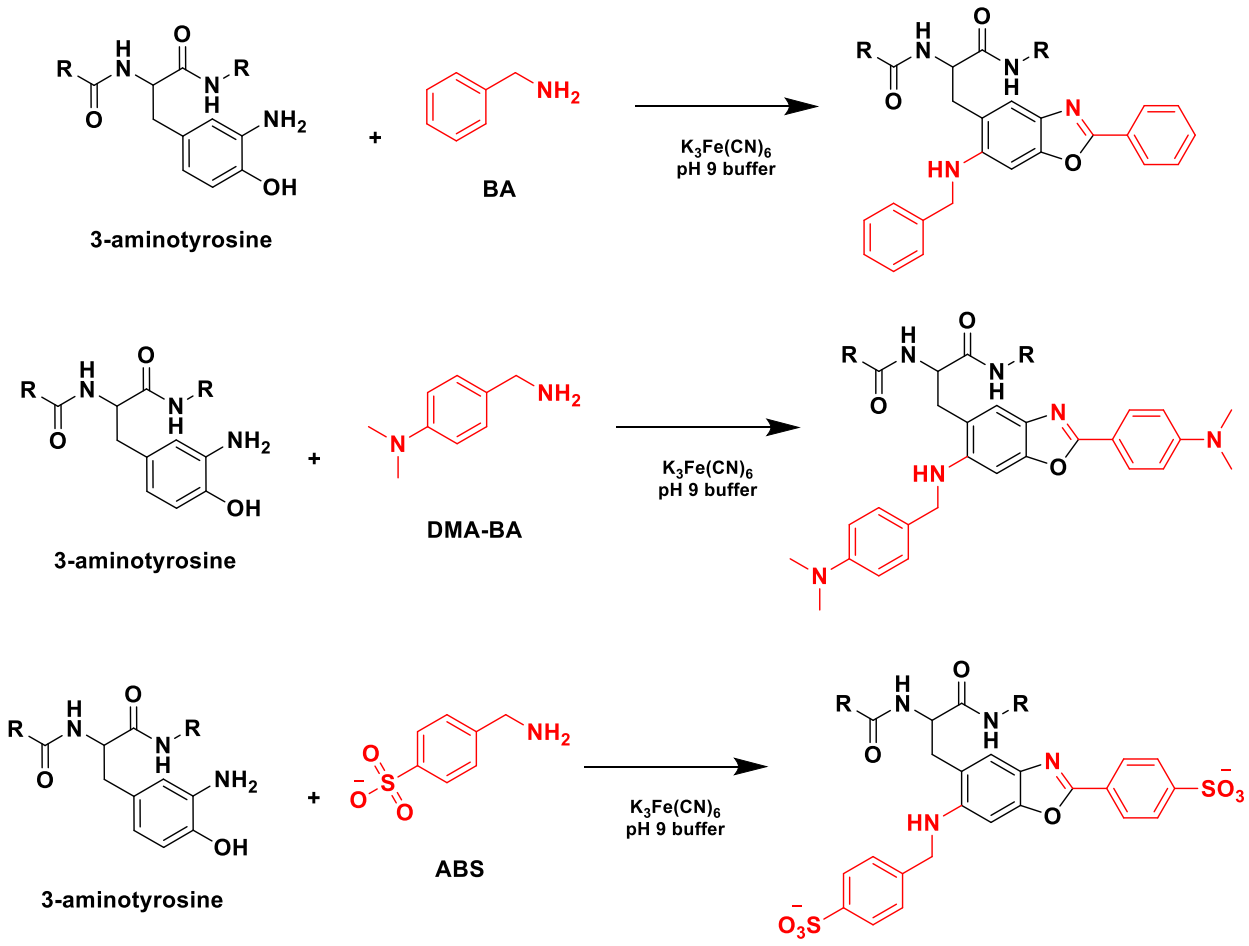

Figure 4-2. Derivatization reactions of the three BA based reagents. (Top) Benzylamine (BA) derivatization. (Middle) 4-Dimethylaminobenzlamine (DMA-BA) derivatization. (Bottom) 4-aminomethylbenzenesulfonic acid (ABS) derivatization.

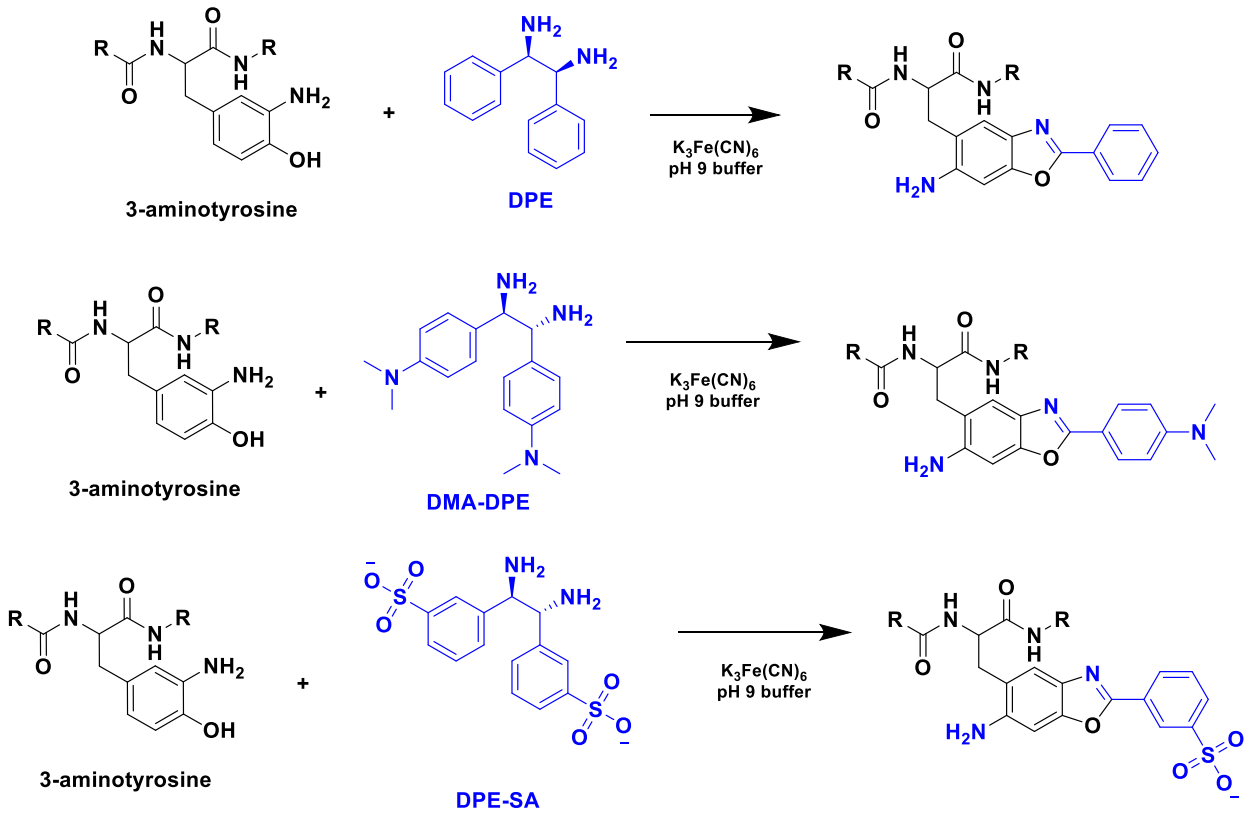

Figure 4-3. Derivatization reactions of the three DPE based derivatization reagents. (Top) Diphenylethylenediamine (DPE) derivatization. (Middle) 1,2-bis(4-(dimethylamino)phenyl)ethylenediamine (DMA-DPE) derivatization. (Bottom) 3,3'-(1,2-diaminoethane-1,2-diyl)dibenzenesulfonic acid (DPE-SA) derivatization.

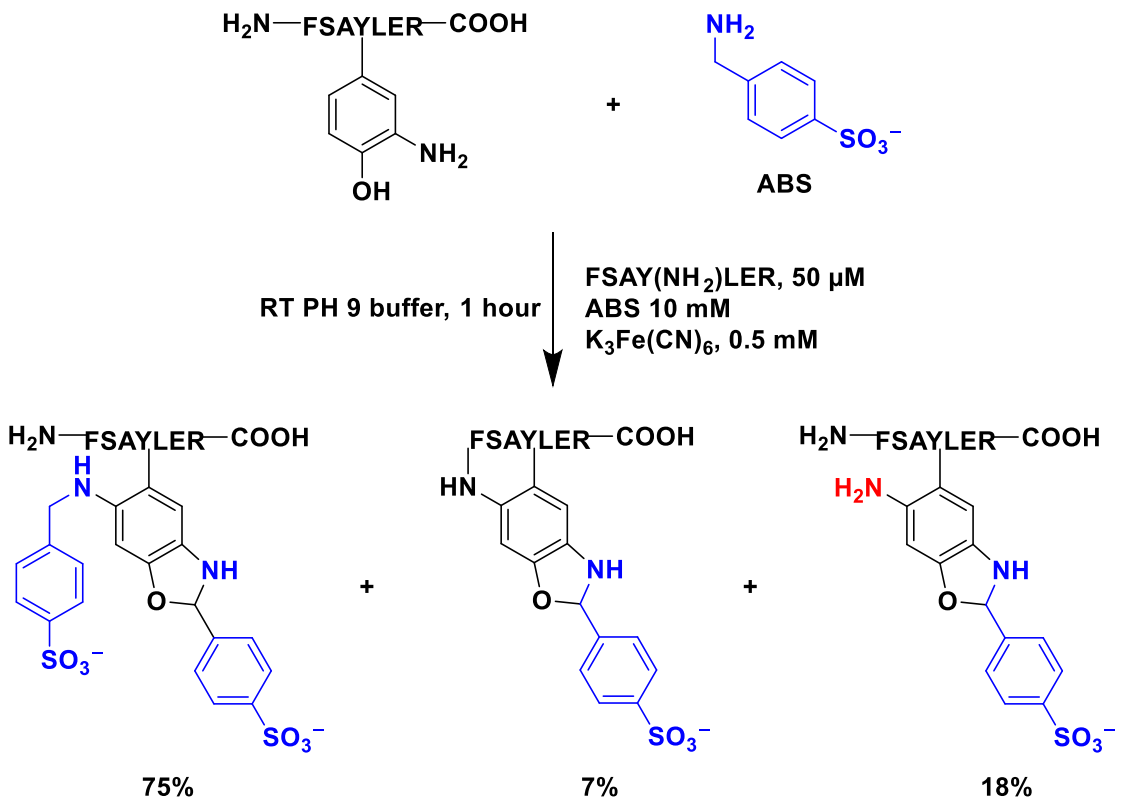

Figure 4-4. ABS derivatization showing potential product distribution with 75% expected benzoxazole product, 7% intramolecular product, and 18% DPE-SA product.

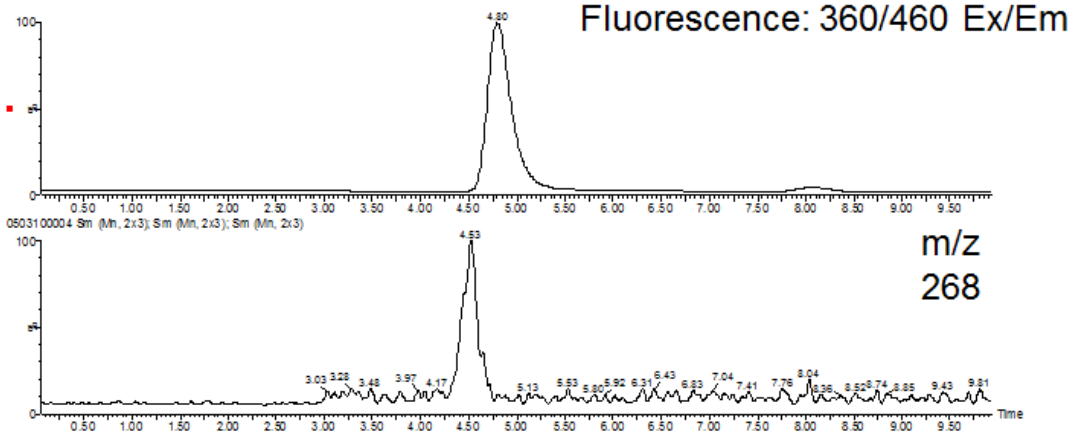

Figure 4-5. LC-MS-FL chromatograms showing DPE derivatization of 2-aminocresol producing product peak mass which matches fluorescence.

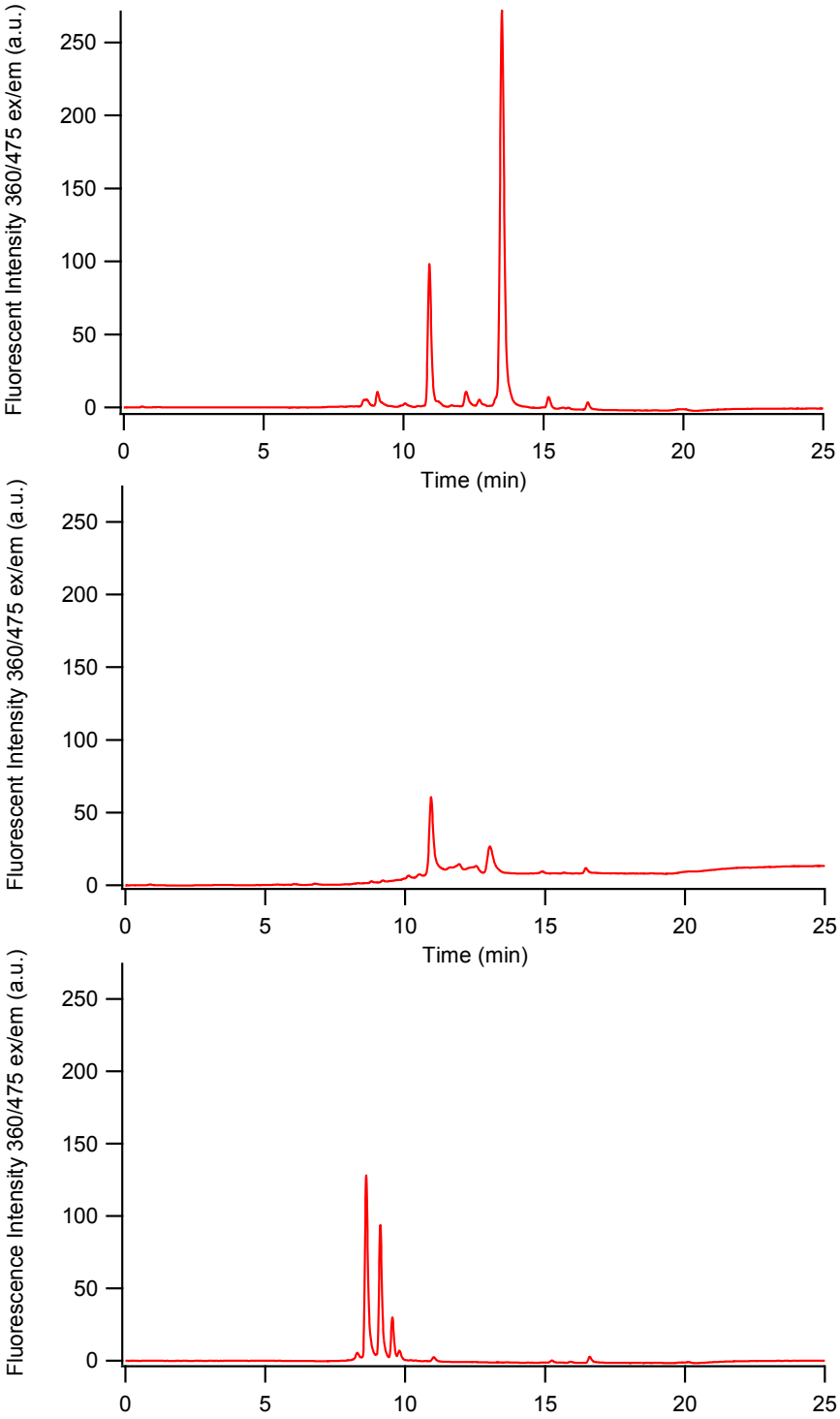

Figure 4-6. HPLC-FL chromatograms from three different BA based derivatization reactions. (Top)BA derivatization of FSAY(NH2)LER with BA product at 13.5 min and DPE product at 11 min. (Middle) DMA-BA derivatization of FSAY(NH2)LER showing no product. (Bottom) ABS derivatization of FSAY(NH2)LER showing ABS product at 8.5 min and side product at 9.5 min.

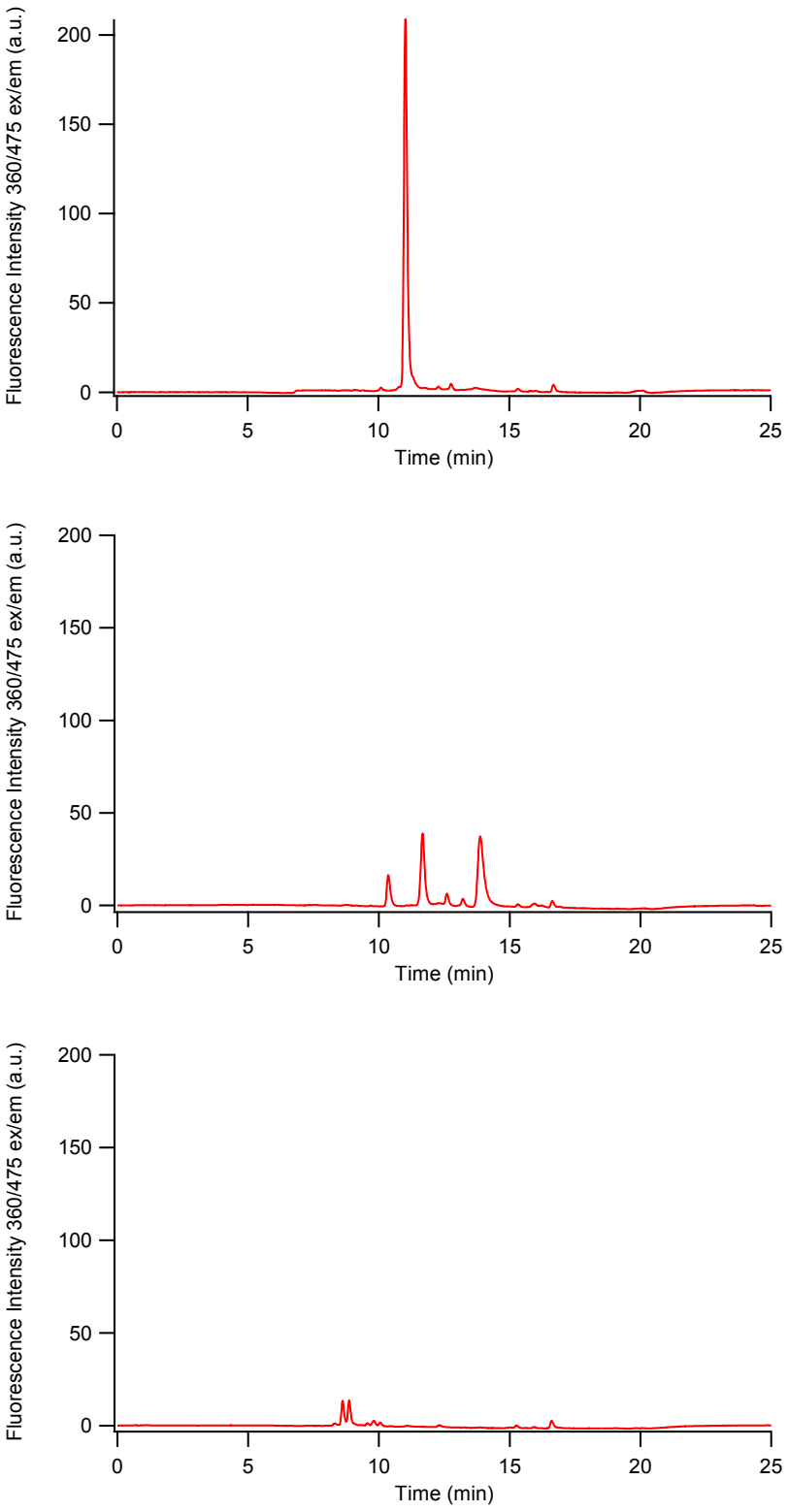

Figure 4-7. HPLC-FL chromatograms from three different DPE based derivatization reactions. (Top) DPE derivatization of FSAY(NH2)LER with expected product at 11 min. (Middle) DMA-DPE derivatization of FSAY(NH2)LER showing expected product at 11.7 min. (Bottom) DPE-SA derivatization of FSAY(NH2)LER showing split product peak at 8.6 and 8.9 min.

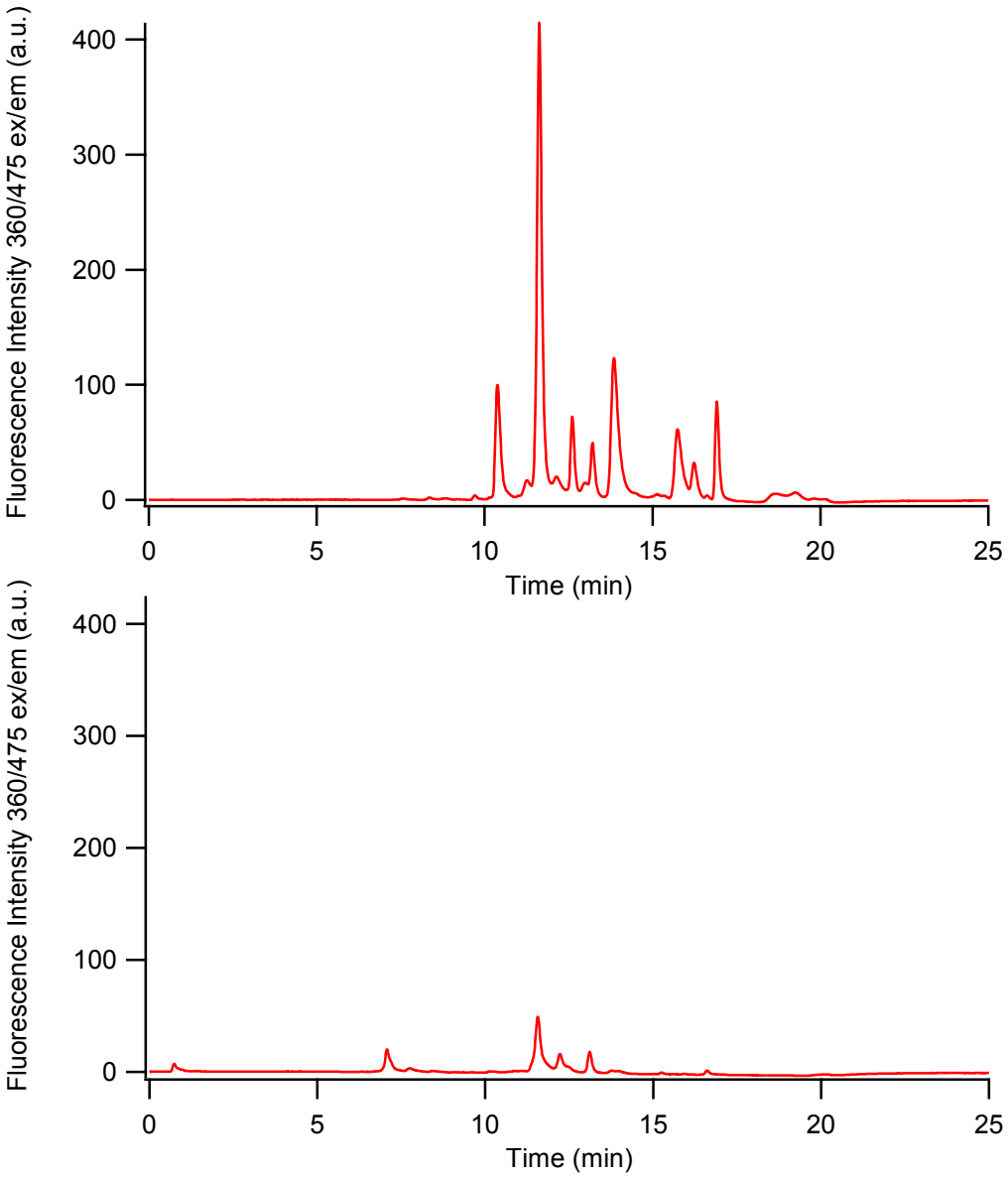

Figure 4-8. HPLC-FL chromatograms of (Top) DMA-DPE derivatization reaction with increased FSAY(NH2)LER concentration showing increase in reaction product at 11.7 minutes and (Bottom) DMA-BA reaction with increased FSAY(NH2)LER concentration showing no product formation.

Reagent	Retention Time (min)	Peak Area	Average Area	Relative Yield
BA	13.5	2987776	2962565	100.0000
		2959201		
		2940719		
BA (DPE Product)	11	814382	843005	28.4552
		863546		
		851087		
ABS	8.5	1064783	973501	32.8601
		956125		
		899596		
ABS (DPE Product)	9.5	222346	225237	7.6028
		230600		
		222766		
DMA-BA	NA	NA	NA	NA
DPE	11	1911932	2037267	68.7670
		1915638		
		2284230		
DMA-DPE	11.7	415441	394584	13.3190
		377857		
		390453		
DPE-SA	8.6	93736	99336	3.3530
		113496		
		90776		
DPE-SA	8.9	94261	108558	3.6643
		128032		
		103380		

Table 4-1. HPLC-FL results from derivatization of FSAY(NH2)LER by six different derivatization reagents. Relative yields are normalized to BA derivatization product peak area.

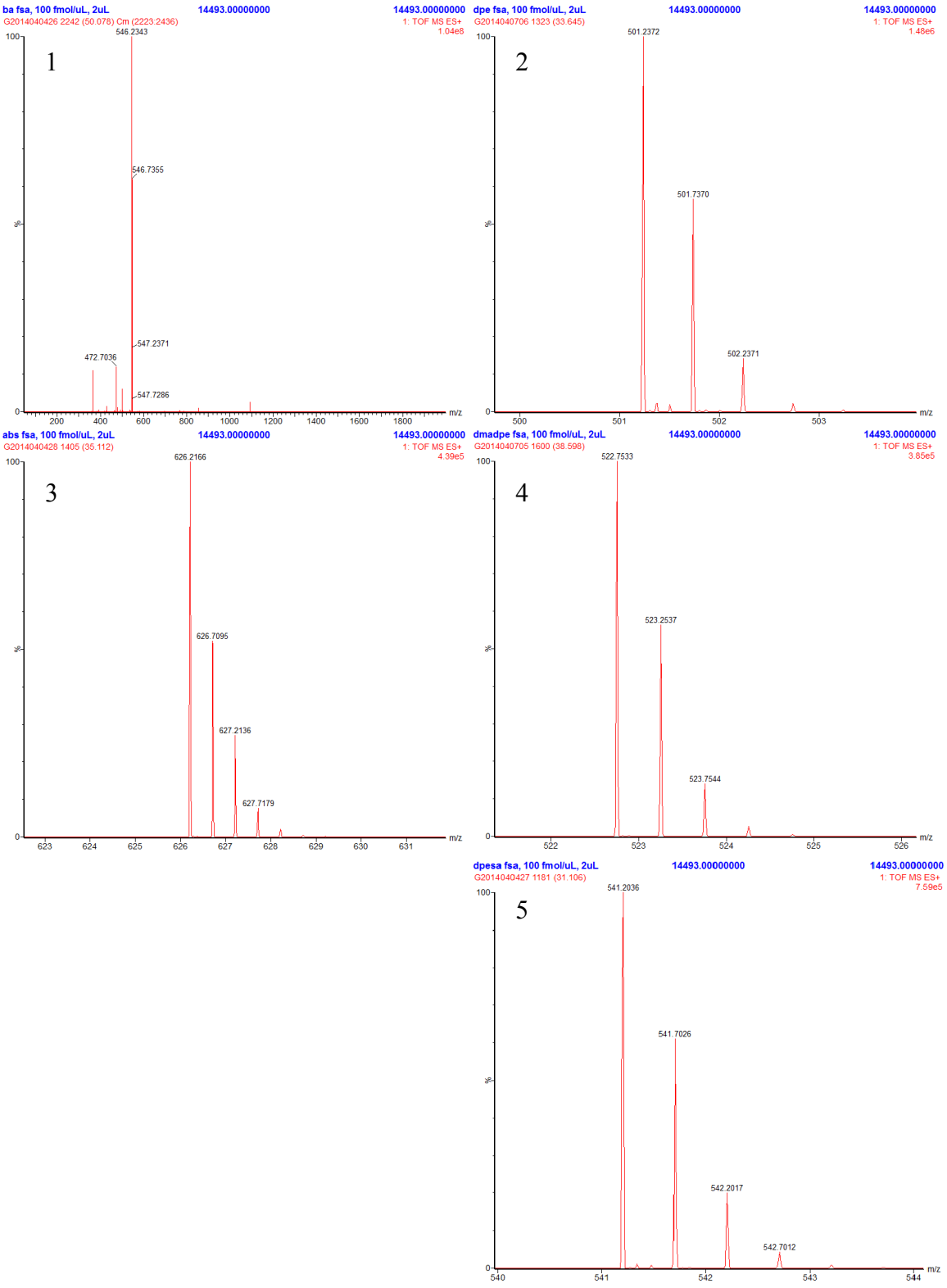

Figure 4-9. Derivatization product spectra from derivatization of FSAY(NH2)LER by (1) BA, (2) DPE, (3) ABS, (4) DMA-DPE, and (5) DPE-SA

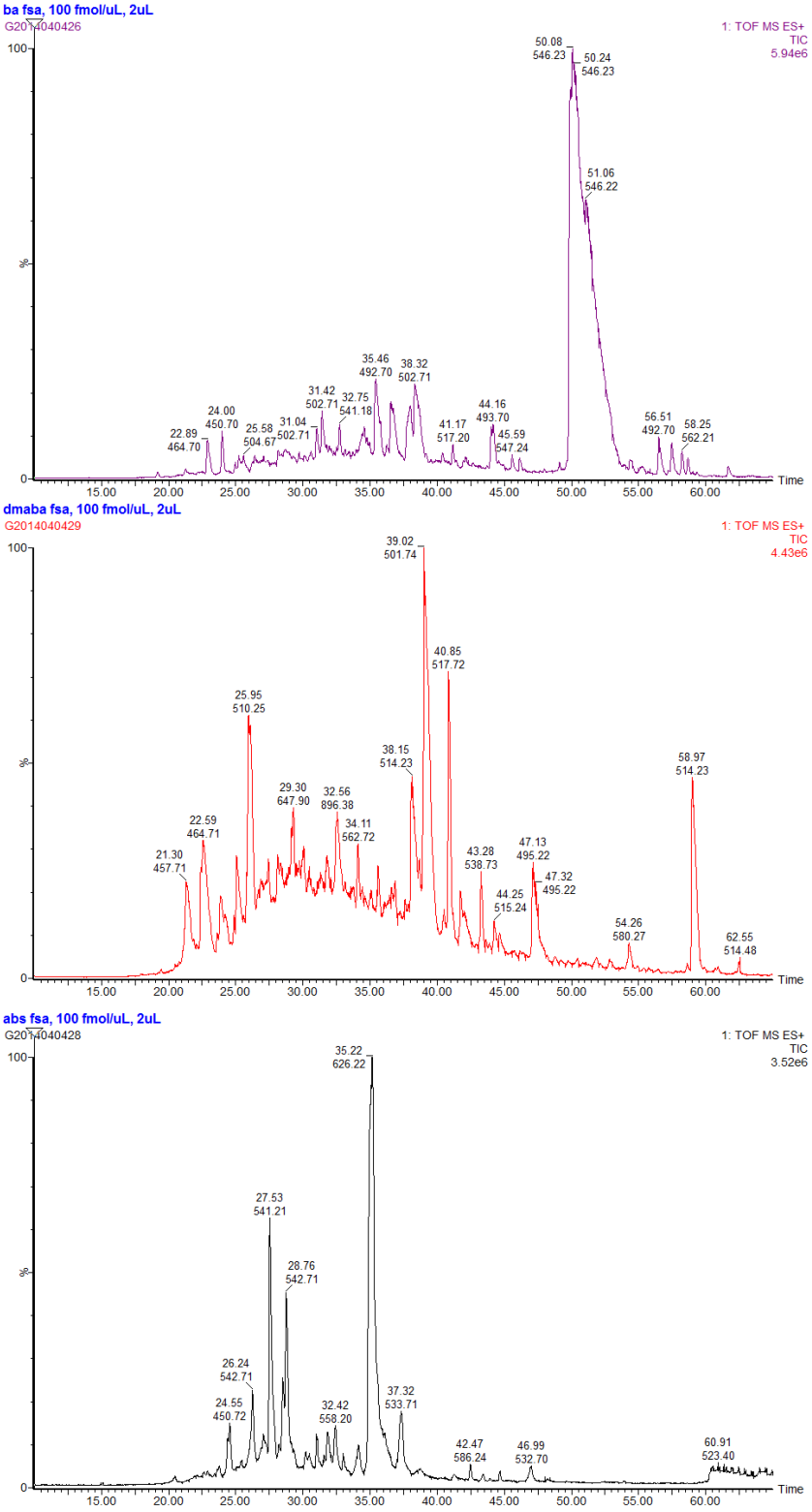

Figure 4-10. UPLC-MS chromatograms from derivatization of FSAY(NH2)LER by (Top) BA, (Middle) DMA-BA, and (Bottom) ABS.

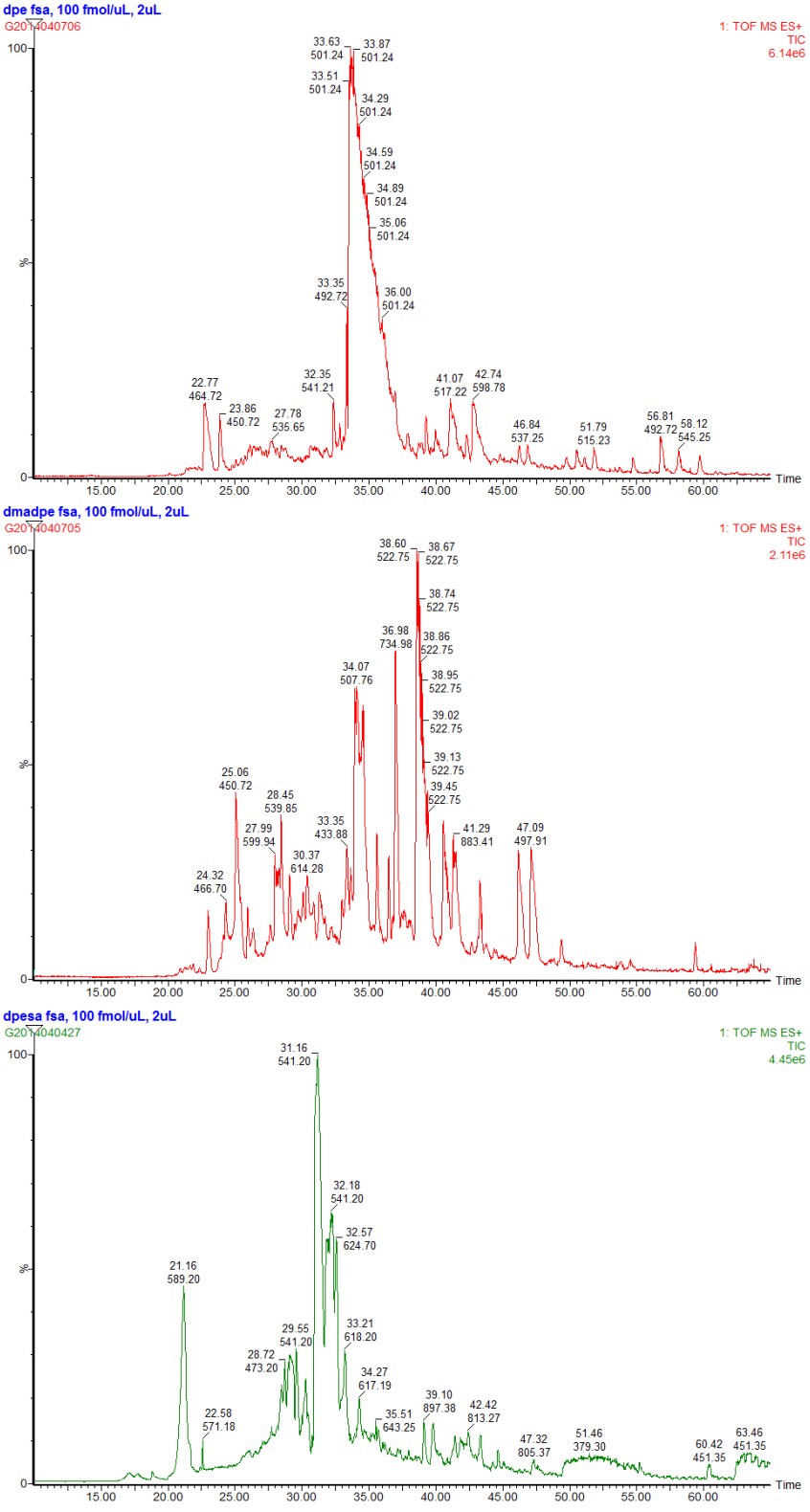

Figure 4-11. UPLC-MS chromatograms from derivatization of FSAY(NH_2)LER by (Top) DPE, (Middle) DMA-DPE, and (Bottom) DPE-SA.

Reagent	Elution Time (min)	Ion Counts (max height)	Peak Area	Relative BA Yield
	50.1	4.55E+04	1.04E+08	100.0000
product)	36.5	1.32E+05	2.88E+06	2.7692
molecular product)	35.4	2.35E+05	4.85E+06	4.6635
	NA	NA	NA	NA
(DPE product)	39.0	1.93E+05	2.04E+06	1.9615
(Intramolecular				
	38.2	3.65E+05	8.55E+06	8.2212
	35.5	4.39E+05	1.27E+08	122.1154
product)	27.5	5.49E+05	5.49E+06	5.2788
amolecular product)	31	4.49E+04	3.98E+05	0.3827
	34.5	1.48E+06	1.45E+08	139.4231
E	38.6	3.85E+05	1.39E+07	13.3654
	31.1	7.59E+05	1.92E+07	18.4615
	31.6	5.09E+05	1.29E+07	12.4038

Table 4-2. UPLC-MS data of FSAY(NH2)LER derivatization showing relative ion counts for six different derivatizations along with products found within each reaction. Yields are normalized to BA derivatization product.

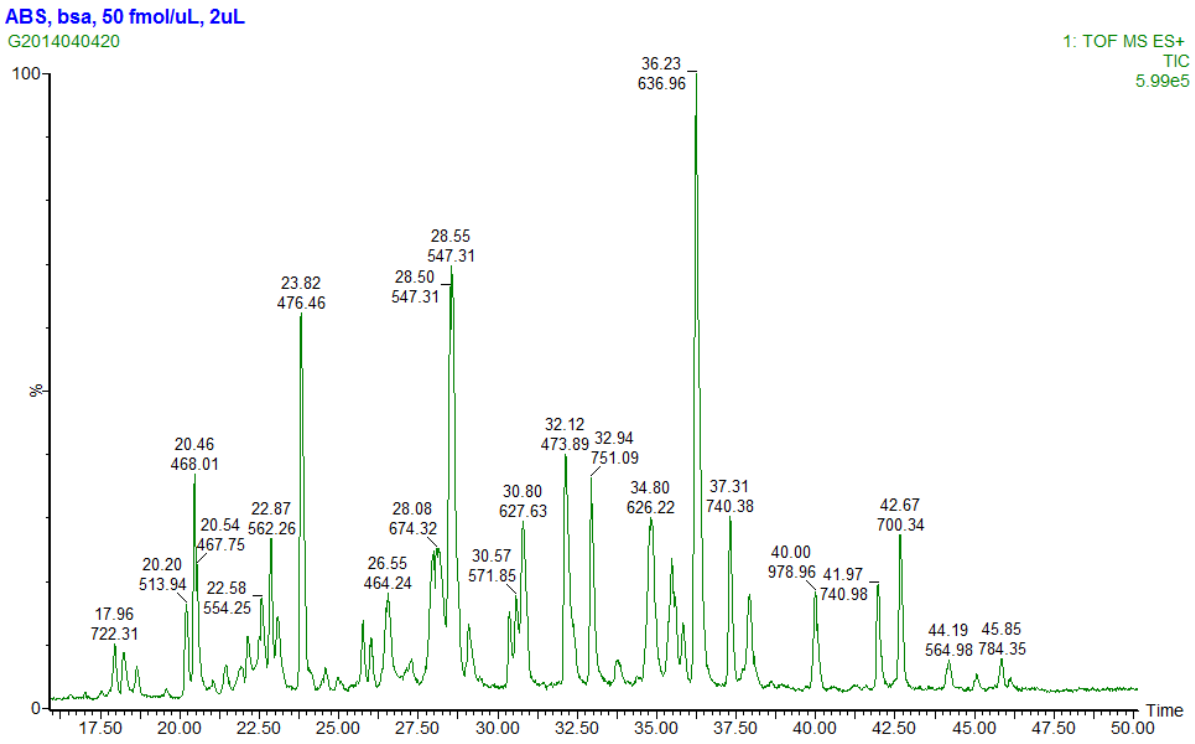

Figure 4-12. UPLC-MS chromatogram of bovine serum albumin digest. FSAY(NH2)LER was spiked into the digest and the peptide solution underwent derivatization by ABS. ABS product peak shows at 34.8 minutes with product mass of 626.22.

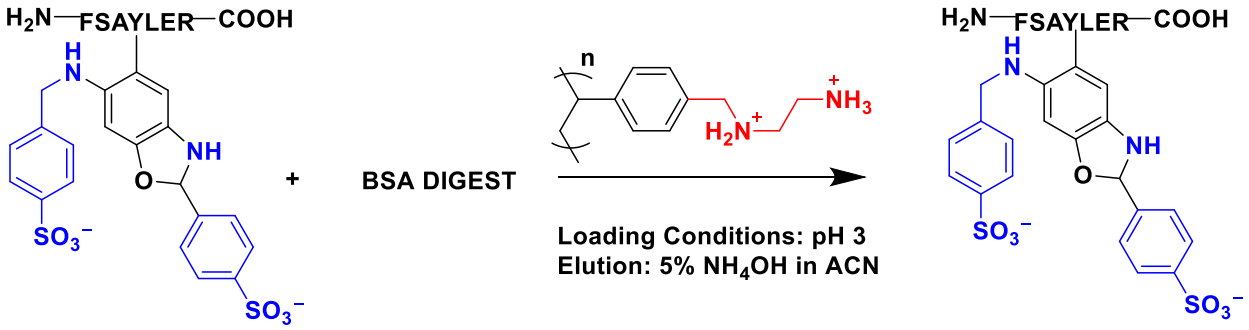

Figure 4-13. ABS product extraction from a BSA digest derivatization solution. Reaction product extracted on a phenomenex strata x-aw SPE cartridge for isolation and enrichment.

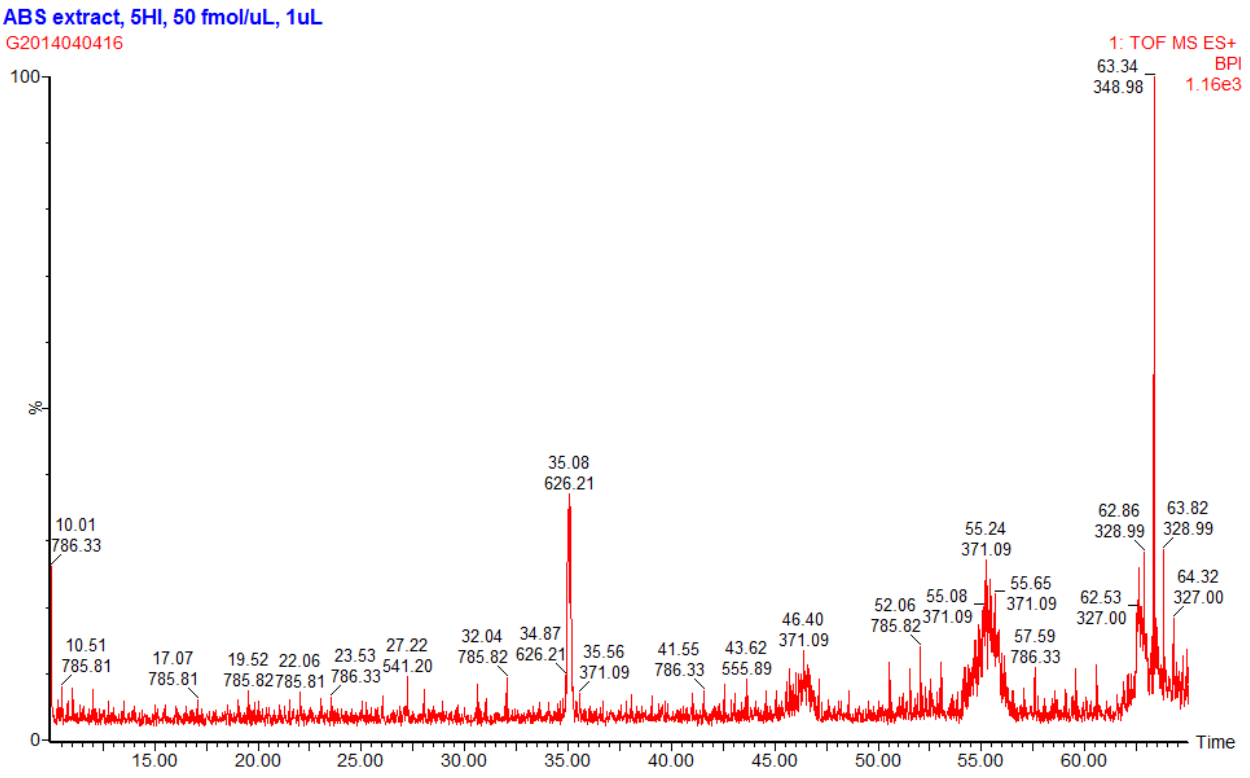

Figure 4-14. UPLC-MS chromatogram of ABS reaction product post extraction and subsequent dilution to pre-extraction concentration.

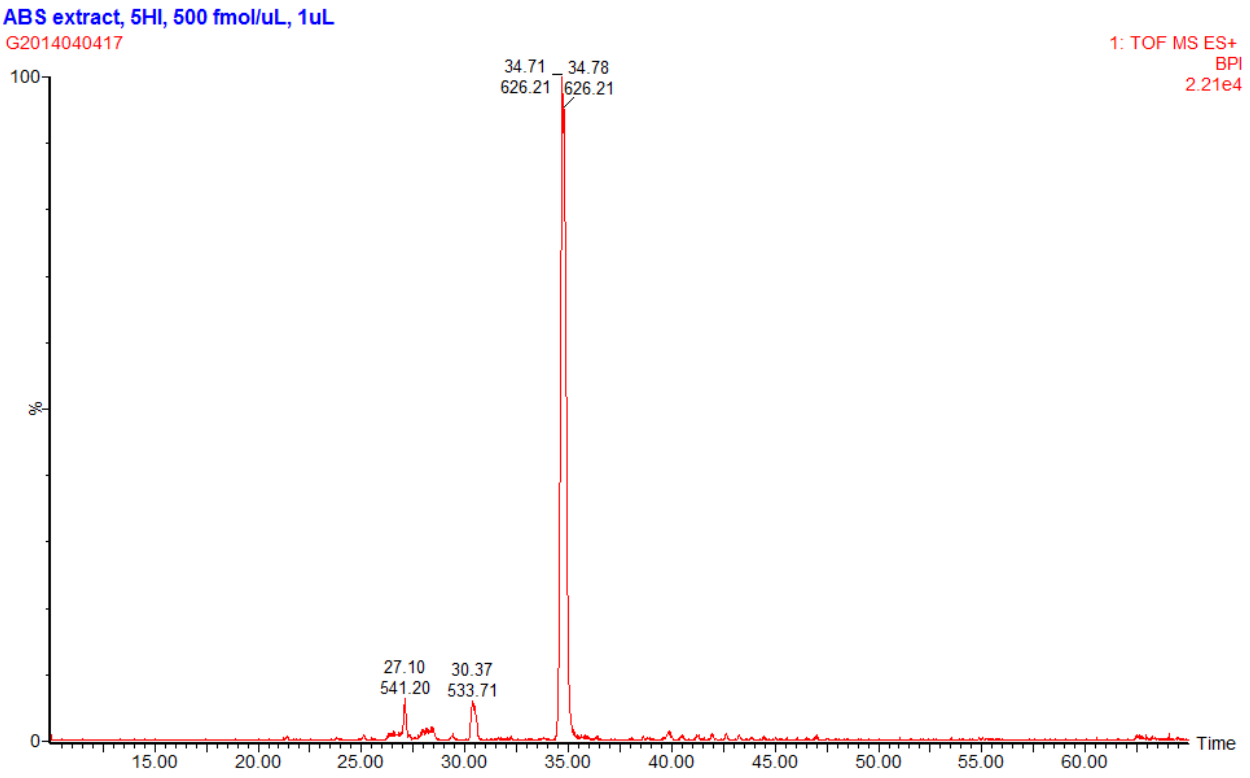

Figure 4-15. UPLC-MS chromatogram of ABS derivatization product after SPE and subsequent enrichment by reconstitution in ten times less solvent.

4.6 Chapter 4 References

[1] J. M. Souza, G. Peluffo and R. Radi, *Free Radic Biol Med* **2008**, *45*, 357-366.
[2] R. Radi, *Acc Chem Res* **2013**, *46*, 550-559.
[3] M. H. Shishehbor, R. J. Aviles, M. L. Brennan, X. Fu, M. Goormastic, G. L. Pearce, N. Gokce, J. F. Keaney, Jr., M. S. Penn, D. L. Sprecher, J. A. Vita and S. L. Hazen, *Jama* **2003**, *289*, 1675-1680.
[4] H. Hill, *Bioanalysis* **2009**, *1*, 3-7.
[5] a) P. A. Cruickshank and J. C. Sheehan, *Analytical Chemistry* **1964**, *36*, 1191-1197; b) D. Morse and B. L. Horecker, *Analytical Biochemistry* **1966**, *14*, 429-433.
[6] J. Pennington, C. Schöneich and J. Stobaugh, *Chromatographia* **2007**, *66*, 649-659.
[7] a) V. S. Sharov, E. S. Dremina, N. A. Galeva, G. S. Gerstenecker, X. Li, R. T. Dobrowsky, J. F. Stobaugh and C. Schoneich, *Chromatographia* **2010**, *71*, 37-53; b) V. S. Sharov, E. S. Dremina, J. Pennington, J. Killmer, C. Asmus, M. Thorson, S. J. Hong, X. Li, J. F. Stobaugh and C. Schoneich, *Methods Enzymol* **2008**, *441*, 19-32.
[8] E. S. Dremina, X. Li, N. A. Galeva, V. S. Sharov, J. F. Stobaugh and C. Schoneich, *Anal Biochem* **2011**, *418*, 184-196.
[9] H. Mirzaei and F. Regnier, *Analytical Chemistry* **2005**, *78*, 770-778.
[10] M. Zabet-Moghaddam, T. Kawamura, E. Yatagai and S. Niwayama, *Bioorganic & Medicinal Chemistry Letters* **2008**, *18*, 4891-4895.
[11] R. Aebersold and M. Mann, *Nature* **2003**, *422*, 198-207.
[12] T. Nakamura and Y. Oda, *Biotechnol Genet Eng Rev* **2007**, *24*, 147-163.
[13] A. M. Kamel, P. R. Brown and B. Munson, *Anal Chem* **1999**, *71*, 5481-5492.
[14] W. C. Lee and K. H. Lee, *Anal Biochem* **2004**, *324*, 1-10.

Appendix

Implementation of Chromatographic Systems Which Surpass Commercial Pressure Limits for Enhanced Resolution and Peak Capacity

A1.1 Introduction

A1.1.1 Current challenges in proteomics

In the wake of the completion of the human genome project, it has come to light that humans make use of approximately 30,000 protein encoding genes[1]. It has since been estimated that these genes encode for close to one million different proteins when structural variants and post-translational modifications are taken into account [2]. Current techniques for biomarker discovery are arduous feats at best that require substantial steps in protein purification. Purified proteins are commonly digested into substituent peptides making them more amenable towards analysis. The de facto tool for identification post sample clean-up and digestion is LC-MS. Mass spectrometry provides a powerful tool for qualitative identification of peptides allowing for computational identification of parent proteins[3]. Recent advances in ionization techniques and computational analysis has allowed for label-free quantitation. Despite promising advances in mass spectrometry, biomarker discovery is still complex due to the need for extensive sample pre-treatment to reduce sample complexity as well as remove substances not of interest that have detrimental efforts on the chromatographic and mass spectrometry systems.

Recent considerations to reduce the complexity of sample clean-up have aimed at improving chromatographic performance[4]. Although mass spectrometry does not require baseline resolution for identification of peptides, co-elution can result in ion suppression and added complication during construction of tandem mass spectrometry data sets that are essential for protein identification[5]. The requirement for sample clean-up stems from the inability of current chromatographic methods to efficiently separate more than several dozens of peptides. As a cellular compartment can contain thousands of different proteins made of tens to hundreds of peptides, the current sample preparation strategies are extensive in order to provide pure protein digests which current chromatography columns

are able to efficiently separate. Increases in column performance could lead to direct gains in sensitivity by excluding the need for preparatory steps which could result in loss of protein.

A1.1.2 Theoretical Basis for Long Axial Columns

Column separation efficiency is quantitatively described by the number of theoretical plates, N, represented in equation 1 where L represents column length and H represents the height equivalent of

$$N = \frac{L}{H} \tag{1}$$

a theoretical plate. From equation 1 it is seen that separation efficiency is directly proportional to column length, which will be the focus of the proceeding work. However, several other factors directly affect separation efficiency that should not be ignored.

H can be generally described by the van Deemter equation (2) where *u* represents linear velocity, the A term represent eddy diffusion, the B term represents longitudinal diffusion, and the C term represents resistance to mass transfer. Each term can be examined in greater

$$H = A + \frac{B}{u} + C \tag{2}$$

detail by the expanded van Deemter equation 3 where λ represents particle shape, d_p represents particle diameter, D_m is the diffusion coefficient of the analyte in the mobile phase, *u* is the linear velocity, and γ and ω are constants. Several conclusions can be drawn from the expanded van Deemter.

$$H = \lambda d_p + \frac{2\gamma D_m}{u} + \frac{\omega d_p^2 u}{D_m} \tag{3}$$

First we see that eddy diffusion is determined by particle size and shape. Irregular particle shape can create different sized channels through which analytes diffuse. Diffusion of analyte through several different sized channels results in peak broadening. Following from this, more uniform particle shape along with smaller particle size can lead to more uniform inter-particle channels, thus minimizing the A term. From the B term we see that longitudinal diffusion is determined by analyte diffusion coefficients and linear velocity. As such, it is usually seen as constant for a given analyte on a given column and can only be adjusted through changes in linear velocity. Finally, the C term shows that mass transfer is affected by analyte diffusion coefficients, linear velocity, and most importantly particle size. The importance of the C term which one can intuit that smaller the particle size, the more efficient the mass transfer of an analyte from stationary phase to mobile phase, which ultimately results in a more efficient separation.

Overall, examination of the van Deemter equation allows one to quantitatively explain how separation efficiency can be increased through use of small particles and optimal linear velocities. The van Deemter minimum for most columns utilizes a linear velocity of 0.1 cm/s. Despite this, linear velocities of 0.2 cm/s are much more common to mitigate the amount of time needed to operate at van Deemter minimums. The loss in efficiency due to increasing linear velocity can be mitigated through use of smaller particles.

A1.1.3 Pressure Limitations

As discussed, chromatographic separation efficiency can be increased through decreasing particle size and increasing column length. The consequence of both of those changes is an increase in back pressure. For comparison, conventional HPLC utilizes columns between two and 25 cms in length containing a 4.6 mm inner diameter (ID) with particles ranging from 3-5 microns. Expected back

pressure for conventional HPLC is from 1,000 to 4,000 psi. More recently, UPLC utilizes 1-3 micron particles in columns 10 to 25 cm in length with an internal diameter of 2.1 mm. Expected back pressure for UPLC is from 4,000 to 10,000 psi. Currently, there is not a commercially available instrument designed for pressures above 15,000 psi. As discussed by Jorgenson[6], if pressure was not a limiting factor, particle size and column length can be optimized for a given pressure. At 45,000 psi, optimal particle size is one µm and optimal column length is 30 cm[6]. With those parameters in mind, his lab constructed apparatus capable of packing sub-two micron particles into fused silica capillary columns up to two meters long. Additionally, his lab modified a Waters nanoACQUITY[7] in order to utilize the custom-made columns. Reported in the following work is the attempt to replicate production of long axial columns utilizing sub two micron particles at KU.

A1.2 Long Axial Column Packing and Preparation

The goal of the present work is to produce increases in peak capacity through longer columns. The following sections describe the process of packing sub-2 µm particles into fused-silica capillary to create columns of higher plate counts than those commercially available. Fused silica capillary (75µm ID) was selected for use in packing. BEH ACQUITY particles (dp = 1.7 µm) were used for all packing operations, which allow for direct comparisons to commercially available columns

A1.2.1 Procedures for Fritting

It should first be noted for all fritting procedures that cleanliness is of extreme importance, as dust particles can have unwanted consequences for packing procedures. Lab space used for fritting should be thoroughly cleaned prior to set up and fritting. Appropriate protection equipment should be worn including a lab coat, safety glasses, and most importantly, nitrile gloves. There are several methods to producing column frits which are well covered in literature and fall beyond the scope of the current

project. For the purpose of producing meter long columns, two general procedures were used. Both procedures used a mixture of kasil and formamide which polymerizes in the end of the capillary tube.

For the first procedure, a 3:1 mixture of kasil:formamide was mixed in a 1.5 mL Eppendorf vial. A 1.3 m piece of 75 µm ID 360 µm OD length of capillary was dipped end-wise (approximately 1 cm deep) into the vial. The end was immediately removed and placed in an oven set at 70° C and allowed to cure overnight. Prior to packing, the same end was cut leaving a 1-2 mm frit at the outlet end of the capillary and the rest of the fritted section was thrown to waste.

The second procedure follows more closely to the procedures used at the University of North Carolina. A kasil solution (20 µL) was placed and absorbed onto a piece of filter paper (Fisherbrand Glass Fiber Filter Circles; G4). Formamide (20 µL) was placed directly on top of the kasil spot on the filter paper. The outlet end of a 1.3 m piece of 75 µm ID x 360 µm OD length of capillary was dabbed onto the kasil solution spot. Gentle twisting motions were applied to the capillary and small holes were bored through the filter paper. The capillary was then placed in an oven at 70° C for at least two hours prior to packing.

A1.2.2 Packing station

For packing columns of up to two meters in length, a packing station was used according to Figures 2 and 3. The stations consist of a Haskel DSF-100 and a Haskel RDSXHF-903 air drive liquid pumps. The former pump operates well in the one to twenty thousand psi range and the latter in the five to 75 thousand psi range. Liquid reservoirs for push solvents are stored in the top rack above the pumps. The solvents are connected to the DSF-100 pump which is then connected in series to the RDSXHR-903 pump. The outlet of the latter pump is then connected to the custom made packing bomb. The packing bomb (Figure A-3) consists of a solvent reservoir capable of holding ~1 mL of fluid with

bomb inlet facing the pumps and bomb outlet pointing up. The bomb contains a micro magnetic stir-bar and sits upon a stir plate.

A1.2.3 High pressure fittings

Every fused-silica capillary connection (both for packing procedures and for all connections in XUPLC system utilization), which must contain pressures greater than 10,000 psi is made with proprietary high-pressure fittings obtained from the University of North Carolina. The fittings, seen in Figure A-1, consist of a backing nut, a backing ferrule, a union nut, a peek ferrule, and a capillary sleeve (not shown). The peek ferrule is drilled out to 380 μm prior to making a connection. The capillary is fitted with the sleeve (1/32" x 0.15") and all fitting pieces save the drilled ferrule are placed over the sleeve in the appropriate order as displayed in Figure A-1. The drilled ferrule is placed directly on the polyamide coating at the head of the capillary where the connection is to be made. The union nut is screwed down against the peek ferrule at the desired connection point with appropriate force to hold pressure, but taking care not to break the union. The backing ferrule is screwed down over the Teflon sleeve by the backing nut. The backing ferrule applies appropriate force along the length of the sleeve to keep the column from sliding out of the primary ferrule.

A1.2.4 Column packing

It should first be noted that cleanliness is a high priority for all packing procedures as contamination of packing equipment, fused-silica capillary, or slurry preparation by dust particles leads to packing failure. Appropriate protective lab wear should be adhered to including lab coat, protective eye wear, and nitrile gloves. Without proper cleanliness at all stages of packing, there is a high probability of packing failure. Prior to packing, a 1.3 m piece of capillary is fritted on one end according to previously describe fritting procedures. The fritted end will be the outlet of the column. The packing material is prepared as a 50 mg/mL slurry in methanol, vortex mixed for 15 second, then placed into a

sonic water bath for 15 minutes. The slurry is then vortex mixed for an additional 15 seconds and 400 µL of the suspension is placed into the packing bomb using a one mL Hamilton syringe (Hamilton #81316; 1001LTN 1.0 mL (22/2"/3)). The non-fitted inlet of the capillary is fitted to a half-inch adapter piece by a high pressure fitting with 3.5 cm of the capillary extended beyond the connection end of the adapter. The protruding length of the capillary is cleaned by wiping with a methanol wetted Kimwipe. The capillary is placed into the packing bomb taking care not to bump the fragile end of the capillary. The adapter is tightened to hold pressure up to 45,0000 psi.

The stir plate is switched on to a speed of six. The DSF-100 pump is turned on and pressurized to approximately 1,000 psi using acetone (HPLC grade) as a packing solvent. Appropriate care should be considered at this point to avoid failure of the kasil frit as failure will result in spraying silica particles over the work area. In such an event, the system needs to be immediately shut off and packing material cleaned from the work area. If the frit holds, the column outlet needs to be monitored for bed formation. After one to two cm of bed has formed, the RDSXHF-903 can be activated and slowly pressurized. Care should be taken as the second pump does not pressurize until approximately 5-10k psi. Pressure on the high pressure pump should be increased to 40k psi at a rate of 5k psi per cm of bed formed. Frit failure is of high concern until the system is fully pressurized. Attention should also be given to the high-pressure capillary connection at the bomb exit to monitor for a leak.

After the system has come to pressure with no leaks detected, the column should be allowed to pack fully, with monitoring possible using a low-amplification microscope. A one meter column should pack in under three hours. If at any point there is an interruption in packing (such as a clog in the packing inlet), the pump pressure can be released and immediately reapplied in an attempt to resume packing. After the column has packed, air supply to liquid pumps should be turned off to allow the column to very slowly depressurize over the course of half an hour and the stir plate should be turned

off. The half inch adapter can be unscrewed from the packing bomb, but the column should remain fitted to the adapter for washing.

A1.2.5 Column Washing

In order to allow the column bed to settle appropriately, columns are washed after packing at higher pressures than they are packed. A 1:1 solution of acetonitrile:water (HPLC grade acetonitrile and Millipore water) is used as washing solvent and the appropriate reservoir is attached to the washing station pump. The packed column with half-inch adapter still attached is attached to the washing station. The 3.5 cm piece of column protruding from the adapter is cut and the adapter is attached to the high pressure haskel 903 pump. The pump is pressurized to approximately 50k psi and the column is allowed to wash for at least ten column volumes. After the appropriate time has passed, the air supply to the pumps can be turned off so the column slowly depressurizes. After the column is fully depressurized, the pump is turned back on and pressurized up to 10k psi. A temporary frit is then fabricated on the inlet side of the column by placement of the capillary between the jaws of a Teledyne Stripall device (Model TWC-1) using setting 4-5 for approximately 60 seconds. The column can then be detached, taking care not to break the newly formed temporary frit, and is allowed to dry. After drying, the temporary frit is cut off and a permanent frit is made at the inlet according to previously described kasil fritting procedure. The column inlet is tested for strength by connection to a high pressure pump, pressurizing the column to 40k psi, and rapid depressurization. A column is deemed fit for use if the inlet frit survives 4-5 rapid decompressions without particles leaking out of the inlet.

A1.3 Extreme Ultra-High Pressure Liquid Chromatography (XUPLC)

A1.3.1 UPLC modification

For utilization of long axial columns packed longer than 25 cm's, the following modifications have been made to a Waters nanoACQUITY UPLC (Figure A-4). From the 6-port Rheodyne valve located at the top right side of the sample manager, a connection capillary (Waters part number 430002242) was fitted leading out from the 6-port valve to a valco T (part MT.5XCS6, 1/32" x 0.006"). From the valco T, a 17 cm length of 75 μm ID capillary leads to the 10k psi pin valve labeled Valve 2 and is connected at the valve's front port. The side port on Valve 2 is connected to appropriate tubing (1/16" ID) leading to waste.

From the remaining port on the Valco T, a 23 cm length of 75 μm ID fused-silica capillary leads to a 40k psi pin valve labeled Valve 3 and is connected to the side port of the valve. A 52 cm piece of 75 μm fused silica capillary connected by Waters high pressure fittings leads out of the front port on Valve 3. The same piece of capillary is connected to the column Valco T, which sets inside the column heater, by a high pressure fitting. Of the two remaining ports on the column Valco T, the column inlet is attached through a high pressure fitting. The column outlet is attached to a "pig tail". The pig tail is a 15 cm piece of 20 μm fused silica capillary that connects the column to the nanoESI source. The column pig tail fitting is a 4 mm piece of Teflon tubing (1/16" x 0.008"), which has been drilled out to 360 μm. This piece of Teflon tubing is then slid over the column outlet and pig tail, connecting the two.

The remaining port on the column Valco T which sits in the column heater is connected to a 1/32" x 0.005" X 40 m long piece of stainless steel tubing which serves as the gradient storage loop. The gradient storage loop is connected at the other end to a vent Valco T. Of the two remaining ports on the vent Valco T, one is attached to a 10 cm piece of stainless steel tubing (1/32" x 0.005"). The other end of the stainless steel tubing is attached at the front port of a 40k psi pin valve. The side port on the 40k psi pin valve is attached to appropriate plumbing for waste.

The remaining port on the vent Valco T is attached to 140 cm of 20 µm fused silica capillary by a high pressure fitting. This same piece of capillary is attached through a high pressure fitting to a 0.5" adapter. The adapter is connected to a HiP 3-way valve. One port on the HiP valve is connected appropriately to waste with the remaining port connected through stainless steel connections and tubing to the Haskell 903. 50:50 Water:Acetonitrile is plumbed appropriately to the Haskell pump and used as push solvent. The assembled additions can be seen in Figure A-5.

A1.3.2 General Operation Notes

With regards to operation of the XUPLC, there are two general directions solvent can be pushed. For loading-type events, such as gradient loading, sample loading, or storage loop flushing, valve two remains closed while valves three and four are open. This allows solvent to fill the gradient storage loop and be pushed through the end of the loop to waste. For operation and data collection, valves three and four are closed, valve two is opened, and the Haskell pump is turned on. In this state, the current contents of the gradient storage loop are forced through the analytical column. Valve two remains open during operation to prevent pressure build-up from the nanoACQUITY and also serves to prevent the nanoACQUITY from experiencing higher than designed for pressure in the event of valve three failures.

A1.3.3 New Operation and Leak Checking

Whenever a high pressure connection is made, or after a change to XUPLC operation is made, a pressure check should always be performed. The main cause of experimental failure for XUPLC operation is due to a leak in the system. Most leaks can be found prior to operation which saves hours of experimental time.

Leak checking should be approached from two directions with valve three as a mid-point. From the nanoACQUITY side, a standard pressure check should be performed under the Intellistart diagnostics

menu found in the BSM (Binary Solvent Manager) sub-section. Prior to this test, valves two and three should be set to the off position. With those valves closed, the leak test should pass at under 30 nL/min of solvent loss at 10,000 psi. If more solvent is lost than acceptable, lines of capillary can be frozen to determine where the leak is occurring. An easy way to accomplish freezing is by turning a can of compressed air upside down and spraying the appropriate length of capillary. Connection points where fittings occur tend to be the highest probable sites where leaks are occurring.

Leak testing from the Haskell side can be a bit more troublesome as there are more potential sites of leakage, which also need to hold higher pressures. With the appropriate valves toggled for the system to be in operating mode, the Haskell pump can be turned on and all connection points should be inspected for fluid accumulation after 15-20 minutes of the pump being activated. To ensure normal operation will proceed as planned, the Haskell pump should be pressured to 40,000 psi for leak checking. If a leak event is not discovered after 20 minutes at 40,000 psi, the pump pressure can be dialed down to normal operation pressure of 30,000 psi. If fluid is detected, the fitting should be re-made and rechecked. In addition to waiting for fluid formation, the Haskell pump itself can often times give clues to leaking. If the drive shaft is visibly moving when the pump is on, there is a leak present. In addition to checking fittings for visible fluid accumulation, the waste ports of pin valves should also be examined for leakage.

A1.3.4 New Column Use

The day before a new column is to be used, the column needs to be fitted to the XUPLC for rinsing. An experimental file using 95% organic modifier should be used to flush the column overnight and can be created by modifying experimental files seen in Figures 8 and 9. The method for doing so is as follows. Valve 4 and Valve 3 should be set to on for them to open with Valve 2 set to off to direct solvent flow through the gradient storage loop. The inlet method file should be set to 95% organic for 15

minutes at 20 µL/min to flush the loop. After this flushing period, at time 15.1 Valve 2 is set to on, at 15.2 Valve 3 is set to off, at 15.3 Valve 4 is set to off, and at 15.4 Valve 1 is set to on. This pushes solvent through the long axial column. The method file should be set to end after 4 hours. The file can be used consecutively in order to achieve flushing overnight. After column flushing, the column should be re-equilibrated before data acquisition.

A1.3.5 Sample Acquisition

As shown in Figure A-6, and more closely in Figure A-7, a single injection is split into four different sample lines within the MassLynx sample queue. This style of setup has the benefit of directly controlling gradient loop contents, sample injection, gradient formation, and data collection. Additionally, this separation of sample acquisition events allows the software to avoid file sizes which are too big for data analysis.

A1.3.6 Gradient Loop Flushing

The first file line corresponds to gradient loop flushing and can be used as an optional command line. The method and valve controls, which can be seen in Figures 8 and 9, follow from the column flushing for new column use and are as follows. Initial valve states should be Valve 1 off, Valve 2 on, Valve 3 on, and Valve 4 on. At time 0.1, Valve 2 is set to off. The inlet method should be set to 20 µL/min of 97% A for 18 minutes followed by 0.01 µL/min at time 18.1 minutes. At 18 minutes, Valve 2 should be set to on.

This method can be altered for column equilibration as follows. Initial valve conditions remain the same. At time 0.1 Valve 2 is set to off. The inlet method should be set to 20 µl/min of 97% A for 5 minutes followed by 0.1 µl/min at time 5.1 minutes. At this point, valves should be changed to Valve 2

on at 5.1, Valve 3 off at 5.2, Valve 4 off at 5.3, and Valve 1 on at 5.4. Valve 1 should be set to off at 19.9 minutes and the method file should end at 20 minutes.

A1.3.7 Gradient Formation

Parallel to conventional chromatography where practical gradient elution is considered in percent organic modifier change per minute, for a constant pressure set up where flow rate is variable, the gradient program is considered in percent organic modifier change per column volume. The analyst should aim for a 2% change in modifier per column volume. For a meter long column packed with 1.9 µm particles, this equates to an approximate 60 µL gradient. For illustration purposes and to access system suitability, an ambitious 12 µL gradient is shown in Figures 10 and 11 as an example. By changing the time it takes to reach 4% organic modifier on row 6 of the inlet method file, the analyst can change the size of the gradient accordingly with a 0.1 min change providing a one µL change in gradient size. It should be noted that all lines proceeding row 6 and method endpoints should be changed accordingly in parallel with corresponding valve states.

The method file shown in Figure A-10 shows the mobile phase composition and corresponding flow rates. It should be noted that the gradient is loaded before the sample and in an opposite order as during XUPLC operation, components are played back in reverse. All flow rates for gradient loading are done at 10 µL/min and follow curve 6 (linear solvent change during the time interval). Mobile phase composition is set to 4% B initially changing to 85% B at 1.1 min till 1.3 min, 40% B at 1.4 min, and 4% at 2.6 min till 3 min. Corresponding valves states, seen in Figure A-11, are Valve 1 off, Valve 2 on, Valve 3 on, and Valve 4 on initially, which changes to Valve 2 to off at 0.01 min, Valve 3 off at 3.0 min, and Valve 2 on at 3.0 min.

A1.3.8 Sample Loading

The instrument method for sample loading follows instructions similar to gradient loading. Important primarily to sample loading is the sample plug must be pushed past the column Valco T in order for it to be pushed onto the column during Haskell pump operation. The sample plug is pushed with starting condition mobile phase composed of 4% B. The method file shown in Figures 12 and 13 pushes the sample with 19 µL of mobile phase. While this volume of push solvent has been shown to produce acceptable results, it is not optimized. Optimizing the plug size used can be accomplished by decreasing the push time to shorter than 1.9 min, continuing with data collection, and measuring peak areas to determine if sample has been lost due to insufficient push volume. Future optimization of sample push time will result in significant time savings.

As shown in Figure A-12, sample loading is accomplished by simply making an injection (as indicated in the auto-sample page) and pushing the injection plug for 1.9 minutes at 10 µL/min. Subsequent to pushing the sample plug, the flow rate is set to 0. Meanwhile, shown in Figure A-13, valves states are altered to begin chromatographic sample separation. Initial valve states are Valve 1 off, Valve 2 off, Valve 3 on, and Valve 4 on. At min 2.2, Valve 2 is set to on and Valve 3 begins a toggling event. A toggling event has been programmed into the method sequence to prevent the valve from sticking immediately prior to high pressure use. The toggle event consists of a rapid on-off valve switching every 0.05 min for 0.25 minutes. After the toggling event, Valve 3 is off, Valve 2 is on, Valve 4 is off, and Valve 1 is set to on.

A1.3.9 Data Acquisition

The fourth and final row in the sample queue corresponds to the data file and should be named appropriately (Figures 14 and 15). Valve states follow from row three in the queue and should be initially set at Valves 3 and 4 off with Valves 1 and 2 on. Upon completion of data collection, typically 120 minutes for a one meter column, Valves 1 and 4 are set to off and on respectively to end

chromatographic development. The Inlet method file has the flow rate set to 0.01 for the course of the run and should be set to end at 120 minutes. MS data acquisition file should be set according to needs. A typical MS method used is an MS^e data acquisition with a collision energy ramp from 15 to 40 V set to record at the expected time of peptide elution.

A1.4 Preliminary XUPLC Results

Figure A-16 shows preliminary results which can be expected when utilizing a 100 cm long column. The chromatogram on the top shows a BSA digest standard on a Waters 10 cm 1.7 µm BEH nanoACQUITY column. The bottom chromatogram shows the same BSA digest when developed through a 100 cm column packed with the same Waters 1.7 µm BEH material. The results produced follow from theory and are as expected.

With utilization of the longer column, there is higher resolution observed between two identical sets of peptides. Resolution is defined by equation (4) where t_r is retention time and W is peak width.

$$R = \frac{2[(t_r)_2 - (t_r)_1]}{W_1 + W_2} \quad (4)$$

Using resolution as a means to evaluate column performance, we see the 10 cm commercial column producing a resolution of 0.72 for the two peptides with the 100 cm column producing a resolution of 2.5. As a resolution of 1.5 is considered baseline resolution, this gain in separation efficiency is quite substantial.

It should be noted that there is a general difference between the two chromatograms in that different peaks are seen. More specifically, both chromatograms fail to show the 39 expected peptides which should be present in a BSA digest with the top chromatogram showing approximately 29 separate peaks and the bottom chromatogram showing approximately 26 separate peaks. Furthermore, evaluation of ion intensities between the two chromatograms show a greater than 10-fold decrease in

sensitivity from the top chromatogram to the bottom. This loss of sensitivity was not a consequence of the XUPLC operation. To the contrary, the lower flow rates associated with XUPLC operation should result in a gain of sensitivity. It was discovered over the implementation of the XUPLC that there were several issues with Mass Spec Laboratory nanoACQUITY instrument as regards cleanliness, maintenance habits, and a lack of operation checks to serve as instrumentation readiness criteria. In addition, the detector plate on the Synapt G2 was in the process of lifetime failure, to the point that replacement was required. Despite the promising gains in resolution through an increase in chromatographic space, the considerable effort put forth to reach acceptable operational status when moving to the XUPLC, the existing problems with instrumentation prevented further evaluation of the extended chromatographic system. As a result further efforts to implement the XUPLC system has been placed on hold until new instrumentation can be acquired to avoid the issues noted.

A1.5 Appendix Figures

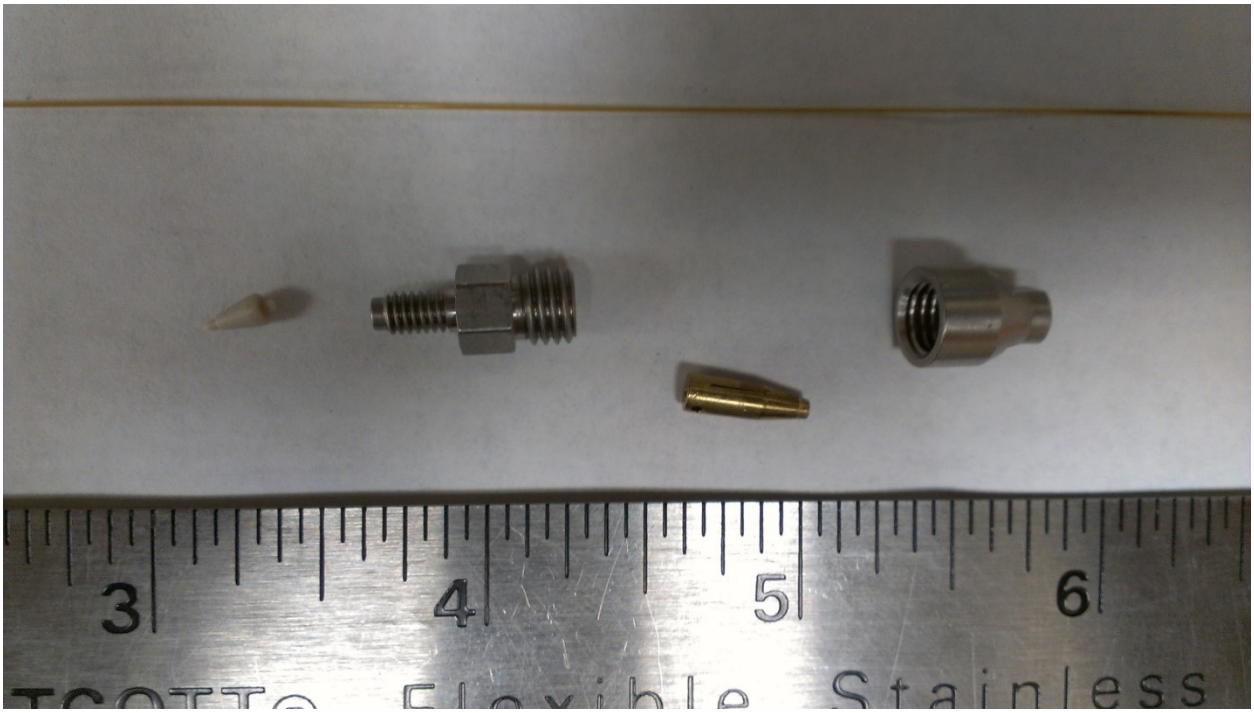

Figure A-1. Custom high-pressure fittings obtained from the University of North Carolina, with Waters approval, next to fused-silica capillary and a ruler for scale. The front ferrule is a Valco high pressure PEEK ferrule which is drilled out to 380 ID prior to use. The connecting nut, back ferrule, and backing nut are custom made. A PEEK sleeve is also used with this connection scheme (not shown).

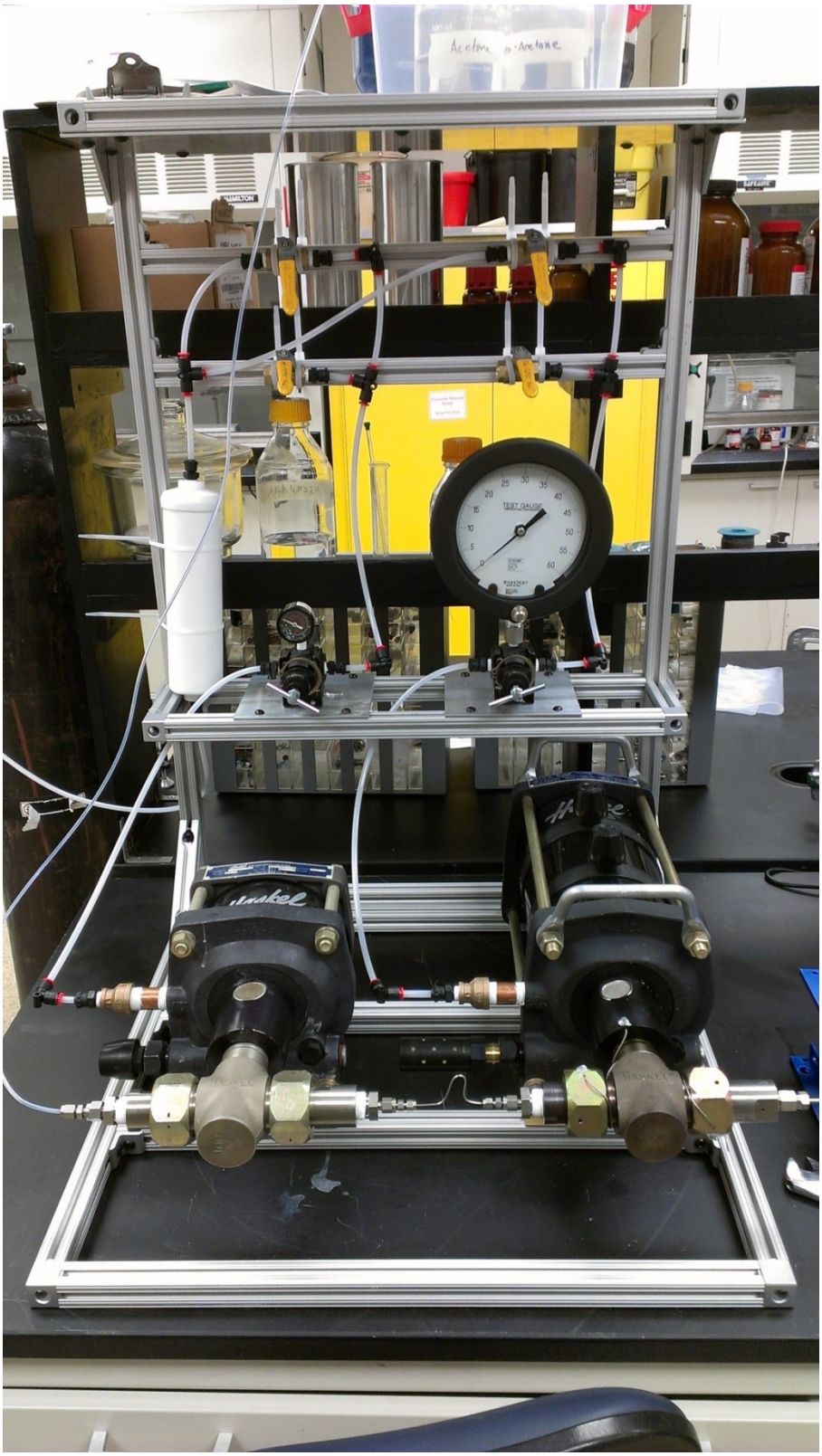

Figure A-2. Packing station set-up showing a Haskel DSF-100 connected to a Haskel RDSXHF-903. Solvent reservoirs are seen above. The Haskel 903 outlet is connected to the packing bomb (Figure A-3).

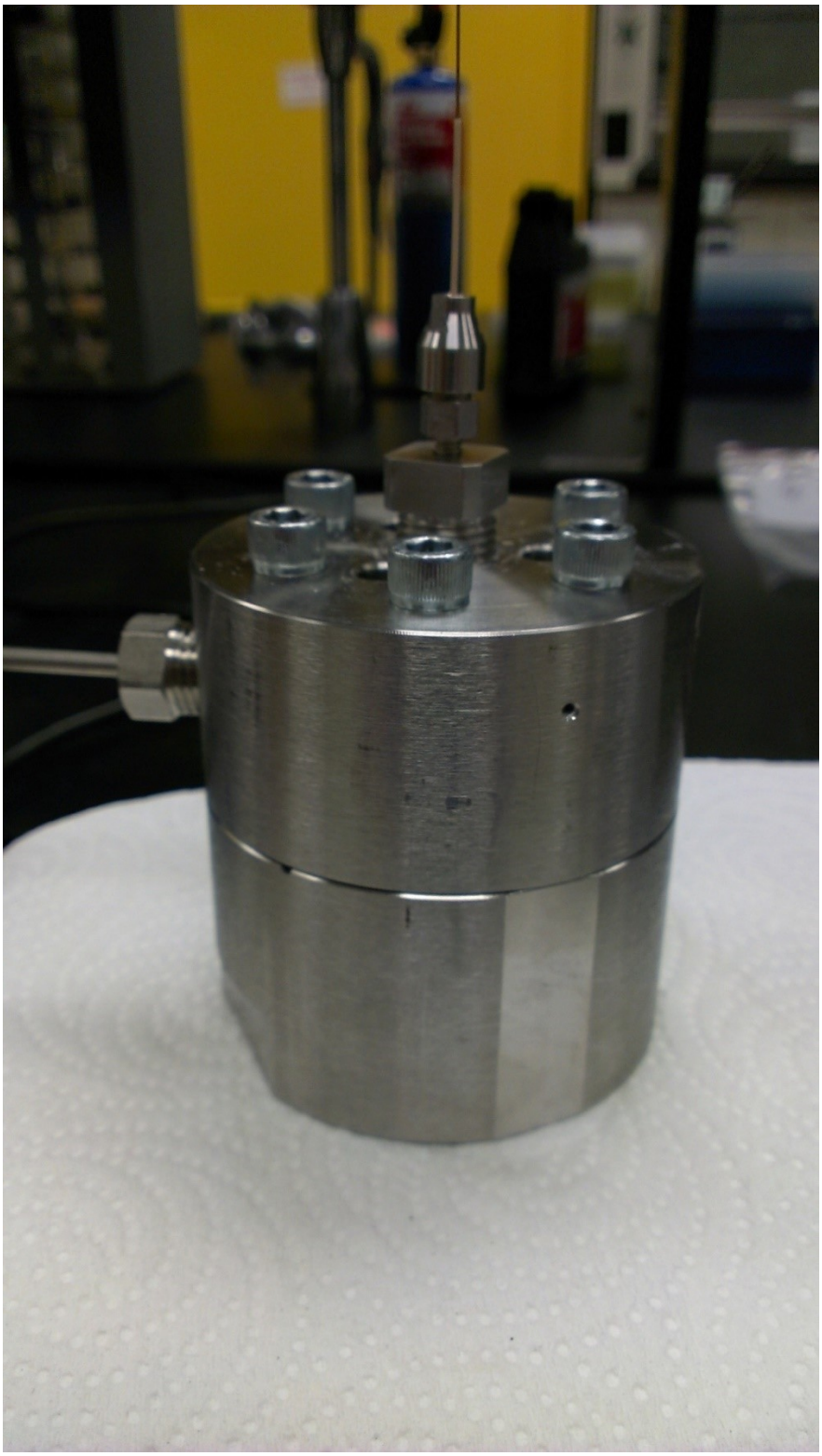

Figure A-3. Packing bomb. Internal volume is approximately 400 µL. The inlet is attached to the Haskel 903 and the outlet can be seen connected to fused-silica capillary for packing.

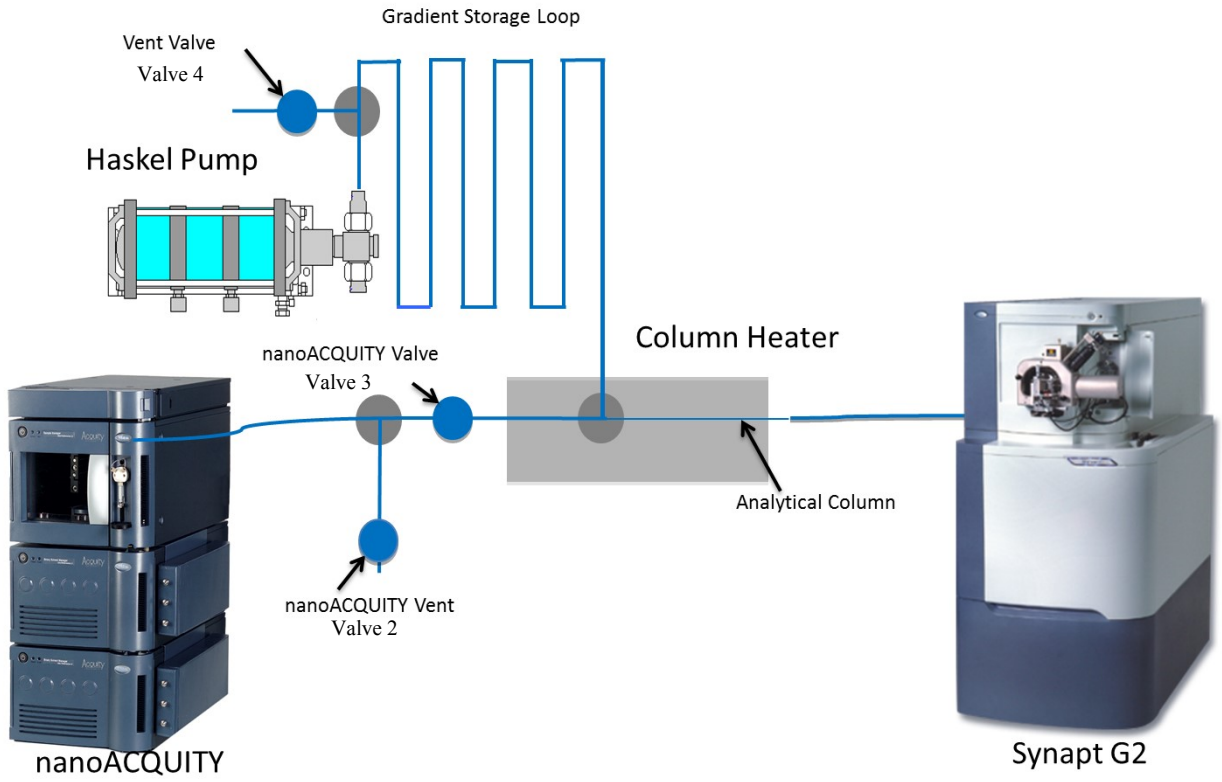

Figure A-4. XUPLC system design featuring connection points between the nanoACQUITY and Synapt G2.

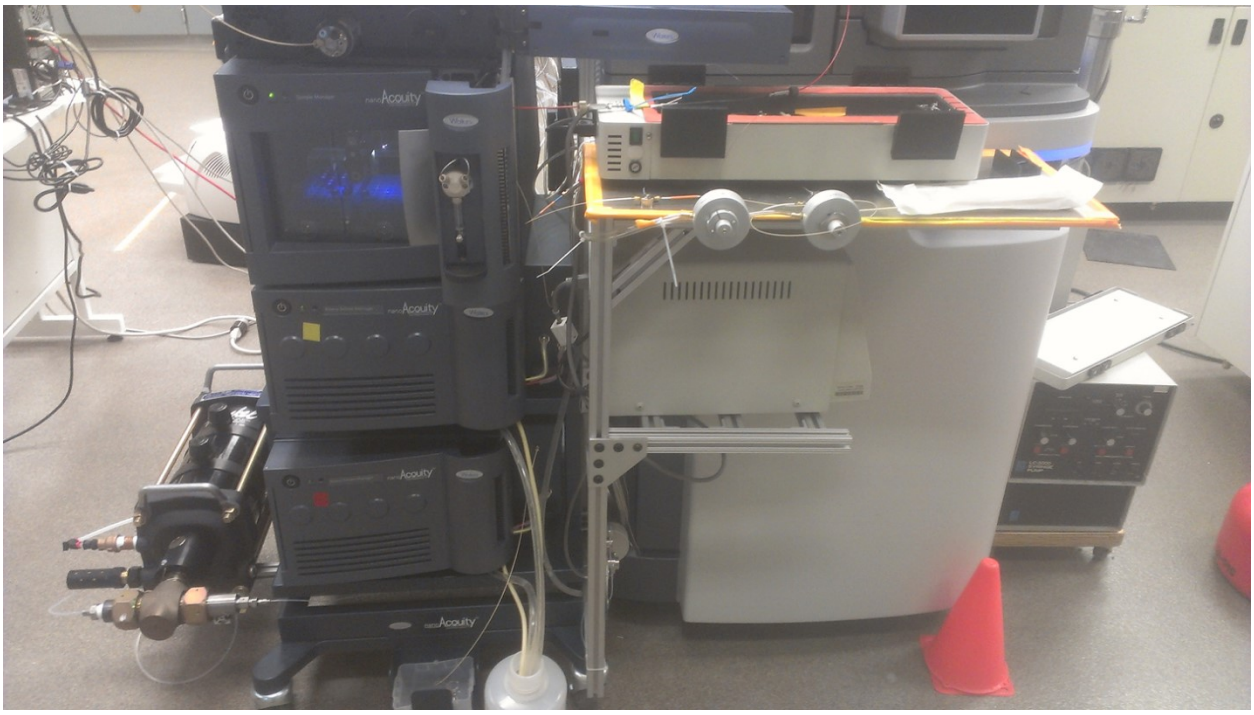

Figure A-5. XUPLC system shown in the KU mass spectrometry laboratory. Haskell 903 can be viewed on the bottom right. To right of the nanoACQUITY is a custom made bench, with pin valves attached, to hold the column heater.

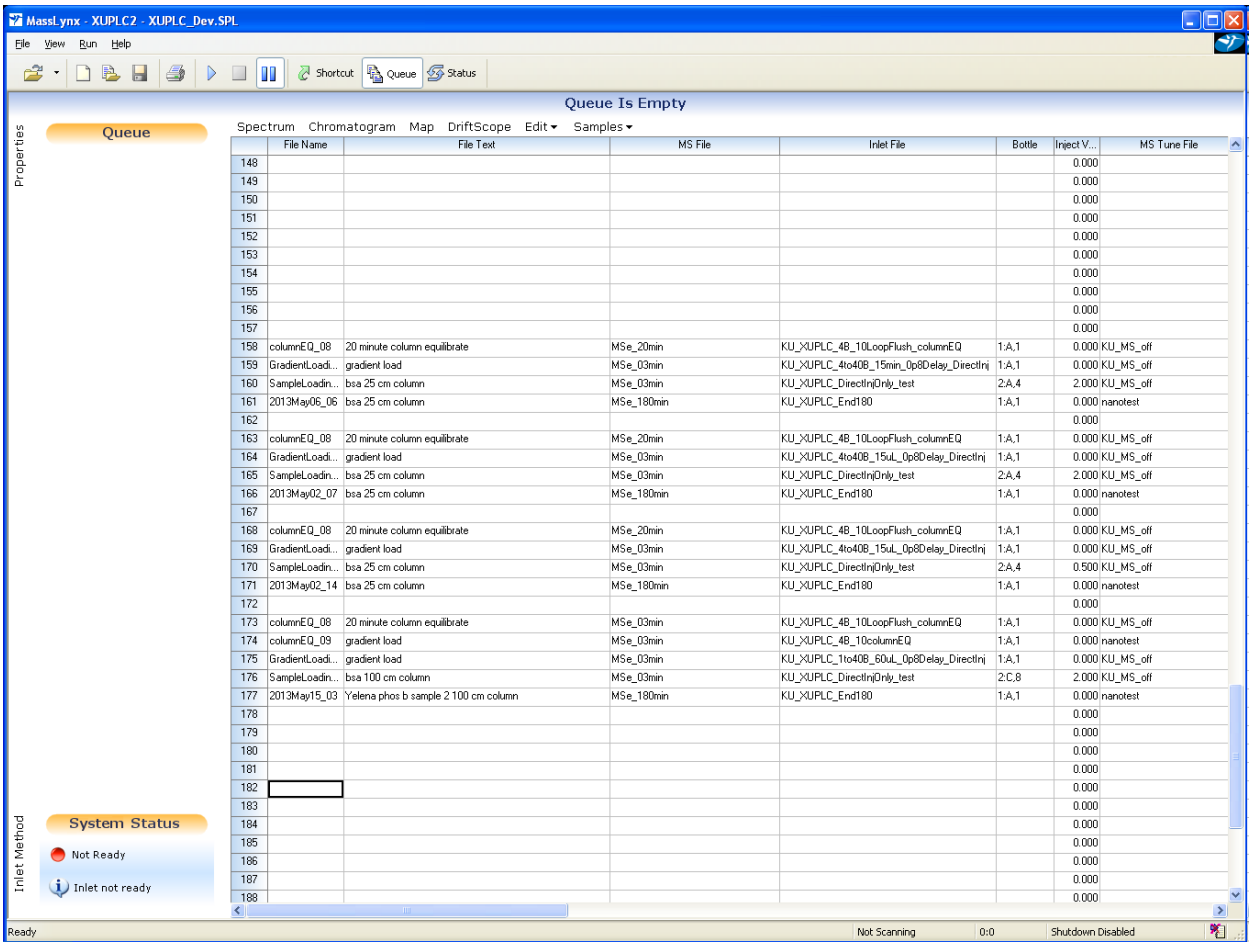

	File Name	File Text	MS File	Inlet File	Bottle	Inject V...	MS Tune File
148						0.000	
149						0.000	
150						0.000	
151						0.000	
152						0.000	
153						0.000	
154						0.000	
155						0.000	
156						0.000	
157						0.000	
158	columnEQ_08	20 minute column equilibrate	MSe_20min	KU_XUPLC_4B_10LoopFlush_columnEQ	1:A,1	0.000	KU_MS_off
159	GradientLoadi...	gradient load	MSe_03min	KU_XUPLC_4to40B_15min_0p8Delay_DirectInj	1:A,1	0.000	KU_MS_off
160	SampleLoadin...	bsa 25 cm column	MSe_03min	KU_XUPLC_DirectInjOnly_test	2:A,4	2.000	KU_MS_off
161	2013May06_06	bsa 25 cm column	MSe_180min	KU_XUPLC_End180	1:A,1	0.000	nanotest
162						0.000	
163	columnEQ_08	20 minute column equilibrate	MSe_20min	KU_XUPLC_4B_10LoopFlush_columnEQ	1:A,1	0.000	KU_MS_off
164	GradientLoadi...	gradient load	MSe_03min	KU_XUPLC_4to40B_15uL_0p8Delay_DirectInj	1:A,1	0.000	KU_MS_off
165	SampleLoadin...	bsa 25 cm column	MSe_03min	KU_XUPLC_DirectInjOnly_test	2:A,4	2.000	KU_MS_off
166	2013May02_07	bsa 25 cm column	MSe_180min	KU_XUPLC_End180	1:A,1	0.000	nanotest
167						0.000	
168	columnEQ_08	20 minute column equilibrate	MSe_20min	KU_XUPLC_4B_10LoopFlush_columnEQ	1:A,1	0.000	KU_MS_off
169	GradientLoadi...	gradient load	MSe_03min	KU_XUPLC_4to40B_15uL_0p8Delay_DirectInj	1:A,1	0.000	KU_MS_off
170	SampleLoadin...	bsa 25 cm column	MSe_03min	KU_XUPLC_DirectInjOnly_test	2:A,4	0.500	KU_MS_off
171	2013May02_14	bsa 25 cm column	MSe_180min	KU_XUPLC_End180	1:A,1	0.000	nanotest
172						0.000	
173	columnEQ_08	20 minute column equilibrate	MSe_03min	KU_XUPLC_4B_10LoopFlush_columnEQ	1:A,1	0.000	KU_MS_off
174	columnEQ_09	gradient load	MSe_03min	KU_XUPLC_4B_10columnEQ	1:A,1	0.000	nanotest
175	GradientLoadi...	gradient load	MSe_03min	KU_XUPLC_1to40B_60uL_0p8Delay_DirectInj	1:A,1	0.000	KU_MS_off
176	SampleLoadin...	bsa 100 cm column	MSe_03min	KU_XUPLC_DirectInjOnly_test	2:C,8	2.000	KU_MS_off
177	2013May15_03	Yelena phos b sample 2 100 cm column	MSe_180min	KU_XUPLC_End180	1:A,1	0.000	nanotest
178						0.000	
179						0.000	
180						0.000	
181						0.000	
182						0.000	
183						0.000	
184						0.000	
185						0.000	
186						0.000	
187						0.000	
188						0.000	

Figure A-6. Screenshot of a typical sample list featuring XUPLC samples. Each individual run is comprised of four to five lines in the sample queue to control gradient formation, sample loading, and file sizes for data acquisition.

158	columnEQ_08	20 minute column equilibrate	MSe_20min	KU_XUPLC_4B_10LoopFlush_columnEQ	1:A,1	0.000	KU_MS_off
159	GradientLoadi...	gradient load	MSe_03min	KU_XUPLC_4to40B_15min_0p8Delay_DirectInj	1:A,1	0.000	KU_MS_off
160	SampleLoadin...	bsa 25 cm column	MSe_03min	KU_XUPLC_DirectInjOnly_test	2:A,4	2.000	KU_MS_off
161	2013May06_06	bsa 25 cm column	MSe_180min	KU_XUPLC_End180	1:A,1	0.000	nanotest

Figure A-7. Expected sample queue information for a single XUPLC injection featuring column equilibration, gradient loading, sample loading, and data acquisition.

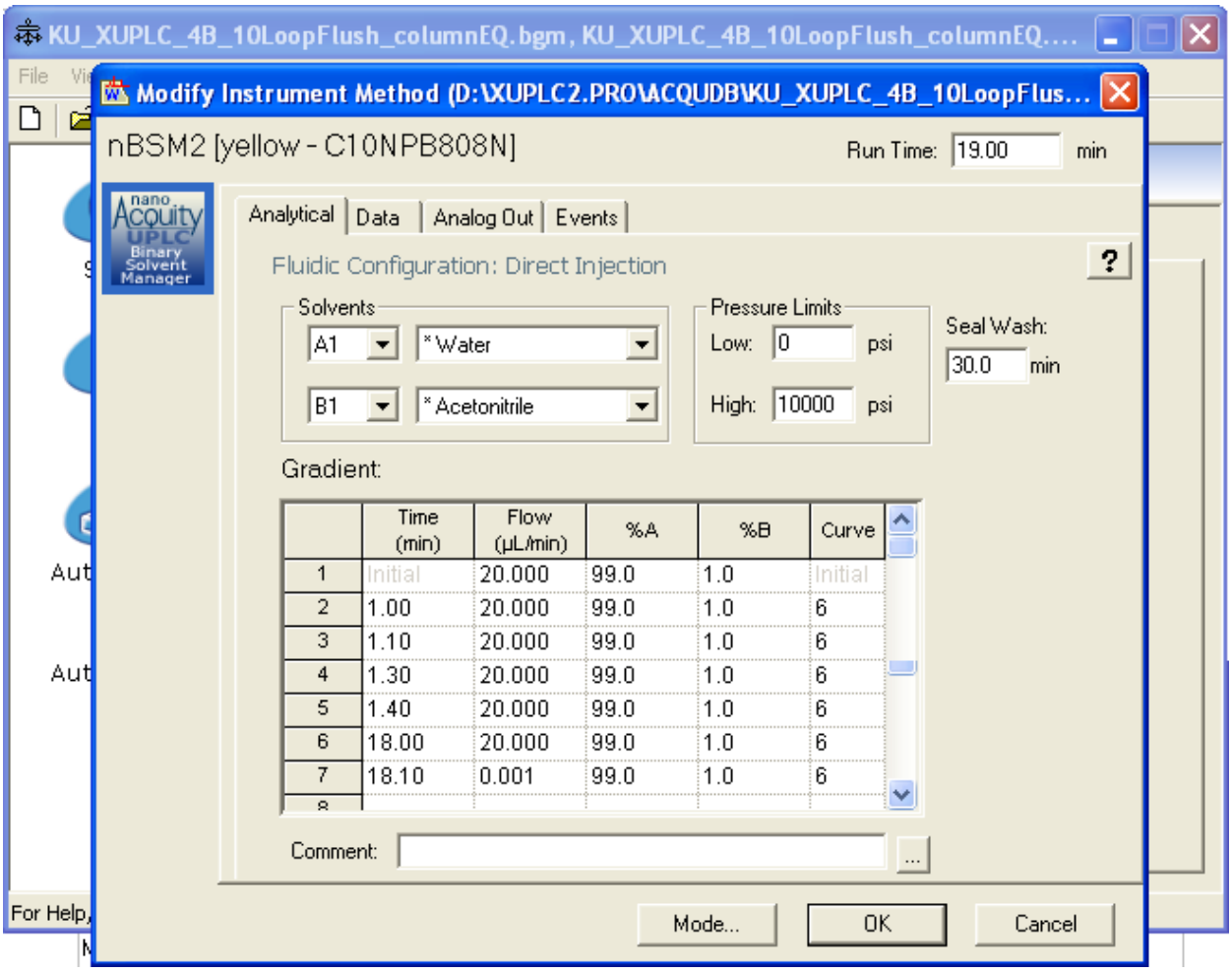

Figure A-8. Inlet method for loop flushing.

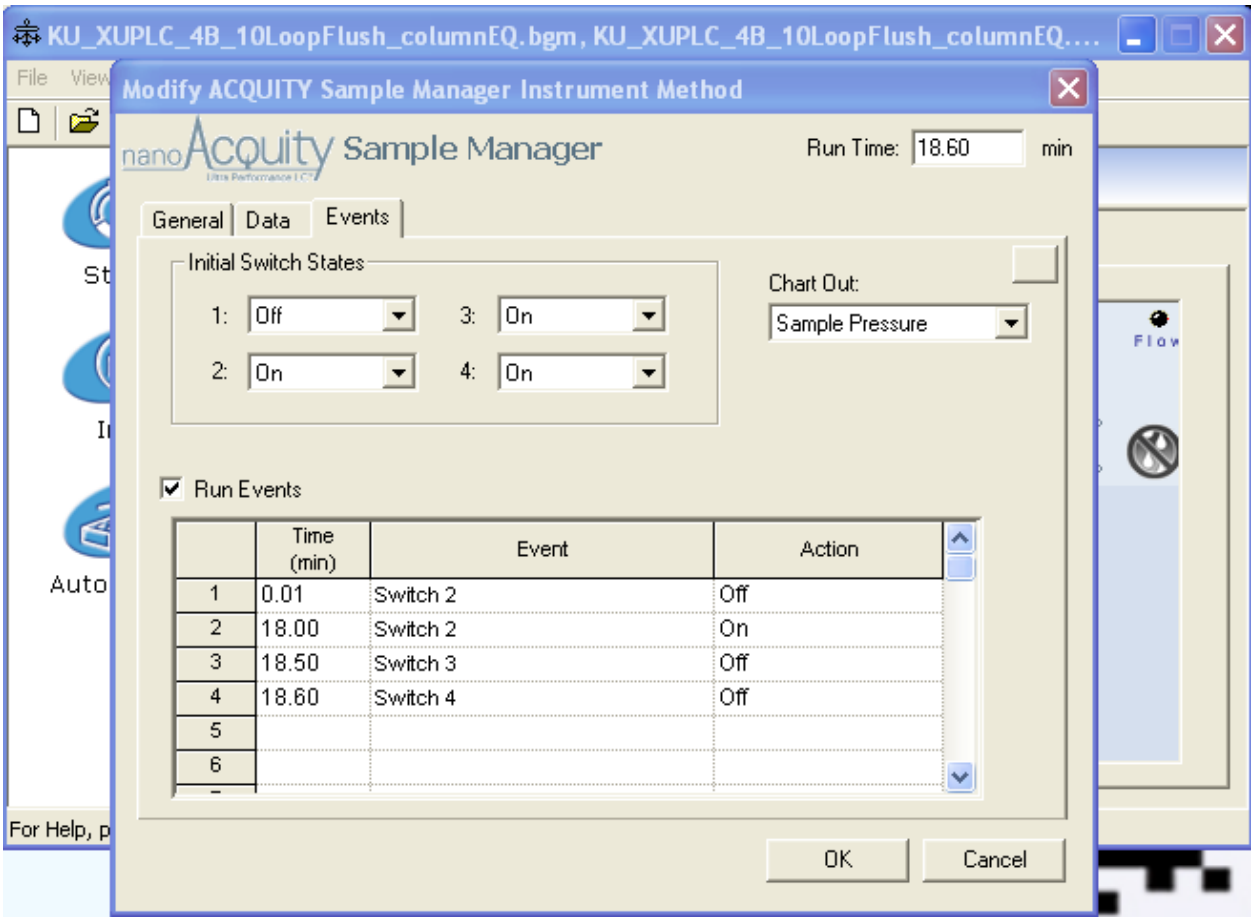

Figure A-9. Sample Manager Events for loop flushing.

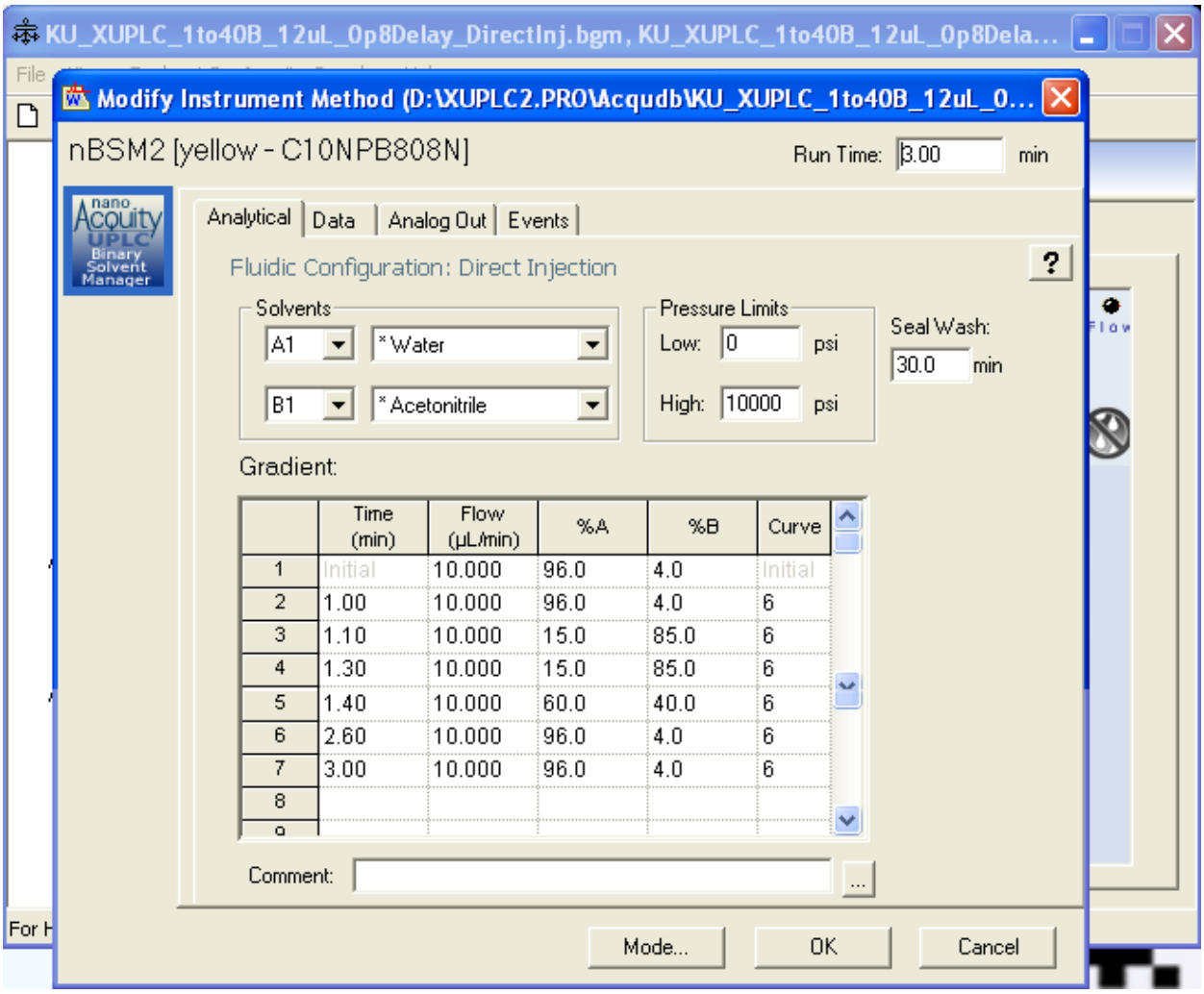

Figure A-10. Inlet method for a 12 µL gradient.

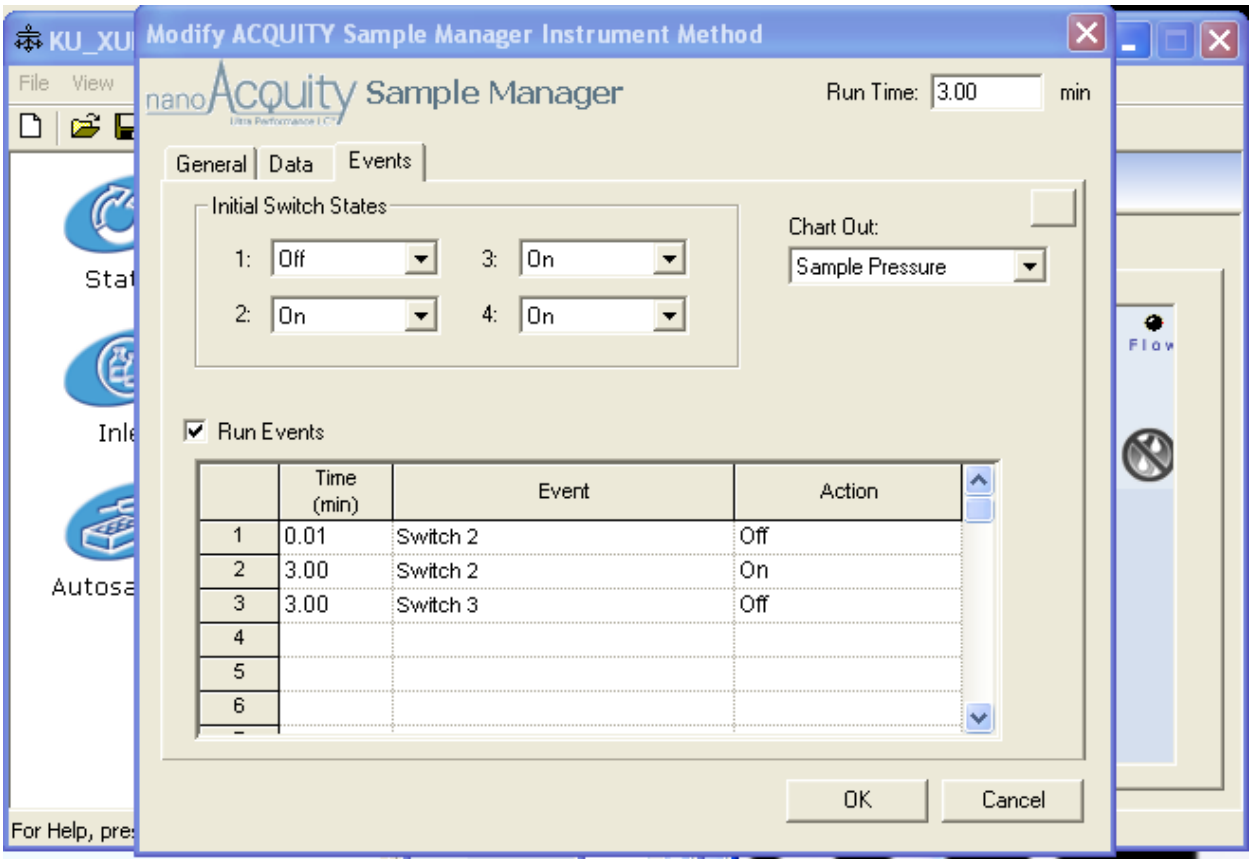

Figure A-11. Sample manager events for gradient loading.

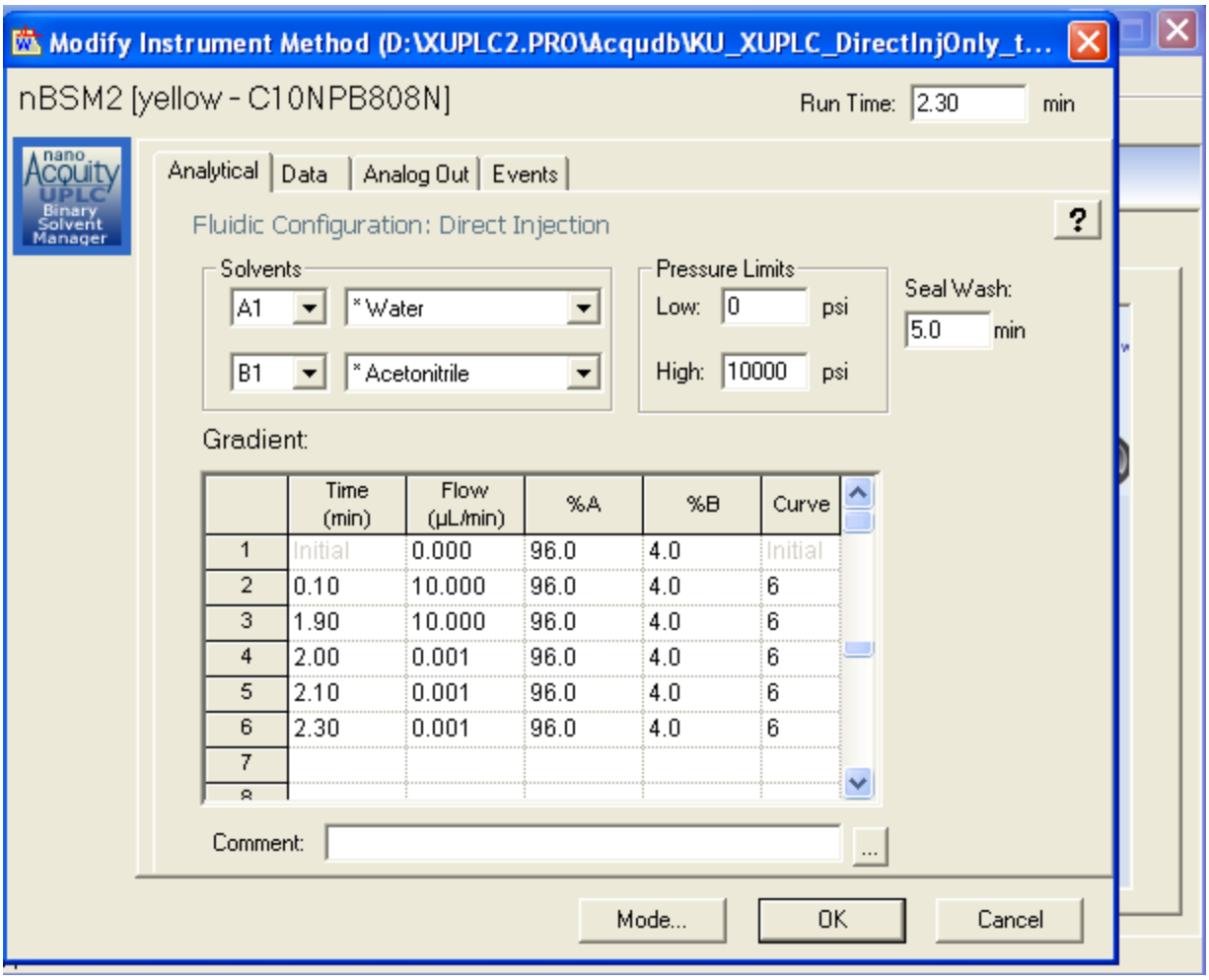

Figure A-12. Inlet method for sample loading with a 19 µL injection push.

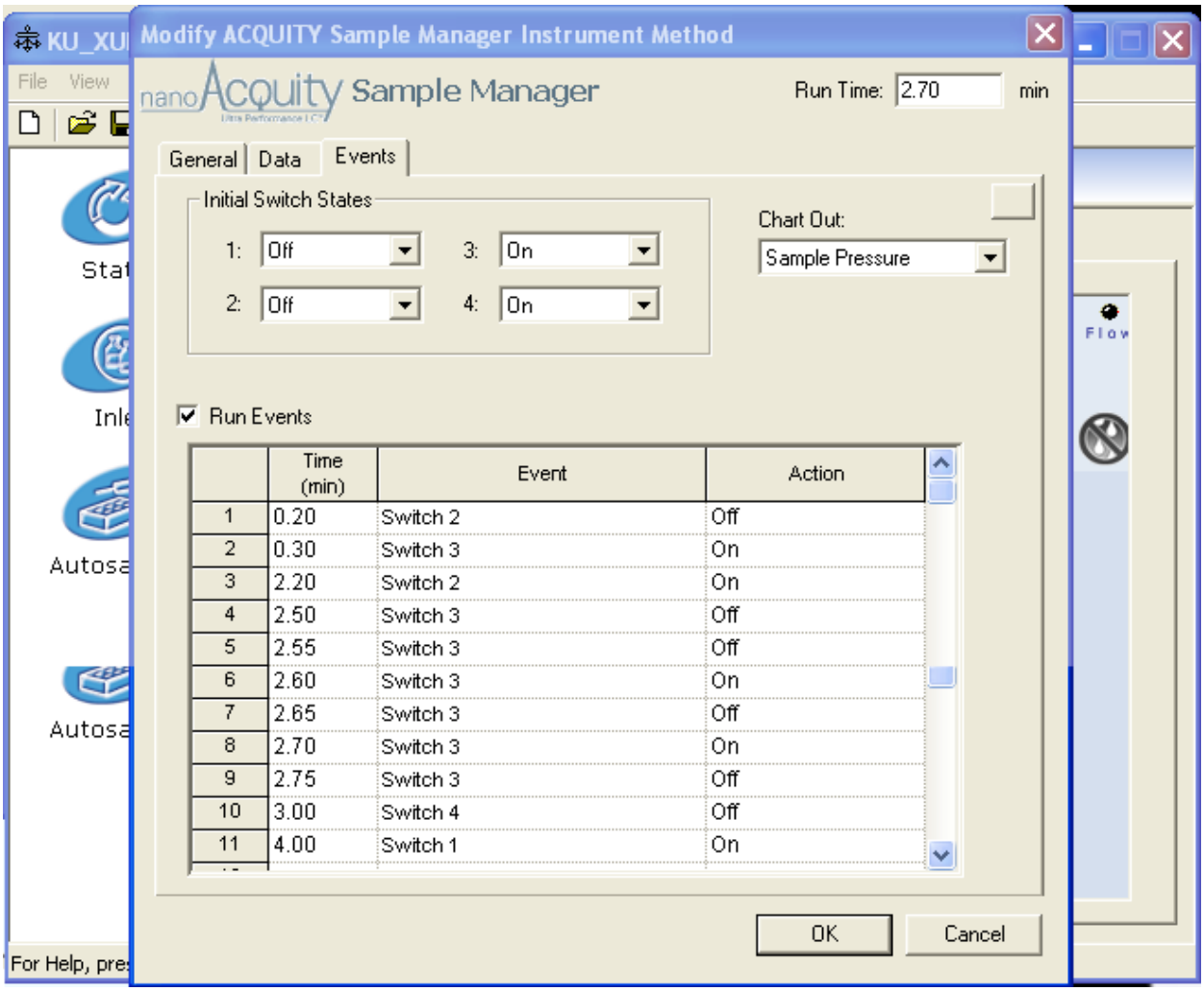

Figure A-13. Sample Manager events for sample loading featuring valve toggling between minute 2.5 and minute 3 and Haskel 903 activation at minute 4.

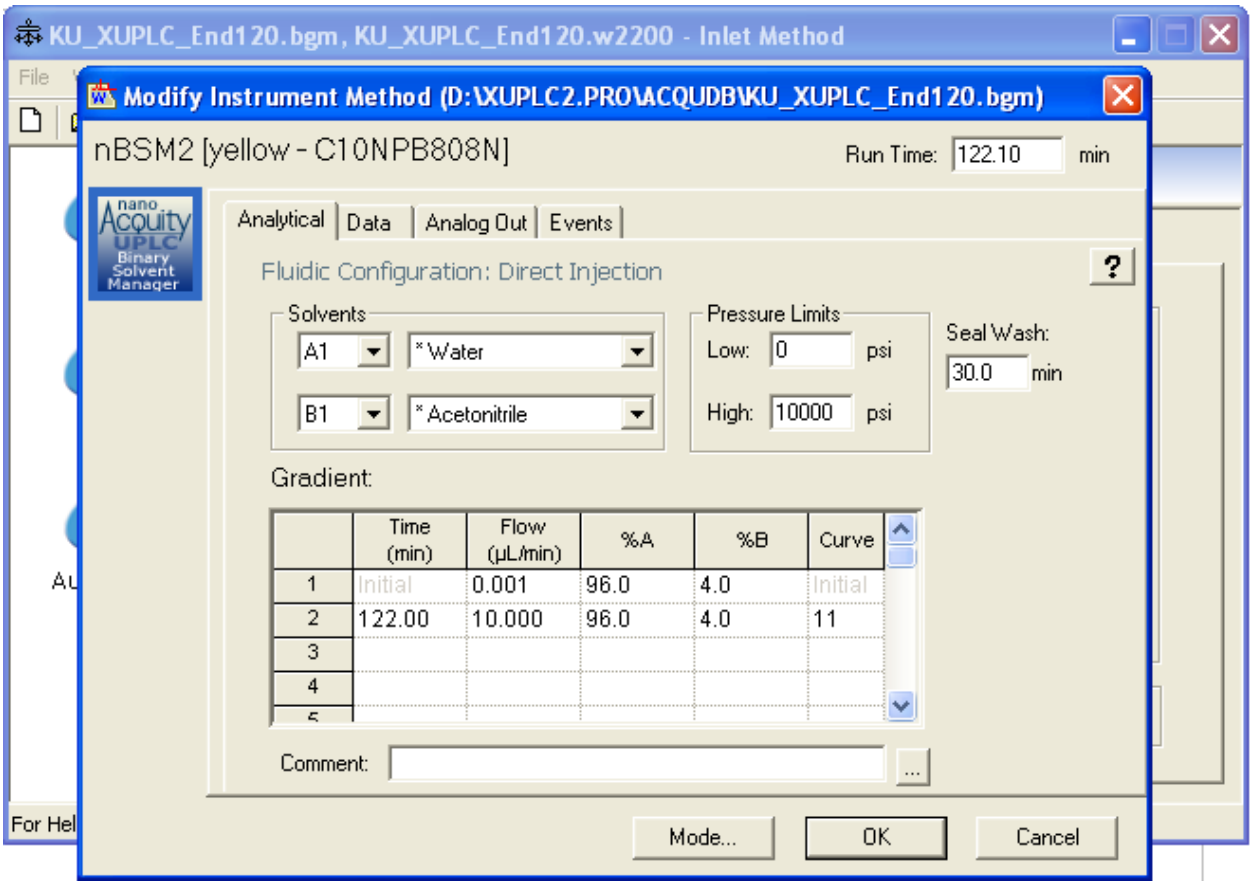

Figure A-14. Inlet method for data acquisition.

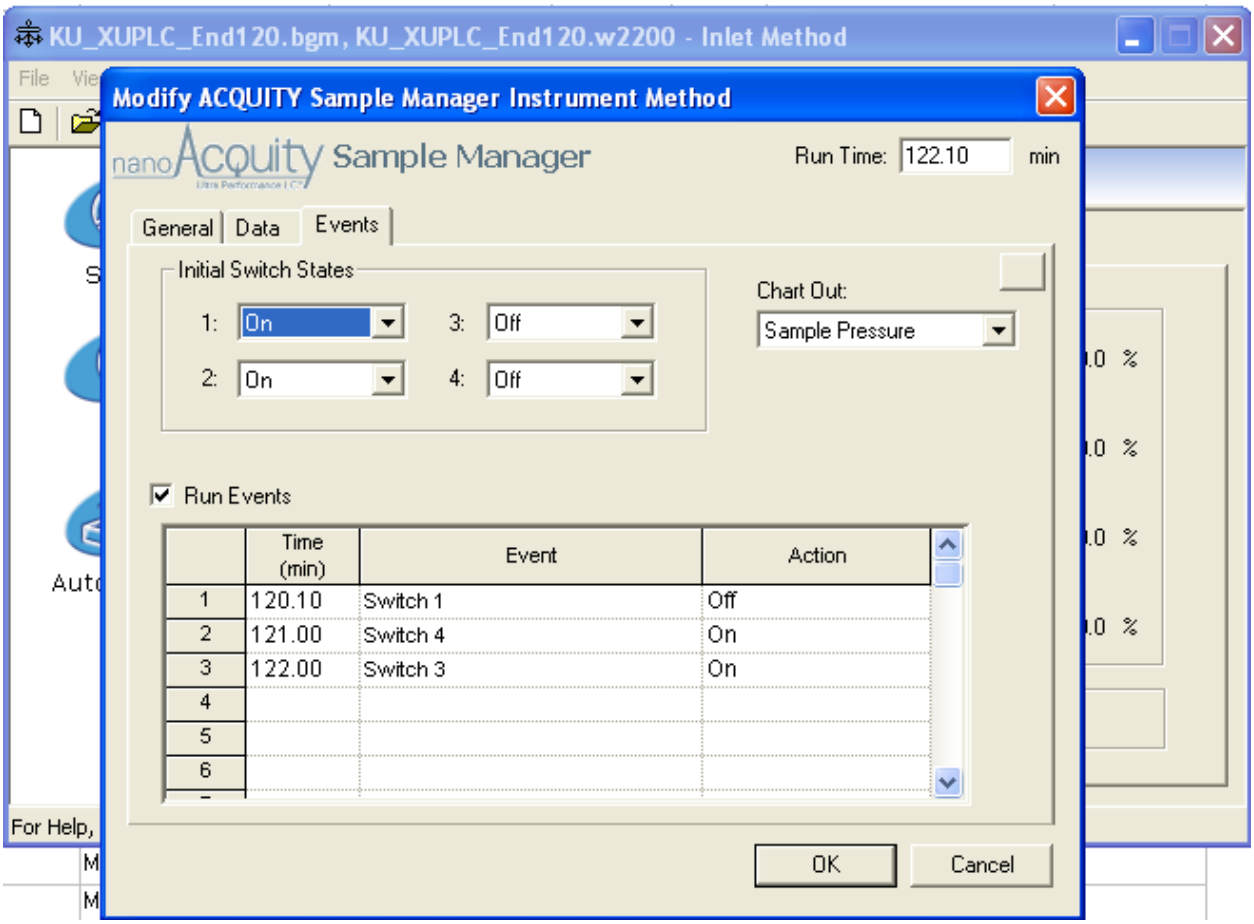

Figure A-15. Sample Manager events for data acquisition featuring Haskel 903 deactivation.

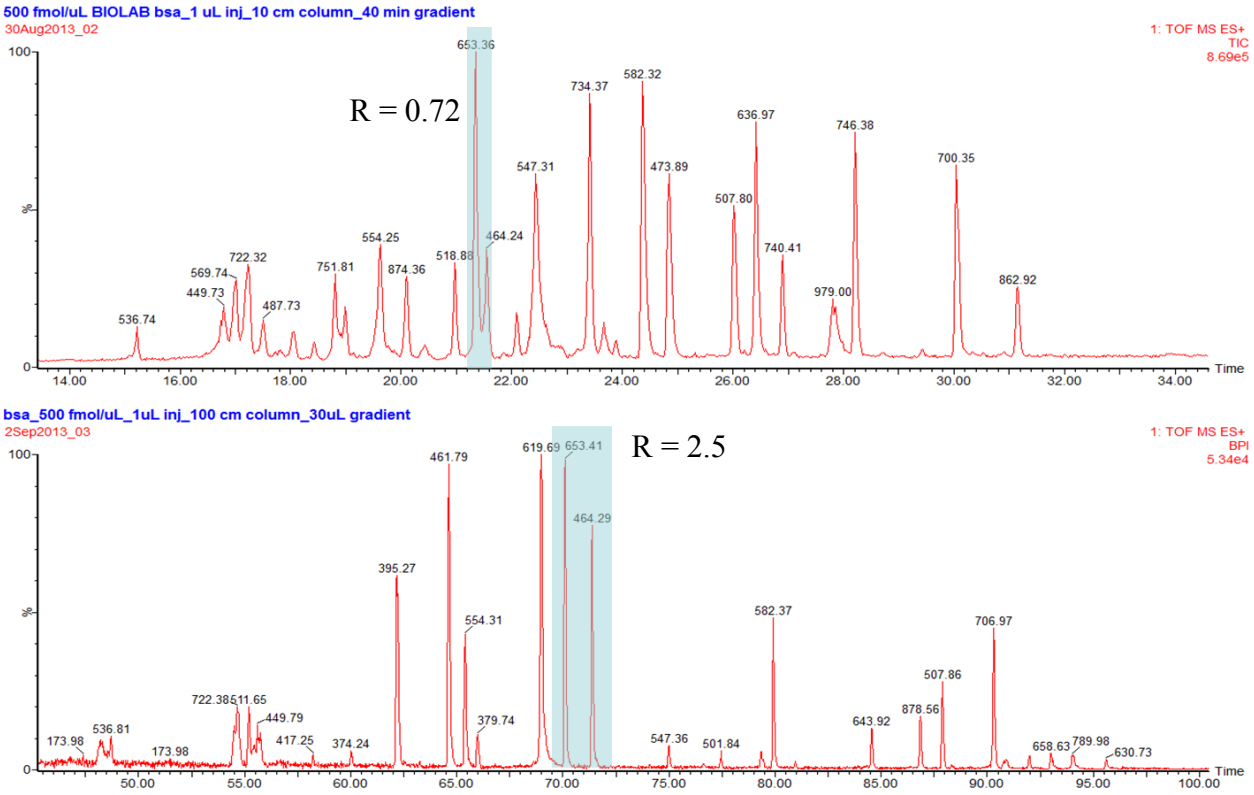

Figure A-16. Comparison of (top) commercial ACQUITY BEH 1.7 µm 10 cm x 75 µm column with a (bottom) custom packed ACQUITY BEH 1.7 µm particles in a 100 cm x 75 µm column. Highlighted areas show identical peptides with a gain in resolution from 0.72 to 2.5 when moving from the 10 cm column to the 100 cm column respectively.

A1.6 Appendix References

[1] D. Baltimore, *Nature* **2001**, *409*, 814-816.
[2] J. Godovac-Zimmermann and L. R. Brown, *Mass Spectrom Rev* **2001**, *20*, 1-57.
[3] E. de Hoffmann and V. Stroobant, *Mass Spectrometry Principles and Applications*, Wiley, **2007**, p.
[4] T. Krüger, T. Lehmann and H. Rhode, *Analytica Chimica Acta* **2013**, *776*, 1-10.
[5] J. Wohlgemuth, M. Karas, T. Eichhorn, R. Hendriks and S. Andrecht, *Anal Biochem* **2009**, *395*, 178-188.
[6] J. W. Jorgenson, *Annu Rev Anal Chem (Palo Alto Calif)* **2010**, *3*, 129-150.
[7] a) J. T. Stobaugh in *Startegies for Differential Proteomic Analysis by Liquid Chromatography-Mass Spectrometry*, *Vol.* University of North Carolina, Chapel Hill, **2012**; b) E. G. Franklin in *Utilization of Long Columns Packed with Sub-2 µm Particles Operated at High Pressures and Elevated Temperatures for High-Efficiency One-Dimensional Liquid Chromatographic Separations*, *Vol.* Univeristy of North Carolina, Chapel Hill, **2012**.